MISSILE GUIDANCE WITH IMPACT ANGLE CONSTRAINT

A THESIS SUBMITTED TO
THE GRADUATE SCHOOL OF NATURAL AND APPLIED SCIENCES
OF
MIDDLE EAST TECHNICAL UNIVERSITY

BY

BARKAN ÇİLEK

IN PARTIAL FULFILLMENT OF THE REQUIREMENTS
FOR
THE DEGREE OF MASTER OF SCIENCE
IN
AEROSPACE ENGINEERING

DECEMBER 2014

Approval of the thesis:

MISSILE GUIDANCE WITH IMPACT ANGLE CONSTRAINT

submitted by **BARKAN ÇİLEK** in partial fulfillment of the requirements for the degree of **Master of Science in Aerospace Engineering Department, Middle East Technical University** by,

Prof. Dr. Gülbin Dural Ünver ___________
Dean, Graduate School of **Natural and Applied Sciences**

Prof. Dr. Ozan Tekinalp ___________
Head of Department, **Aerospace Engineering**

Assist. Prof. Dr. Ali Türker Kutay ___________
Supervisor, **Aerospace Engineering Dept., METU**

Examining Committee Members:

Prof. Dr. Ozan Tekinalp _____________
Aerospace Engineering Dept., METU

Asst. Prof. Dr. Ali Türker Kutay ____________
Aerospace Engineering Dept., METU

Assoc. Prof. Dr. İlkay Yavrucuk _____________
Aerospace Engineering Dept., METU

Prof. Dr. Kemal Leblebicioğlu _____________
Electrical and Electronics Engineering Dept., METU

Prof. Dr. Kemal Özgören _____________
Mechanical Engineering Dept., METU

Date: ______________

I hereby declare that all information in this document has been obtained and presented in accordance with academic rules and ethical conduct. I also declare that, as required by these rules and conduct, I have fully cited and referenced all material and results that are not original to this work.

Name, Last name: Barkan ÇİLEK

Signature :

ABSTRACT

MISSILE GUIDANCE WITH IMPACT ANGLE CONSTRAINT

Çilek, Barkan

M.S., Department of Aerospace Engineering

Supervisor: Assist. Prof. Dr. Ali Türker Kutay

December 2014, 100 Pages

Missile flight control systems are the brains of missiles. One key element of a missile FCS is the guidance module. It basically generates the necessary command inputs to the autopilot.

Guidance algorithm selection depends on the purpose of the corresponding missile type. In this thesis, missile guidance design problem with impact angle constraint is studied which is the main concern of anti-tank and anti-ship missiles. Different algorithms existing in the literature have been investigated using various analysis techniques some of which are not present in the literature.

For the algorithms that need time-to-go information, sensitivity of the algorithm to the errors in time-to-go measurement is analyzed. In this context, apart from the time-to-go methods that are used in corresponding algorithms, a different time-to-go

method[1] is employed and sensitivity analysis is repeated. Results with different time-to-go methods are compared.

Keywords: Impact Angle, Missile Guidance, Launch Envelope, Optimal Guidance, Proportional Guidance, Time-to-Go

ÖZ

VURUŞ AÇISI KISITLI FÜZE GÜDÜMÜ

Çilek, Barkan

Yüksek Lisans, Havacılık ve Uzay Mühendisliği Bölümü

Tez Yöneticisi:Yrd. Doç. Dr. Ali Türker Kutay

Aralık 2014, 100 Sayfa

Füze uçuş kontrol sistemleri (UKS) füzelerin beyinleridir. Bir füze UKS'sinin önemli bir parametresi güdüm modulüdür. Bu modül oto-pilotun girdi olarak alacağı gerekli komutları üretir.

Güdüm algoritması seçimi ilgili füzenin tipine bağlıdır. Bu tezde, daha çok anti-tank ve anti-gemi füzelerinin bir problemi olan vuruş açısı kısıtına göre güdüm tasarımı problemi çalışılmıştır. Literatürde var olan algoritmalar bazıları literatürde var olmayan çeşitli analiz teknikleri kullanılarak incelenmiştir.

Kalan zaman bilgisine ihtiyaç duyan algoritmalar için kalan zaman hesaplamasındaki hataların başarıma etkisi incelenmiştir. Bu kapsamda, ilgili algoritmalardaki vuruşa kalan zaman bilgisinden farklı olarak, farklı bir kalan zaman hesaplama[1] yöntemi

uygulanmış ve başarım analizi tekrar edilmiştir. Farklı kalan zaman hesaplama yöntemiyle olan analizler karşılaştırılmıştır.

Anahtar Kelimeler: Vuruş Açısı, Füze Güdümü, Atış Zarfı, Optimal Güdüm, Doğrusal Güdüm, Vuruşa Kalan Zaman

Beni sevgiyle büyüten anneme;

Ve beni her zaman destekleyen kardeşime.

ACKNOWLEDGEMENTS

I would like to express my sincere appreciation to my supervisor Asst. Prof. Dr. Ali Türker KUTAY for his valuable suggestions, guidance and support throughout the thesis.

TABLE OF CONTENT

LIST OF FIGURES

FIGURES

LIST OF TABLES

TABLES

LIST OF SYMBOLS

α	Angle of Attack
γ_m	Flight Path Angle
λ	Line of Sight Angle
γ_f	Missile Final Flight Path Angle
γ_{m0}	Initial Firing Angle
γ_t	Target Flight Path Angle
γ_{mf}	Impact Angle
γ_d	Desired Impact Angle
σ_m	Missile Look Angle
σ_t	Target Look Angle
τ	Time-to-Go
UKS	Uçuş Kontrol Sistemi (Flight Control System)
LOS	Line of Sight
FCS	Flight Control System
MCLOS	Manuel Commanded Line of Sight
SACLOS	Semi-Automatic Command to Line of Sight
IIR	Imaging Infrared

LADAR	Laser Detection and Ranging
IMU	Inertial Measurement Unit
CIWS	Closed in Weapon System
PNG	Proportional Navigation Guidance
PN	Proportional Navigation
PPN	Pure Proportional Navigation
TPN	True Proportional Navigation
BPN	Biased Proportional Navigation
BPPN	Biased Pure Proportional Navigation
ACPNG	Angle Constrained Biased Proportional Navigation
BSBPN	Biased Shaping Biased Proportional Guidance
IACBPPN	Impact Angle Constrained Biased Pure Proportional Guidance
GENEX	Generalized Vector Explicit Guidance
SDREGL	State Dependent Riccati Equation Guidance Law
OG	Orientation Guidance
TGH	Terminal Guidance Handover
ZEM	Zero Effort Miss
GUI	Graphical User Interface
SWIL	Software-in-the-Loop

CHAPTER 1

INTRODUCTION

1.1. Missiles Overview

In a modern military usage, a missile is a self-propelled guided weapon system, as opposed to unguided self-propelled munitions, referred to as just a rocket.[2] Depending upon the purpose, missiles can be classified under four different categories as follows.

- Surface to Air
- Surface to Surface
- Air to Surface
- Air to Air

In order to have an overview of the missiles that have been produced up to now, one may refer to [3].

In this study, missile guidance design with impact angle constraint is studied. Impact angle is important for anti-tank and anti-ship missiles. Before explanation of why these constraints refer to this type of missiles, anti-tank and anti-ship missiles are examined briefly in the following sub-sections.

1.1.1 Anti-Tank Missiles

Tanks are important assets to land forces of an army. In land warfare, they are usually supported by air forces and infantry. The schematic of a main battle tank can be seen in the picture below.[4]

Figure 1 Main Battle Tank Components

Guidance techniques that are employed in anti-tank missiles can be classified under three different categories which are as following.

- MCLOS
- SACLOS
- Fire and Forget (Homing Guidance)

Missiles' successes that use MCLOS type of guidance relies hardly upon the operator's skill. Because, the operator watches the missile flight, and uses a signaling system to command the missile back into the straight line between operator and target (LOS). [5]

In SACLOS type of guidance, target tracking is done by operator manually, however control and tracking of missile is done automatically. It is easier than MCLOS due to the fact that operator has to only track the target, not both the missile and the target.

Fire and forget types of missiles are the most advanced of all above. In this type of guidance, operator only fires the missile and there is no need for illumination or other external aids thereafter for the missile to hit the target because missile carries laser, IIR seeker or a radar seeker mounted on the nose of the missile.

An anti-tank missile which is produced by ROKETSAN Missile Industries is shown below. [6]

Figure 2 UMTAS Anti-Tank Missile

1.1.2 **Anti-Ship Missiles**

There are various types of warships classified according to their usage. A list of them can be found in [7]. A sample ship picture which is MİLGEM produced by Istanbul Military Shipyard is shown below.

Figure 3 MİLGEM Warship

Anti-ship missile guidance techniques are similar to the anti-tank missiles. The ones that are used mostly can be classified as following.

- MCLOS Guidance
- SACLOS Guidance
- Beam Riding Guidance
- Homing Guidance (Active, Semi-Active, Passive)

MCLOS and SACLOS guidance was described in the previous sub-section; hence they are not explained in this chapter.

Beam riding guidance is a form of command guidance. In this type of guidance, the target is tracked by means of an electromagnetic beam, which may be transmitted by a ground (or ship or airborne) radar or a laser tracking system (e.g., a LADAR, or laser radar). [8]

The expression homing guidance is used to describe a missile system that can sense the target by some means, and then guide itself to the target by sending commands to its own control surfaces.[8] There are three types of homing guidance. First one is active homing which means the missile illuminates and tracks the target itself without an external aid. Second one is semi-active homing in which the missile tracks the target onboard whereas the target is illuminated by sources outside of the missile (i.e., ground based illumination radar). Final one is the passive homing. In this type of guidance, missile relies on natural sources such as light or heat waves for illumination of the target where tracking is done onboard.

A sample anti-ship missile, Harpoon, produced by McDonell Douglas and Boeing Defense is displayed below.[9]

Figure 4 Harpoon Missile

1.2. Missile Flight Control System Components

A missile flight control system structure is given below.[10]

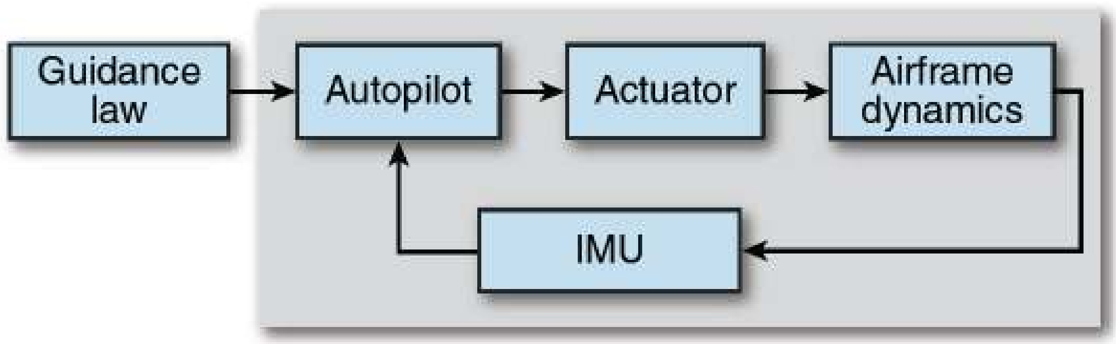

Figure 5 Missile Flight Control System

Guidance law decides the appropriate commands to be sent to autopilot in order to reach the desired destination. Autopilot receives the commands from the guidance law (i.e., acceleration) and calculates the necessary moving surface deflections ordered to the actuators. Actuators are the physical connections that transmit the commands of autopilot to the moving surfaces. Airframe responds the moving surfaces' commands by changing the position and orientation of the airframe. IMU senses these differences for each time step and sends the necessary information to the autopilot.

1.3. Motivation and Purpose of the Work

In literature, there are numerous papers that study the impact angle problem. Nonetheless, no thesis work exists that studies these algorithms extensively in a more systematic manner. Main purpose is to outline these algorithms and analyze 5 of them in a detailed manner.

1.4. Scope and Contributions of the Work

Scope of the thesis is the guidance algorithms that aim to specify the impact angle which finds application of anti-ship and anti-tank missiles. Missile is assumed to have a time constant of 0.25 sec which is modeled with a first order transfer function. However, there is a section which is devoted to the robustness analysis in order to see the effects of different time constants.

There are many simulations each of which aims to extract a specific behavior of the algorithm of interest. TGH orientation analysis, engagement field color-coded graphs and impact angle variance with respect to different target speeds are new analysis' that are not present in the literature. Another contribution is the application of a new time-to-go method [1] which is not used in the algorithms that require time-to-go information. This new time-to-go method is used in time-to-go error analysis which shows the errors induced by wrongly estimated/measured time-to-go in reality using a model from literature.[11]

1.5. Outline

Chapter 2 incorporates the literature survey which is about the guidance algorithms with impact time constraint. Chapter 3 describes and compares the guidance algorithms existing in the literature. Chapter 4 presents the simulation results. Chapter 5 includes the conclusions and future work.

CHAPTER 2

GUIDANCE WITH IMPACT ANGLE CONSTRAINT: A LITERATURE SURVEY

2.1. Constraint Definition

Impact angle of a missile to the target is of growing importance in modern warfare. For instance, in case of wars in urban areas, decreasing the collateral damage may help degrade the civilian casualties. This can be achieved with a direct vertical attack to the enemy units. Hence, achieving an impact angle of 90 degrees is of crucial importance for this case. Second case showing the importance of determining impact angle is for anti-tank missiles. Tanks have different vulnerability characteristics depending on the place where they would be hit. Hence, being able to specify the impact angle stands as a very important advantage. Another situation is the anti-ship missiles. Modern warfare ships have a variety of defenses against anti-ship missiles such as CIWS. CIWS is a naval shipboard weapon system for detecting and destroying incoming anti-ship missiles and enemy aircraft at short range.[12] Because CIWS covers some fan-shaped zone limited in range and azimuth and taking advantage of CIWS' weakness of multi-target engagement, if missiles are fired in a narrow space in azimuth, chance to destroy the target would increase dramatically. Techniques to control impact angle will be discussed in the next section.

2.2 **PN Based Impact Angle Algorithms**

PNG is probably the most popular among all of the guidance methods and vast amount of literature exists of this guidance law. Simply stating, this law tries to nullify the LOS(the line vector that connects the positions of the pursuer and the evader) rate by dictating the pursuer to rotate its velocity vector at a rate that is proportional to the rotation rate of the LOS. Simple scalar form of this law is given as :

$$a_n = NV_c \frac{d\lambda}{dt} \tag{1}$$

a_n= the commanded normal (or lateral) acceleration in ft/sec2 or m/sec2

N= the navigation constant (also known as navigation ratio, effective navigation ratio and navigation gain), a positive real number (dimensionless) usually between 3-5

Vc= the closing velocity [ft/sec] or [m/sec]

($\frac{d\lambda}{dt}$)=the LOS rate measured by the missile seeker[rad/sec]

PPN is one of the forms of proportional navigation. The pursuer issues acceleration commands perpendicular to its velocity vector. PPN is usually applicable to endo-atmospheric engagements where control forces are generated by aerodynamic lift, because we do not have control authority to realize the forward velocity requirement which is the case with TPN. In TPN, on the contrary, acceleration commands are perpendicular to instantaneous LOS. It is usually employed in exo-atmospheric missiles where acceleration commands are realized by thrust vectoring so that forward velocity component of the acceleration command can be satisfied. Neither of TPN or PPN can control the impact angle.

Another form of PN is BPN with which impact angle can be controlled. In this type of navigation, a bias term is added to the proportional navigation term where this bias term might be a function of many variables.

2.2.1 **Biased PN Based Impact Angle Algorithms for Stationary Targets**

Erer and Merttopçuoğlu [13] used Biased Pure Proportional Navigation (BPPN) to intercept stationary targets aiming to control the impact angle. In the paper, non-linear equations representing the BPPN kinematics with a stationary target are solved in closed form. After that introducing non-dimensional range and time into the non-linear equations, authors derived a stability criterion which defines the conditions that the engagement will lead to a capture. What follows is the outline of the two phase guidance scheme which uses bias action to postpone the rotating of the pursuer's velocity vector to target until the bias value is reached. After the bias value is reached, missile flies with PPN only. It is important to note that only LOS rate is required to realize this law which corresponds to ease of implementation to the actual missile.

Jeong et al.[14] proposed a so called angle constrained biased PNG (ACBPNG) law to control impact angle. The required bias angle is analytically calculated. Acceleration histories, trajectories and flight path angles of ACBPNG and conventional PNG are compared. Moreover, maneuverability, anti-detection and sensitivity to navigational errors are analyzed. In the end, simulations are carried out to see the variation of vertical distance, commanded acceleration and flight path angle with respect to initial range, initial vertical distance, impact angle and closing velocity. Authors underline the reality that this law does not guarantee optimality in any point of view.

Kim et al.[15] propose a bias shaping method based on the two-phase BPN guidance which can achieve both terminal angle constraint and look angle limitation to maintain the seeker lock-on condition with the acceleration capability being limited. Bias shaping is done on the requirement that the integral of the bias should have the required value before the interception. Law basically consists of two time-varying biases and switching logic. The method does not require time-to-go or range information, only LOS rate is required. Because of these, this law can easily be implemented on a missile with a passive seeker.

Ratnoo and Ghose [16] propose a PNG based guidance law for capturing all possible impact angles in a surface-to-surface planar engagement against a stationary target. For the initial phase, an orientation guidance scheme is proposed. After following the orientation trajectory, missile can switch over to a navigation constant N>=2 to achieve the desired impact angle. The navigation constant through the orientation phase changes according to the initial engagement geometry. Simulations are carried out for constant speed missile model and realistic missile model for which ideal and first order autopilot cases are considered.

2.2.2 **Biased PN Based Impact Angle Algorithms for Non-Stationary Targets**

Kim et al.[17] derived a guidance law based on non-linear engagement model. Usage of nonlinear kinematics made it possible to derive analytic conditions for fulfilling the guidance law. The new law is a modification of the classical PNG law which includes a time-varying bias. One important advantage of the proposed guidance law is that it does not require time to go information which may be corrupted by noise or estimation errors in reality. Moreover, by comparing an optimal linear law, it is proved that the proposed law is optimal near collision course provided that constants in the proposed law are equal to some specific integer values.

Model et al.[18] designed a guidance law named Modified angle constrained biased proportional navigation guidance (MACBPNG). MACBPNG is capable of achieving a wide range of impact angles in which the required bias term is derived in a closed form considering non-linear equations of motion (EOM). The commanded acceleration is perpendicular to LOS which means this law can be thought as a form of TPN. Bias term is updated at every iteration to get better accuracy. In the end, the law is compared with an existing law[14]. It is seen that MACBPNG has a wider launch envelope than ACBPNG.

Ratnoo and Ghose[19] improved their guidance law for non-stationary non-maneuvering targets. Similar to the former paper they released, they presented an orientation scheme for the first phase after which scheme is turned to PNG with N=3. The navigation constant used in the orientation phase depends on the initial geometry between the target and the interceptor. Simulations are carried out for constant speed and realistic interceptor models with ideal and 1^{st} order autopilot. Robustness of the law is verified with this 1^{st} order autopilot model.

Lee et al.[20] examined the effects of system lag on performance of a generalized impact-angle-control-guidance law, analytic solutions of the proposed guidance law is derived for a first order system. This analytic solution is obtained by solving a third order linear time-varying ordinary differential equation. Terminal misses due to system lag have been investigated using the analytic solutions; the effects of guidance coefficients on the terminal misses have been discussed.[20] Moreover, sensitivity of impact angle error and miss distance is analyzed with respect to impact angle and initial heading angle. Finally, analytic solutions have been compared with the linear and nonlinear simulations.

Ratnoo and Ghoose [19] improved their first algorithm for non-stationary targets. For initial phase, orientation guidance is proposed like in [19]. For the initial phase, there are additional terms like velocity ratio of target and interceptor and interceptor's flight path angle. While deriving the orientation guidance constant, zero interceptor flight path angle is assumed. A proof is also given stating that if the missile can be brought to point 3 on the orientation trajectory, any impact angle can be achieved between $-\pi$ and 0. After that, the proposed guidance law is given concisely in a well-defined manner. Up to now, constant speed missile is assumed. One more derivation is given for realistic missile model in which first order autopilot lag is assumed. Simulations are carried out for both cases.

2.3 **Optimal Control Theory Based Impact Angle Algorithms**

In some impact angle problems, optimal control theory is used to solve the constraints imposed on the problem. These problems incorporate a cost function in which the performance measure of interest exists. This measure may be time to go, altitude climbed, control effort. For instance, if cost function's parameter is acceleration effort squared[21], it is defined as below.

$$J = \int_0^{t_f} n_c^2 \, dt \tag{2}$$

After defining the cost function, it is tried to be minimized using optimal control algorithms which depend on the problem characteristics**.** The following papers present these issues.

2.3.1 Optimal Control Theory Based Impact Angle Algorithms for Stationary Targets

Kim and Grider [22] published the first paper that discusses the impact angle control problem. Two problems are defined depending on the auto-pilot lag. First problem has no autopilot lag where the nonlinear engagement kinematics is expressed in state-space form. Second problem is defined with auto-pilot lag which is also in state-space form with nonlinear variables. Cost function is expressed in terms of the input to the autopilot (fin angle) and the final states of range vector projected on the ground and body attitude angle. Optimal control is then expressed in terms of state variables with the gains changing with respect to time. Effects of "soft" and "hard" constraints on acceleration were shown. Finally, initial states for which the miss distance and attitude angle at impact are satisfactory are extracted by solving the equations backward in time.

Ryoo et al.[1] generalized optimal guidance laws specifying impact angle and zero miss distance for arbitrary missile dynamics. The optimal guidance command is represented by a linear combination of the ramp and the step responses of the missile's lateral acceleration. The guidance law is investigated for ideal autopilot and first order lag autopilot models. New time to go calculation methods are proposed considering path curvature. In the end, nonlinear and adjoint simulations are carried out and comparisons are made with biased PN law.[17] It is seen that OGL spends less control energy than BPN. Moreover, OGL has finite lateral acceleration demand as the missile approaches the target whereas BPN's demand shoots up to infinity.

Subchan [23] presents some computational results of the optimal trajectory of missile by minimizing the integrated altitude along the optimal trajectory especially to avoid increasing anti-missile capability. In order to solve this problem, author first introduced nonlinear equations of motion of a point mass moving over a flat non-rotating earth. After that, aerodynamic parameters and constraints are outlined. The motion is divided into three phases. In the 1st phase interceptor is moving steady and level. In the 2nd phase it climbs and dives into the target thereafter. Optimization problem is solved using direct collocation(for more information reader may refer to [24]) method. In the end, simulations are carried out and comments are made.

Ryoo et al.[25] proposed a new guidance law based on linear quadratic optimal control theory with terminal constraints on miss distance and impact angle for a constant speed missile against a stationary target. Cost function is weighted by a power of time-to-go. Selection of guidance gains and trajectory shaping are possible by varying the exponent of the weighting function. An important contribution of this paper is that it incorporates a new time to go calculation method. Non-linear and adjoint simulations are made and law is compared with a Biased PNG Law [17]and it is shown that performance of the new law is better than BPNG law especially in the terminal homing phase.

Yao et al.[11] derived an energy optimal guidance law aiming to minimize the control effort and the induced drag which causes velocity loss. The law composes of two terms one of which representing the proportional navigation term that ensures impact point accuracy and the other symbolizing the authority on the impact angle. It is said that the law bases on linearization and small angle assumption. However, reader cannot see a derivation or any results showing the acceleration demand of the derived law. Assuming point mass, constant missile velocity and movement in the vertical plane; authors outlined non-linear equations of motion. Using these equations, simulations are carried out for large impact angles and it is seen that both impact point and angle requirements are satisfied. This implies that the guidance law derived using small angle assumption also works for the large angle cases. Finally, the error analysis by adding some terms on time to go equation which is assumed that it is calculated by range over closing velocity is done. It turns out to be so that the closer the interceptor to the target the less the error is calculated.

Lee et al.[26] try to find the feasible set of weighting functions that lead to analytical forms of weighted guidance laws. Firstly, a cost function is introduced. In the cost function, there exists an acceleration term squared and a weighting function. The problem is then started to be solved with linear engagement kinematics. After that using the Schwarz's inequality, an optimal acceleration command is derived. This term includes the weighting function term which is trying to be shaped. A proof is given saying that any weighting function can provide the analytical form of optimal solution if up to triple integrations of the inverse of the weighting functions are analytically given. This is the most important output of this work. In the end of the paper, using two sample weighting functions acceleration demands are derived.

Ratnoo and Ghose[27] solve the impact angle constrained guidance problem against a stationary target using the SDRE technique. Firstly, nonlinear engagement kinematics is outlined and state matrices are formed. Cost function Q is assumed to be a function of time to go to include the target information in the guidance logic. After that, an acceleration command is derived. An important thing to note here is that constant speed assumption is used in the development process. However, in simulation studies, realistic interceptor model is used with the corresponding aerodynamic properties. The effect of initial firing angle, impact angle and effect of guidance parameter N is studied while the other variables being the same in each simulation. In the end, robustness is studied with respect to autopilot lags and it is seen that the proposed law shows very low errors for first order delays up to 0.5 seconds.

Park et al.[28] propose a new optimal guidance law considering seeker's Field of View (FOV) limits for a missile with a strapdown seeker. The strapdown seeker has a narrower FOV than that of a gimbaled seeker; hence designer must ensure the FOV limitations of the missile are not violated during the engagement. In the beginning of the paper, problem formulation is outlined in which constraints and state equations are given. After that, using Hamiltonian equations, optimal acceleration commands are derived for initial, midcourse and final phases. In the end, comparison is made with other existing guidance laws and it is seen that proposed law is more efficient in terms of control energy.

Lee et al.[29] derived closed-form solutions of an optimal impact-angle-control guidance against a stationary target for a first-order lag system. First order missile with constant speed and small flight path angle assumption is made. Based on these assumptions, mathematical problem is solved by introducing a third order linear time varying ordinary differential equation. Linear and nonlinear simulations are performed and the results of them are compared with the analytic solution.

2.3.2 Optimal Control Theory Based Impact Angle Algorithms for Non-Stationary Targets

Savkin et al.[30] outlined precision missile guidance problem where the successful intercept criterion has been defined in terms of both minimizing the miss distance and controlling the missile body attitude with respect to target at the terminal point. Kinematics are formulated in matrix form, then standard LQR approach and H^{∞} formulations (both in state feedback and output feedback form) were used to derive the optimal control command. Sinusoidal form of maneuvering target model is considered. It has been shown that H^{∞} control theory if suitably modified stands as a powerful tool to solve the precision missile guidance problem.

Ohlmeyer and Phillips[31] propose a new guidance law called generalized vector explicit guidance (GENEX). Aim of the law is to specify the final missile target relative orientation called impact angle and make the miss distance zero. A cost function in terms of time to go and demanded acceleration is introduced with a weighting factor “n”. Afterwards, using Hamiltonian equations, an acceleration demand term is derived and the results are applied to proportional navigation. Since proportional navigation does not specify any final orientation, one more derivation is done in order to include the impact angle. An advantage of this law is that it is in vector form which means one can apply this law to 3-dimensional problems. Authors also reduced the problem to 2-D problem to illustrate the law in single plane. In the end, simulations are carried out for two different scenarios. As a future work, authors suggested applying this law to higher fidelity weapon models incorporating 6-DOF dynamics, nonlinear and coupled aerodynamics, and detailed autopilot descriptions.

A new precision guidance law with impact angle constraint for 2-D planar engagement case is outlined by Manchester and Savkin[32]. In this method, it is proposed that at every point in space, a different “desired circular path” exists. It is derived assuming two sets of information, one being restricted than other. For each set, a different law outcomes. It is compared with a BPNG law in the literature[17] via simulations for the cases with a limited and unlimited missile acceleration capability. It is seen that in terms of target speed and the desired impact angle, proposed law has a wider envelope than that of BPNG. One important advantage of the proposed law is that it does not require range to target information where all other impact-angle constrained guidance laws of which the authors are aware require. Final thing that should be noted is that this law does not claim any optimality in the sense of acceleration energy where BPNG is nearly optimal in this sense when the missile starts to close to the collision course.

In this paper, Yoon[33] introduced a circular reference curve on a moving frame fixed to the target. Using the Frenet formulas, RCNG law for the impact angle control problem is developed. It is theoretically shown that the proposed law can solve the impact angle control problem for virtually any initial arrangement of pursuer and target and any desired impact angle. Moreover, a bound of impact angle errors under the RCNG law was derived. The proposed law is compared with [32] and [17]. The 3-D version of this law is available.[34]

CHAPTER 3

GUIDANCE ALGORITHMS MATHEMATICAL ANALYSIS

Some of the guidance laws outlined in previous chapter will be discussed and analyzed in more detail in this chapter. In all laws, 2-D engagement will be assumed. Following engagement geometry for stationary targets and non-stationary targets will be employed respectively.

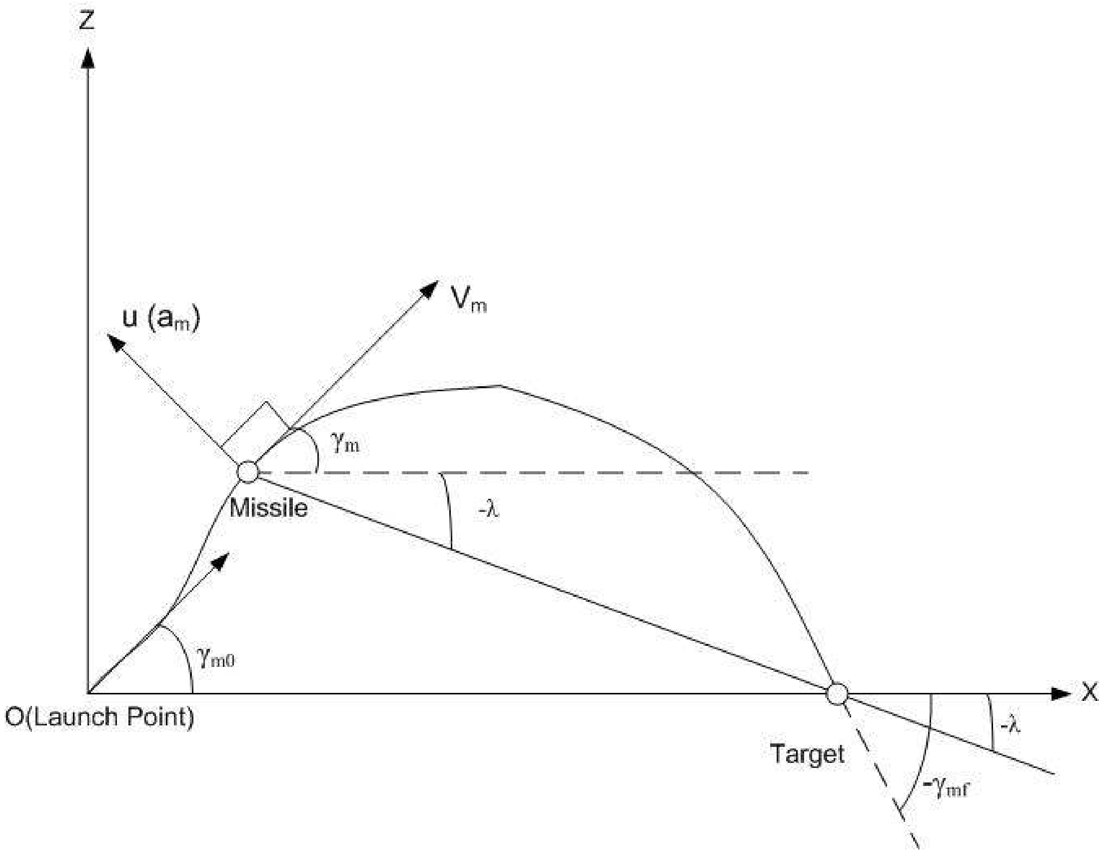

Figure 6 Engagement Schematic for Stationary Target

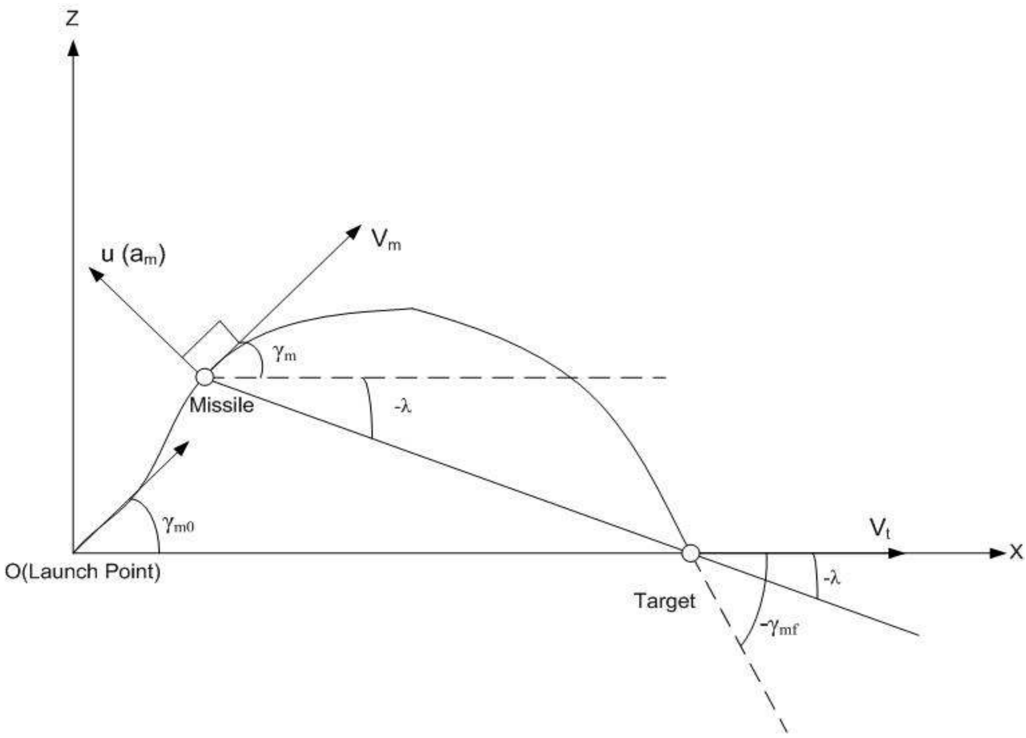

Figure 7 Engagement Schematic for a Non Stationary Target

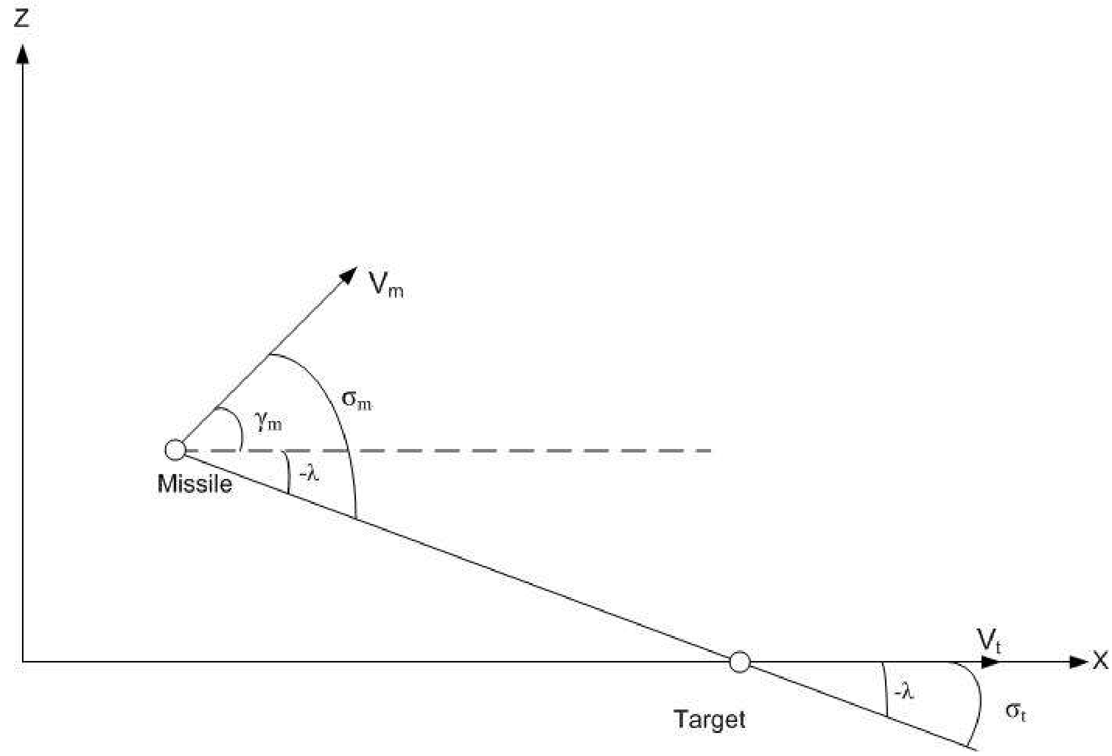

Figure 8 Engagement Schematic (refined)

3.1 PNG Algorithms Detailed Analysis

PNG without a bias term cannot control the impact angle. Hence, bias is added to the PNG algorithms generally to gain the freedom to specify the impact angle before the engagement. There are some algorithms developed in the literature to this end. They differ in the sense of choosing the bias and shaping the bias during the engagement. One may take the seeker gimbal angle limits, physical acceleration limits, fin actuator rates etc. into account while shaping the bias.

3.1.1 PNG Characteristics without A Bias Term

In this thesis, planar interception problem is studied. Hence, 3-D PNG law will not be explained here. Interested readers may refer to [35] for a complete 3-D PNG law derivation.

As stated in the previous section, there are two main forms of PNG law. One is true proportional navigation guidance and the other is pure proportional navigation guidance. Neither of these two laws can control the impact angle of which the interceptor missile hits the target. Hence, the impact angle is arbitrary in these laws. However, it is useful to investigate the characteristics of PNG law. Because, some forms of optimal control based guidance laws and all forms of biased PNG laws make use of some of the properties of PNG laws, especially the navigation constant plays an important role. Not all navigation constants result in a satisfactory performance in terms of miss distance. The main problem is the saturation of the commanded acceleration in the final moments. For navigation constants N≥2, there exists finite commanded acceleration near the interception.[8] Thus, one must choose a navigation constant equal to or greater than 2 in order to achieve the intercept.

In TPNG or PPNG, there exists a navigation constant that is optimal in terms of energy spent. The cost function is described as[36]:

$$J = \frac{1}{2} C y^2(t_f) + \int_0^{t_f} (a_m{}^2(t))dt \tag{3}$$

The optimal control problem aims to find a_m that minimizes the functional (3). For engagement schematic used in this thesis y can be replaced by z which is altitude. Using optimal control techniques, the solution comes out to be[36]:

$$a_m(t) = \frac{3\tau}{{}^3/_C + \tau^3}(z(t) + \dot{z}(t)\tau) \tag{4}$$

In order to have zero miss distance, C must go to infinity. Thus, optimal guidance law becomes:

$$a_m(t) = \frac{3}{\tau^2}(z(t) + \dot{z}(t)\tau) \tag{5}$$

If linear approximation is used,

$$\lambda = {}^z/_R \text{ where } R \cong V_{cl}\tau \tag{6}$$

Taking the derivative of (6);

$$\dot{\lambda}(t) = \frac{\dot{z}(t)r(t) + z(t)V_{cl}}{r^2} = \frac{\dot{z}(t)\tau + z(t)}{V_{cl}\tau^2} \tag{7}$$

Inserting (7) to (5);

$$a_m(t) = 3V_{cl}\dot{\lambda}(t) \tag{8}$$

Equation (8) is analogous to equation (1) in which N is replaced by 3. This means that optimal navigation gain in PNG laws is 3 in the sense of energy used. It is important to note that when the navigation gain is higher than 3, heading error which is defined as the angle deviation from the collision course can be removed more quickly than that with 3. However, in that case the effects of guidance noise associated with $\dot{\lambda}(t)$ becomes more significant.[8]

3.2 **Biased PNG Algorithms Detailed Analysis**

Bias is added to the PNG algorithms generally to gain the freedom to specify the impact angle before the engagement. There are some algorithms developed in the literature to this end. They differ in the sense of choosing the bias and shaping the bias during the engagement. One may take the seeker gimbal angle limits, physical acceleration limits, fin actuator rates etc. into account while shaping the bias.

3.2.1 **Indirect Impact-Angle-Control Against Stationary Targets Using Biased Pure Proportional Navigation(IACBPPN)**[13]

Erer and Merttopçuoğlu's paper [13] can be summarized as following.

$$a_c = V_m \dot{\gamma}_m \tag{9}$$

To control the impact angle, one may add a bias term as following;

$$\dot{\gamma}_m = N\dot{\lambda} + b \tag{10}$$

Plugging equation (10) into (9), one may get;

$$a_c = V_m(N\dot{\lambda} + bias) \tag{11}$$

If ideal autopilot is assumed, commanded acceleration (a_c) is equal to missile acceleration (a_m).

Look angle should be zero at the instant of impact to have the desired impact angle. Thus, integrating equation (11) and setting $-\lambda_f = -\gamma_m$ yields the following:

$$\gamma_f = \frac{N\lambda_i - \gamma_{m0} - \int_{t_i}^{t_f} bdt}{N - 1} \tag{12}$$

In order to have the desired impact angle γ_d, the bias profile should be selected accordingly. This profile can be anything including intervals of zero value. However, a systematic approach should be taken to satisfy the desired impact angle. Two different approaches are proposed. First approach which is more convenient is as follows.

Bias is applied till the value γ_f is equal to desired impact angle. The missile flies with PPN thereafter. The bias application time should be less than total engagement time, hence setting it to range over closing velocity (or missile velocity) guarantees this. Moreover, setting γ_f to γ_d , equation (12) can be manipulated to find the initial bias value as follows.

$$b_i = \frac{N\lambda_i - \gamma_{m0} - (N-1)\gamma_d}{{r_i}/{v_i}} \tag{13}$$

In order to eliminate the adverse effects of velocity change, velocity weighting is proposed as following:

$$b = b_i * \frac{v}{v_i} \tag{14}$$

Second approach is to use a full biasing tactic until the impact. This is not a realistic choice since the successful bias value can be only found by trial and error.

3.2.2 Bias Shaping Method for Biased Proportional Navigation with Terminal Impact Angle Constraint(BSBPN)[15]

In two phase guidance schemes proposed, in both [13], [15] only LOS rate information is required which enables these guidance laws' application to passive homing missiles. However, in these papers, acceleration capabilities and look angle limits of the missile are not included in bias design.

BPN guidance can be simply stated as:

$$a_c = V_m(N\dot{\lambda}_m + bias) \tag{15}$$

where $\dot{\gamma}_m = N\dot{\lambda}_m + bias$

Integrating $\dot{\gamma}_m$;

$$\gamma(t) = \gamma_{m0} + N\lambda(t) + \int_0^t b\, dt \tag{16}$$

In the case of successful interception of the target with the desired impact angle, look angle is zero. In this case $\gamma_m = \lambda_m$. Then one can have;

$$\int_0^{t_f} b dt = (1 - N)\gamma_{mf} - \gamma_{m0} \tag{17}$$

Up to this point, Erer and Merttopçuoğlu's paper[13] was summarized. In this paper[15], a different bias shaping method is proposed which can provide a continuous guidance command near the target as well as satisfy the look-angle limit to maintain the seeker lock-on condition. In this paper, angle of attack is considered to be small, hence look angle is equal to gimbal angle.

Proposed bias shaping method can be summarized with the following figure. [15]

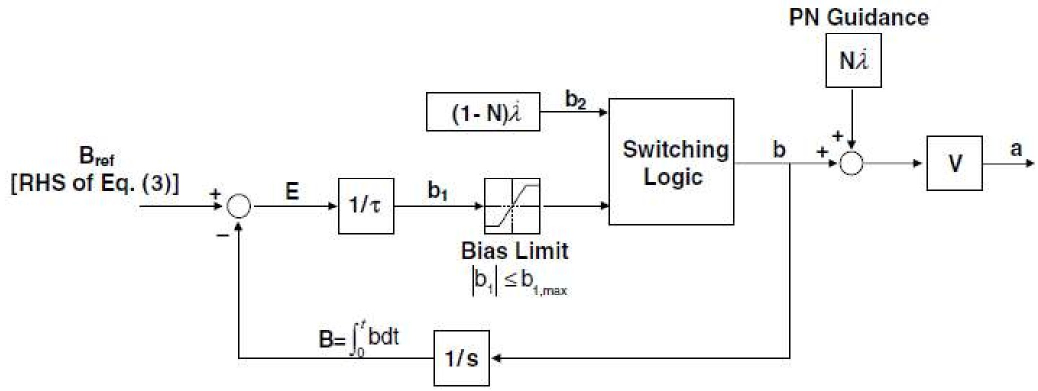

Figure 9 Bias Switching Logic

In the figure above, RHS of equation (3) is actually equation (17) in this thesis. The first, b_1, is the time varying bias calculated by the difference between the required integral value, $Bref = (1 - N)\gamma_f - \gamma_0$, and the integral of bias, B. The second time-varying bias, b_2, is to maintain the constant look (gimbal) angle, which is used if the look angle approaches the maximum look-angle limit σ_{max}. The switching logic is to decide which one of the two biases is used to generate the guidance command. In order to understand the concept better, two different cases are outlined.

Case 1: Assume $0 < \sigma_0 < \sigma_{max}$ for the initial moment and look angle (gimbal angle) does not violate the limits of gimbal angle. For this case, $b=b_1$ and is exponentially varied as:

$$b(t) = \frac{B_{ref}}{\tau} e^{\frac{-t}{\tau}} \tag{18}$$

Taking the integral:

$$B(t) = \int_0^t b dt = (1 - e^{\frac{-t}{\tau}}) B_{ref} \tag{19}$$

In order to satisfy the impact angle constraint, B should reach B_{ref} before the interception of the target, thus τ should be sufficiently small. It is important to note that; if $\tau \leq \frac{r_0}{7v}$, $B \cong 0.999B_{ref}$for $t \geq 7\tau$ since the length of the curved trajectory for the impact angle control is larger than the straight line which is initial range r_0. Another aspect is that one should put a bound on b_1 to keep the guidance command within the acceleration limit a_{max} because a large bias may be produced owing to the difference between B and B_{ref} in the initial homing phase. Hence $b_{1,max} = \frac{a_{max}}{V}$ is implemented.

Case 2: Being same with the Case 1, $0 < \sigma_0 < \sigma_{max}$ for launching moment however for this case, $|\sigma| > \sigma_{max}$ occur at a time during engagement. This means that desired impact angle is greater than that of case 1. For this case, $b = b_1$is initially used. However, when $|\sigma| > \sigma_{max}$ occurs, bias is switched to $b = b_2 = (1 - N)\dot{\lambda}$ to maintain maximum look angle. In this case, look angle rate is zero as:

$$\dot{\sigma} = \dot{\gamma} - \dot{\lambda} = N\dot{\lambda} + b_2 - \dot{\lambda} = 0 \tag{20}$$

and the LOS rate is:

$$\dot{\lambda} = \frac{-V}{R} \sin \sigma_{max} < 0 \; for \; \sigma_{max} \in (0, \frac{\pi}{2}) \tag{21}$$

During this phase, look angle is held constant at its maximum value and the guidance command is $a = V\dot{\lambda}$ identical to PN with N=1.

As the missile approaches the target, $b_2$with $N \geq 2$ gradually increases due to an increase in $|\dot{\lambda}|$ given in equation (21) while $b_1 \to 0$ because $B \to B_{ref}$. Bias is no longer needed if B is equal to B_{ref}. Hence, it is necessary to switch back to b_1 when $|b_1| \leq |b_2|$ to satisfy the desired impact angle and avoid an instantaneous acceleration change. To summarize the proposed law;

$$b = \begin{cases} b_1 \;\; for \; initial \; phase \; of \; engagement \\ b_2 \; if \; \sigma(t) \geq \sigma_{max} \\ b_1 \; if \; |b_1| \leq |b_2| \; and \; until \; interception \end{cases} \tag{22}$$

Equation (22) means the guidance algorithms has 3 modes. 1st mode will increase the look angle to gimbal angle limits. 2nd mode will maintain the maximum look angle and 3rd mode will enable to intercept the target with the desired impact angle while look angle is going essentially to zero.

3.2.3 **Orientation Guidance (OG)** [19]

Recalling simple PNG law;

$$\dot{\gamma}_m = N\dot{\lambda} \tag{23}$$

Integrating the equation above,

$$\frac{\gamma_{mf} - \gamma_{m0}}{\lambda_f - \lambda_0} = N \tag{24}$$

For interception, the target and interceptor velocity components normal to the line of sight should be equal, that is,

$$V_m \sin(\gamma_{mf} - \lambda_f) = V_t \sin(\gamma_t - \lambda_f) \tag{25}$$

From this equation, one can extract $\lambda_f$as following:

$$\lambda_f = \tan^{-1}\left[\frac{\sin\gamma_{mf} - \beta\sin\gamma_t}{\cos\gamma_{mf} - \beta\cos\gamma_t}\right] \tag{26}$$

where β represents target to interceptor velocity ratio. Plugging (26) into (24) one can have;

$$N = (\gamma_{mf} - \gamma_0)/\left(\tan^{-1}\left[\frac{\sin\gamma_{mf} - \beta\sin\gamma_t}{\cos\gamma_{mf} - \beta\cos\gamma_t}\right] - \lambda_0\right) \tag{27}$$

After a set of algebraic operations, impact angle set using PN guidance only is as following:

$$\gamma_f \in [\,\gamma_{mf}{}^* \quad \lambda_0 + \sin^{-1}(-\beta\sin\lambda_0)\,] \quad N \geq 3 \tag{28}$$

where $\gamma_{mf}{}^*$ is the solution of the case where $N = 3$.

For all impact angles outside the range given by equation (28), authors propose an orientation guidance algorithm. It states that for all impact angles outside the given range, interceptor follows an orientation trajectory until the following relation becomes equal to 3;

$$N = (\gamma_{mf} - \gamma) / \left(\tan^{-1} \left[\frac{\sin \gamma_{mf} - \beta \sin \gamma_t}{\cos \gamma_{mf} - \beta \cos \gamma_t} \right] - \lambda \right) \tag{29}$$

After that, the interceptor follows PN guidance with N=3. The detailed proof is given in the paper.

The question is to find the orientation guidance command constant which drives the interceptor to end of the orientation trajectory. If the desired impact angle is –π , the interceptor should reach point 3 in the orientation trajectory. In this case with $\alpha_t = 0$ and $\gamma_{mf} = -\pi$, equation (26) gives the result $\lambda_f = -\pi$. Substituting these values into equation (29), we have at point 3,

$$\frac{-\pi - \gamma_m}{-\pi - \lambda} = 3 \quad \gg \quad \gamma_m = 2\pi + 3\lambda \tag{30}$$

If λ is selected to be 0, γ_m becomes $-2\pi/3$. To take the interceptor from point 1 to point 3 on the orientation trajectory, using equation (24) we have;

$$N = \frac{\gamma_{m0} - 0}{0 - (-2\pi/3)} = \frac{3\gamma_{m0}}{2\pi} \tag{31}$$

Therefore, the acceleration command is:

$$a_m = \frac{3\gamma_{m0}}{2\pi} * V_m * \dot{\lambda} \tag{32}$$

The proposed guidance law can be concisely stated as:

$$a_m = N * V_m * \dot{\lambda} \tag{33}$$

For engagement geometries with;

$$\frac{\gamma_{mf} - \gamma_0}{\lambda_f - \lambda_0} \geq 3$$

$$\text{Guidance parameter N:} \tag{34}$$

$$N = \frac{\gamma_{mf} - \gamma_0}{\lambda_f - \lambda_0}$$

For engagement geometries with:

$$\frac{\gamma_{mf} - \gamma_0}{\lambda_f - \lambda_0} < 3$$

Guidance parameter N:

$$N = \frac{3\gamma_{m0}}{2\pi} \quad if\ t < t_s \tag{35}$$

$$N = 3\ if\ t \geq t_s$$

T_s is the switching time when the value of expression $\frac{\gamma_{mf}-\gamma}{\lambda_f-\lambda}$ increases to 3.

For realistic interceptor a different law is proposed based on the same algorithm. It assumes the guidance loop is closed after the boost phase is over. Thus, equation (31) is modified as:

$$N = \frac{-0 - \gamma_{mglc}}{(-2\pi/3) - \lambda_{glc}} = \frac{\gamma_{mglc}}{2\pi/_3 + \lambda_{glc}} \tag{36}$$

γ_{mglc} and λ_{glc} represent the interceptor heading and the line of sight angle at the instant of guidance loop closure(GLC).

Eqaution (26) shows that for a prescribed impact angle value γ_{mf} the value $\lambda_f$varies with the interceptor speed. Hence, for realistic missile model case, the value $\frac{\gamma_{mf}-\gamma}{\lambda_f-\lambda}$ might deviate from the switching value as the interceptor speed changes and may fall below the acceptable guidance parameter limit $2(1+\beta)$. There is an extrat term for gravity compensation which will not be considered since gravity is neglected in the simulations in this thesis. The new law can be stated as below.

For engagement geometries with;

$$\frac{\gamma_{mf} - \gamma_0}{\lambda_f - \lambda_0} \geq 3$$

Guidance parameter N: (37)

$$N = \frac{\gamma_{mf} - \gamma}{\lambda_f - \lambda}$$

For engagement geometries with:

$$\frac{\gamma_{mf} - \gamma_0}{\lambda_f - \lambda_0} < 3$$

Guidance parameter N:

$$N = \frac{\gamma_{mglc}}{2\pi/_3 + \lambda_{glc}} \;\; if \; \frac{\gamma_{mf} - \gamma_m}{\lambda_f - \lambda} < 3, t < t_s$$

$$N = 3 \; if \; \frac{\gamma_{mf} - \gamma_m}{\lambda_f - \lambda} > 2(1+\beta), t > t_s, \tag{38}$$

$$N = 2(1+\beta) \; if \; \frac{\gamma_{mf} - \gamma_m}{\lambda_f - \lambda} \leq 2(1+\beta), t > t_s$$

3.3 Optimal Control Theory Based Algorithms Detailed Analysis

3.3.1 Generalized Vector Explicit Guidance(GENEX)[31]

To start, define a set of linear state equations and boundary conditions as follows:

$$\dot{\hat{X}} = A\hat{X} + \hat{b}u \tag{39}$$

$$\hat{X}(t_0) = X_0 \;\; \hat{X}(t_f) = X_f = 0 \tag{40}$$

where **X** is state, u is the control and $\hat{b}$ may be time varying. Introducing a cost function of the form:

$$Q = \int_0^{T_0} \frac{u^2}{2T^n} dT = \int_0^{T_0} L(u,T) dT \tag{41}$$

where $T = T_f - T$ and n is an integer ≥ 0 .

Using Hamiltonian and the minimum principle of Pontryagin an optimal acceleration command is derived and it is shown below:

$$u^* = -(Mb)^T Q^{-1} MXT^n \tag{42}$$

In this formulation M is the fundamental matrix whose definition is given below.

$$\frac{dm}{dT} = MA, \quad M(T=0) = I \tag{43}$$

In order to illustrate the usage of these results, proportional navigation law is considered. Define the lateral separation between the missile and its final point as following:

$$z = z_f - z_m \tag{44}$$

The state is chosen to be zero effort miss(ZEM) which is defined as the distance the missile would miss the target if the target continued along its present course and the missile made no further corrective maneuvers.[21]

The equation for ZEM is:

$$e = z_f - z_m - \dot{z}_m T \tag{45}$$

Taking the derivative of equation (17) gives:

$$\dot{e} = -\dot{z}_m - \ddot{z}_m T - \dot{z}_m \dot{T} = -\ddot{z}_m T \tag{46}$$

because $\dot{T} = -1$. The control is chosen to be the missile acceleration. The equation is transformed into the form of $\dot{\hat{X}} = A\hat{X} + \hat{b}u$ as follows:

$$\dot{\hat{X}} = -uT, \qquad X(0) = X_0\,, \quad X_f = 0 \tag{47}$$

In this equation, it can easily be seen that A=0 and b=-T. Using the definition of the fundamental matrix in equation (43) and cost function in equation (41), cost function comes out to be :

$$Q = \int_0^T T^{n+2}\, dT = \frac{T^{n+3}}{n+3} \tag{48}$$

Substituting equation (48) into equation (42) gives:

$$u^* = T\left[\frac{n+3}{T^{n+3}}\right] X T^n = \left[\frac{n+3}{T^2}\right] X \tag{49}$$

Optimal acceleration command is derived as a function of the state ZEM, weight n and time to go. However, there is no specification up to now for impact angle that may be redefined as final velocity orientation since target is stationary. In order to include that, second state is added which is the difference between current velocity and desired final velocity. It is defined as:

$$X_2 = v = \dot{z}_f - \dot{z}_m \tag{50}$$

where derivatives of states are defined as:

$$\dot{z} = uT \tag{51}$$

$$\dot{v} = -u \tag{52}$$

The matrix form then comes out to be:

$$\begin{bmatrix} \dot{z} \\ \dot{v} \end{bmatrix} = \begin{bmatrix} 0 & 0 \\ 0 & 0 \end{bmatrix} \begin{bmatrix} z \\ v \end{bmatrix} + \begin{bmatrix} -T \\ -1 \end{bmatrix} u \quad (53)$$

Constructing the optimal acceleration command using the same procedure illustrated above, the command is:

$$u^* = 1/T^2[K_1(z_f - z_m - \dot{z_m}T) + K_2(\dot{z_f} - \dot{z_m})T] \quad (54)$$

where *K1=(n+2)(n+3)* and *K2=-(n+1)(n+2)*

So far the command is written for z-axis. It can be assumed that the same procedure is applicable for x-coordinate as well, moreover time to go term can be approximated as range over closing velocity.

$$u = \frac{1}{T^2}[K_1(\hat{R}_f - \hat{R}_m - \hat{V}_m T) + K_2(\hat{v}_f - \hat{v}_m)T] \quad (55)$$

Setting the following parameters;

$$R_f - R_m = R\hat{r} \qquad V_m = V\hat{v} \qquad V_f = V\hat{v}_f \qquad T = R/V \quad (56)$$

Missile is guided to predicted intercept point in this algorithm; hence V also represents the average closing speed to that point. Substituting (40) into (39);

$$\hat{u} = 1/T^2[K_1(R\hat{r} - VT\hat{v}) + K_2VT(\hat{v}_f - \hat{v})] \quad (57)$$

Because $VT = R$, one can have;

$$u = \frac{V^2}{R}[K_1(\hat{r} - \hat{v}) + K_2(\hat{v}_f - \hat{v})] \quad (58)$$

Since the vehicle of interest is an endo-atmospheric missile, one can assume that it has no longitudinal control capability. Thus, the component of **u** normal to velocity vector **v** can be modified as:

$$u_\perp = \frac{V^2}{R}[K_1(\hat{r} - \hat{v}\cos(\gamma_m - \lambda)) + K_2(\hat{v}_f - \hat{v}\cos(\gamma_m - \gamma_{mf}))] \quad (59)$$

Above case is for 3-dimensional case. If the case is planar engagement which is the situation dealt with in this thesis, a reconstruction in the formula above is essential. The detailed analysis is in [30], the result becomes the following:

$$u_\perp = \frac{V^2}{R}[-K_1\sin(\gamma_m - \lambda_m) - K_2\sin(\gamma_m - \gamma_{mf})] \quad (60)$$

3.3.2 **State Dependent Riccati Equation Based Guidance Law for Impact Angle Constrained Trajectories(SDREGL)**[27]

It is important to define the states which are to be regulated. Using the engagement geometry in Figure **6**, states are chosen to be z and γ_m. Nonlinear system dynamics can then be represented as:

$$\dot{z} = V_m \sin\gamma_m \tag{61}$$

$$\dot{\gamma}_m = \frac{a_m}{V_m} \tag{62}$$

Since the problem is formulated as a regulator problem, both states should go to zero. This means the objective is to hit the target with zero impact angle. Later, it will be seen how to generalize it to other impact angles.

Showing the state vector as below:

$$x = \begin{bmatrix} z \\ \gamma_m \end{bmatrix} \tag{63}$$

State dependent coefficient (SDC) form of equations is given as:

$$\dot{x} = A(x)x + Bu \tag{64}$$

Converting equations (42) and (43) into SDC form of (45), one can have:

$$\dot{z} = V_m(\frac{\sin\gamma_m}{\gamma_m})\,\gamma_m \tag{65}$$

$$\dot{\gamma}_m = \frac{a_m}{V_m} \tag{66}$$

From equations (42-46);

$$A(x) = \begin{bmatrix} 0 & \dfrac{v_m \sin\gamma_m}{\gamma_m} \\ 0 & 0 \end{bmatrix} \tag{67}$$

$$B = \begin{bmatrix} 0 \\ \dfrac{1}{V_m} \end{bmatrix} \tag{68}$$

Since the final time is not known, one should consider an infinite-horizon type non-linear regulator problem as following:

$$J = \frac{1}{2}\int_{t_0}^{\infty} [x^T Q x + R u^2(t)]dt \tag{69}$$

In the equation above, R is scalar since we have one control which is a_m. Q is a 2x2 matrix. It is important to note here that Q must be a function of time to go in order to include the target information in the guidance law. Let Q be of the form:

$$Q = \begin{bmatrix} {q_1}^2 & 0 \\ 0 & {q_2}^2 \end{bmatrix} \tag{70}$$

In order to check whether the SDRE solution is asymptotically stable, 5 conditions must be met.[27] After stability analysis which can be observed in the corresponding paper, it came out to be so that the SDRE solution is asymptotically stable.

One must solve the algebraic state-dependent Riccati equation to find the P matrix which exists in the SDRE control solution that is defined as:

$$u^* = -B^T P(x) x \tag{71}$$

Algebraic state dependent Riccati equation is defined as:

$$A^T(x)P(x) + P(x)A(x) - P(x)BR^{-1}B^T P(x) + Q = 0 \tag{72}$$

where *P(x)* is defined as :

$$P(x) = \begin{bmatrix} p_{11} & p_{12} \\ p_{21} & p_{22} \end{bmatrix} \tag{73}$$

Solving equation (72) yields:

$$\begin{gathered} p_{11} = q_1 \frac{\gamma_m}{V_m \sin\gamma_m} \sqrt{{q_2}^2 + 2q_1{v_m}^2 \frac{\sin\gamma_m}{\gamma_m}} \\ p_{12} = q_1 v_m \\ p_{22} = v_m \sqrt{{q_2}^2 + 2q_1{v_m}^2 \frac{\sin\gamma_m}{\gamma_m}} \end{gathered} \tag{74}$$

Optimal command is then derived as :

$$u^* = \left(-q_1 z + \sqrt{{q_2}^2 + 2q_1{v_m}^2 \frac{\sin\gamma_m}{\gamma_m}} \gamma_m \right) \tag{75}$$

Since the value of γ_m in intermediate steps is out of interest, q_2 is set to zero.

On the other hand, z should be controlled tightly for successful interception. Let q_1 a function of time to go as following:

$$q_1 = \left\{ \frac{N}{t_{go}} \right\}^2 \tag{76}$$

Using (57) in (56); one can get the control command as:

$$u^* = -\left\{\left(\frac{N}{t_{go}}\right)^2 z + \frac{\sqrt{2}NV_m}{t_{go}}\sqrt{\frac{\sin\gamma_m}{\gamma_m}}\gamma_m\right\} \tag{77}$$

Geometrically;

$$z = R\sin(-\lambda) \tag{78}$$

Plugging (78) into (77);

$$u^* = -\left\{\left(\frac{N}{t_{go}}\right)^2 R\sin(-\lambda) + \frac{\sqrt{2}NV_m}{t_{go}}\sqrt{\frac{\sin\gamma_m}{\gamma_m}}\gamma_m\right\} \tag{79}$$

In this equation, there exists a time-to-go term. Typically, time-to-go term is calculated as following:

$$t_{go} = \frac{R}{V_{ref}} \tag{80}$$

V_{ref} term usually refers to closing velocity. However, for some engagements with high heading error the closing velocity may be zero or even negative thus resulting in a bad time to go estimation. To avoid this, following logic is employed.

$$v_{ref} = \begin{cases} V_c \; if \; V_c > \dfrac{V_m}{2} \\ \dfrac{V_m}{2} \; if \; V_c \leq \dfrac{V_m}{2} \end{cases} \tag{81}$$

The guidance command in equation (79) was derived for regulator solution which drives both states to zero, resulting in zero impact angle. In order to generalize this to other impact angles, the frame of reference is rotated by an amount γ_{mf} about the origin. This rotation schematic is given below. (Note that notations in the schematic are adapted from paper and is not consistent with the notations of this thesis)

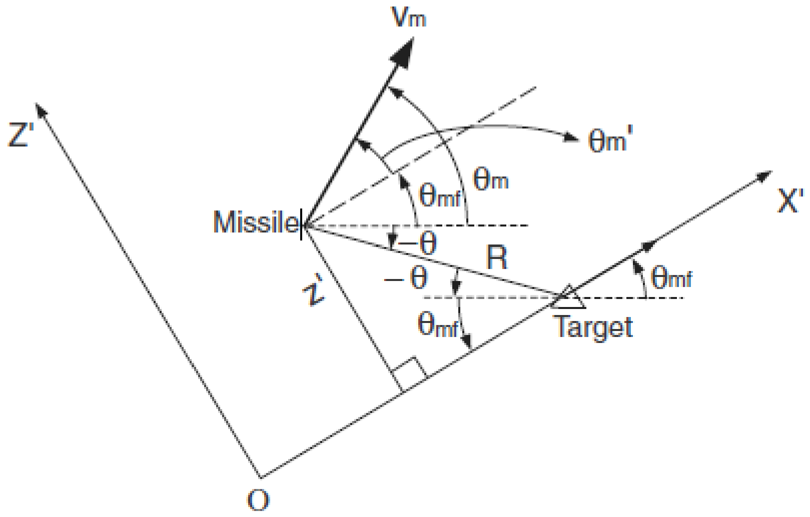

Figure 10 New Reference Frame for SDREGL

In this new frame, missile cross-range z' and heading $\gamma_m'(\theta_m' \; in \; paper \; notation)$ values are calculated as:

$$z' = R\sin(\gamma_{mf} - \lambda)$$
$$\gamma_m' = \gamma_m - \gamma_{mf} \tag{82}$$

Using equations (82) in (79) and adding gravity compensation term, the acceleration command is derived as:

$$u^* = -\left\{\left(\frac{N}{t_{go}}\right)^2 R\sin\left(\gamma_{mf} - \lambda\right) + \frac{\sqrt{2}NV_m}{t_{go}}\sqrt{\frac{\sin(\gamma_m - \gamma_{mf})}{\gamma_m - \gamma_{mf}}}(\gamma_m - \gamma_{mf})\right\} \tag{83}$$
$$+ g\cos\gamma_m$$

CHAPTER 4

SIMULATION

In this section, guidance algorithms that have been investigated in detail in previous chapter are compared according to various aspects. Simulations are run in different conditions some of which are not included in the papers presented. In all simulations, missile speed is assumed to be constant. This actually represents the terminal phase engagement conditions. Midcourse and initial phases are out of scope of this thesis.

The miss distance is calculated when the range rate changes sign (or range rate becomes positive) which means missile got immediate vicinity of the target and started to go away from the target.

All simulation are for planar engagement and bases on point mass assumption.

An important note is the time step of the simulations. It is specified as 10 mili-seconds due to computational speed considerations. This would result in fluctuations in some graphs (i.e. miss distance values in robustness analysis) and variations in miss distance values in the order of 2.5 meters since the speed of the missile is 250 m/sec.

Gravity is neglected in all runs. However, if reader wants to see the effect of gravity, he/she can refer to sections 4.1.1.1 and 4.2.1.1.

4.1 Stationary Target

In this subsection, target is assumed to be stationary. Simulations are carried out for each algorithm outlined in the previous section and results are shown.

4.1.1 Run Type I

IACBPPN, BSBPN and SDREGL are all derived for stationary targets. Hence one should expect them to show satisfactory performance for this case. GENEX and OG are designed both for stationary and non-stationary cases. Thus, no problem should occur with them. A typical scenario for an anti-tank missile should have the following parameters.

Table 1 Scenario I Run I Parameters

Parameters	Values
Missile Initial Position	(3000,500)
Target Position	(5000,0)
Missile Initial Velocity	250 m/s
Missile Initial Orientation	+15 degrees
Gravity	Neglected
Desired Impact Angle	-45 degrees
Acceleration Limits	+7g/-7g

In IACBPPN, two phase bias application mode is used. In GENEX, design parameter N is taken to be 1.

In BSBPN, gimbal limit is taken to be 25 degrees. In this run set, initial look angle is 29 degrees which is higher than the allowable gimbal angle. Hence it is assumed that guidance law starts with mode 2 in which the look angle, 29 degrees, is kept constant and mode 3 follows thereafter in the terminal phase.

Missile time constant is assumed to be 0.25 seconds which is modeled as a first order delay as following:

$$\frac{a_{realized}}{a_{commanded}} = \frac{1}{\tau s + 1} \tag{84}$$

Missile trajectories with the five guidance algorithms studied are presented in Figure 11. Missiles have an initial flight path angle of $+15$ degrees and expected to hit the target with an impact angle of -45 degrees. All five algorithms appear to meet the requirements. For a better assessment of achievement of the angle criterion, flight path angle histories are presented in Figure 12. All algorithms meet the impact angle requirement with less than 1 degree error. Acceleration histories are presented in

Figure 13. BSBPN and OG hit the acceleration saturation limit. IACBPPN provides the most uniform acceleration history.

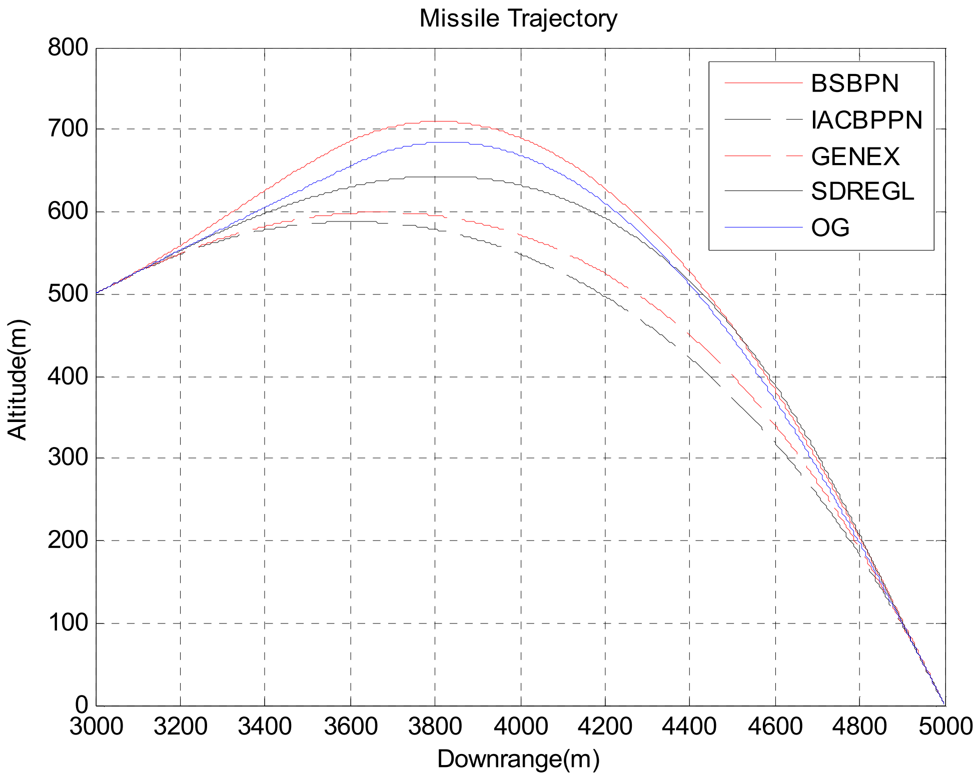

Figure 11 Missile Trajectory Histories

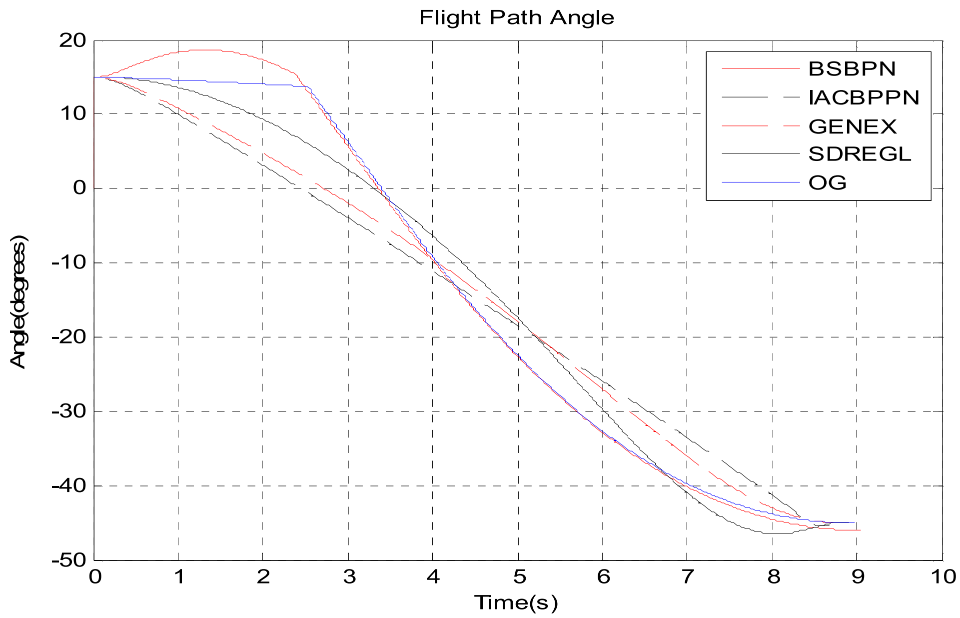

Figure 12 Flight Path Angle Histories

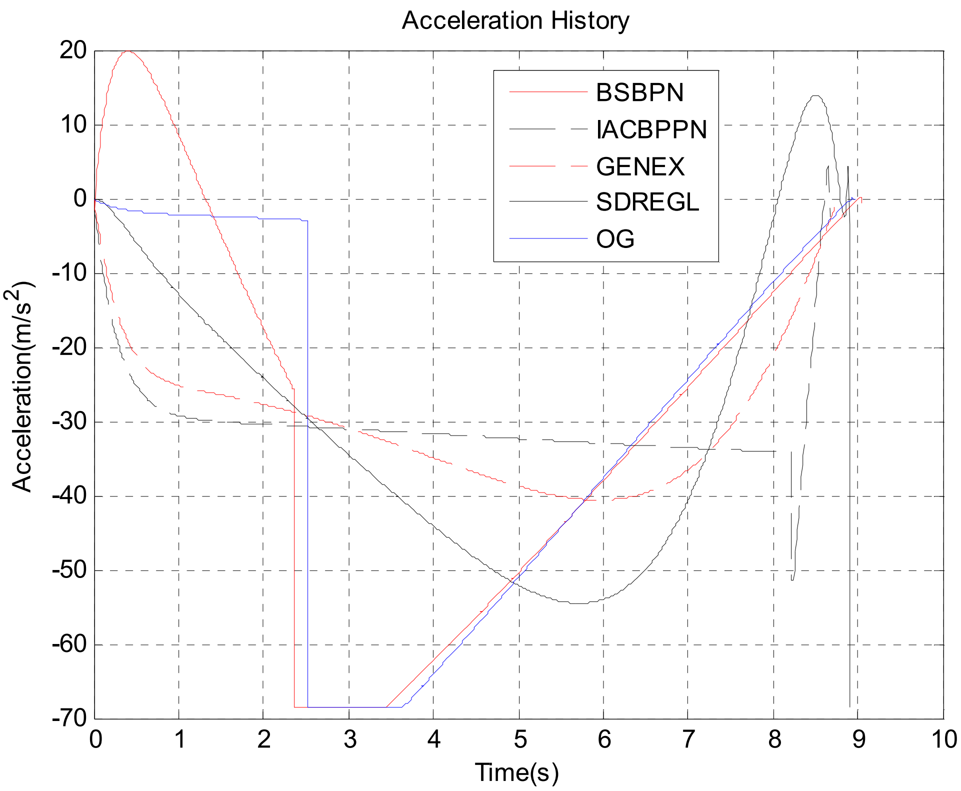

Figure 13 Acceleration Histories

It is observed that all guidance laws perfectly satisfy the performance criterions. In Table 2, the detailed results are presented.

Table 2 Scenario I Run I Results

	BSBPN	IACBPPN	GENEX	SDREGL	OG
Miss Distance(m)	2.4	1.62	0.49	1.37	2.02
Impact Angle(degrees)	-46.0	-45.4	-44.99	-44.98	-45.0
Control Effort(m/s)	298.6	264.1	261.8	275.7	261.9

4.1.1.1 **Simulation with Gravity ON for Stationary Target**

Since the problem of interest is pitch plane type with the gravity direction parallel to inertial z-direction, it would be useful to see what happens when the gravity is on. Gravity is compensated in the lateral direction with a cosine component where in longitudinal direction no compensation is possible. Hence, velocity of the missile varies during engagement. Below, simulation properties with the gravity are seen.

Table 3 Simulation Properties With Gravity for Stationary Target

Parameters	Values
Missile Initial Position	(3000,500)
Target Position	(5000,0)
Missile Initial Velocity	250 m/sn
Missile Initial Orientation	+15 degrees
Gravity	Neglected
Desired Impact Angle	-45 degrees
Acceleration Limits	+7g/-7g
Gravity	ON

Graphs will not be given for sake of brevity. Only tabulated results are shown below.

Table 4 Results with Gravity for Stationary Target

	BSBPN	IACBPPN	GENEX	SDREGL	OG
Miss Distance(m)	0.2	0.2	0.8	2.5	2.4
Impact Angle(degrees)	-46.0	-44.7	-44.9	-45.0	-45.0
Control Effort(m/s)	295.9	263.5	263.2	297.0	258.8

If one compares Table 2 and Table 4 , it can be easily deduced that almost no difference exists between two cases for this scenario except that with SDREGL. It is seen that, in SDREGL, control effort increases when the gravity is taken into consideration which means that it requires a bit more energy in the real applications. However, it has almost no effect on miss distance and impact angle. Due to that reason, it can be neglected.

4.1.2 Run Type II

4.1.2.1 Discrete TGH Region

In the previous section, a scenario was defined where the terminal guidance started from a fixed point with fixed initial conditions and all five algorithms were executed to steer the missile to a stationary target. In this section, the success of the algorithms will be analyzed in terms of different terminal guidance handover (TGH) points with the target being at the same point. Scenario parameters are shown below.

Table 5 Scenario I Run II Parameters

Parameters	Values
Missile Initial Position	Varies in the defined field
Target Initial Position	(5000,0)
Target Velocity	Stationary
Missile Initial Velocity	250 m/sec
Missile Initial Orientation	+15 degrees
Gravity	Neglected
Desired Impact Angle	-45 degrees
Acceleration Limits	+7g/-7g

In the table below, the number “1” indicates the success and the number “0” indicates failure. Rows and columns represent the altitude and downrange respectively for the TGH location. Initial missile velocity and angles are constant for all points in the matrix. Target is at (5000,0).

Success is defined as miss distance being less than 5 meters and absolute impact angle error being less than 5 degrees. Desired impact angle is -45 degrees in all simulations. Failure means not satisfying either or both of the criterions defined above.

Launch envelopes with the five algorithms are presented in Table 6 through Table 10.

For BSBPN, LOF means “lock-on-failure” which means initial look angle is greater than 25 degrees which is nothing but the maximum allowable gimbal angle.

Table 6 BSBPN Launch Envelope for Non-Accelerating Missile against Stationary Target

	0	500	1000	1500	2000	2500	3000	3500	4000	4500
2100	LOF	LOF	LOF	LOF	LOF	LOF	LOF	LOF	LOF	LOF
1700	LOF	LOF	LOF	LOF	LOF	LOF	LOF	LOF	LOF	LOF
1300	LOF	LOF	LOF	LOF	LOF	LOF	LOF	LOF	LOF	LOF
900	1	LOF	LOF	LOF	LOF	LOF	LOF	LOF	LOF	LOF
500	1	1	1	1	1	LOF	LOF	LOF	LOF	LOF
100	0	0	0	0	0	0	0	0	0	LOF

Table 7 IACBPPN Launch Envelope for Non-Accelerating Missile against Stationary Target

	0	500	1000	1500	2000	2500	3000	3500	4000	4500
2100	1	1	1	1	1	1	1	0	0	0
1700	1	1	1	1	1	1	1	0	0	0
1300	1	1	1	1	1	1	1	0	0	0
900	1	1	1	1	1	1	1	1	0	0
500	1	1	1	1	1	1	1	1	0	0
100	1	1	1	1	1	1	1	0	0	0

Table 8 GENEX Launch Envelope for Non-Accelerating Missile against Stationary Target

	0	500	1000	1500	2000	2500	3000	3500	4000	4500
2100	1	1	1	1	1	1	1	1	0	0
1700	1	1	1	1	1	1	1	1	0	0
1300	1	1	1	1	1	1	1	1	0	0
900	1	1	1	1	1	1	1	1	0	0
500	1	1	1	1	1	1	1	1	0	0
100	1	1	1	1	1	1	1	0	0	0

Table 9 SDREGL Launch Envelope for Non-Accelerating Missile against Stationary Target

	0	500	1000	1500	2000	2500	3000	3500	4000	4500
2100	1	1	1	1	1	1	1	0	0	0
1700	1	1	1	1	1	1	1	0	0	0
1300	1	1	1	1	1	1	1	1	0	0
900	1	1	1	1	1	1	1	1	0	0
500	1	1	1	1	1	1	1	1	0	0
100	1	1	1	1	1	1	1	0	0	0

Table 10 OG Launch Envelope for Non-Accelerating Missile against Stationary Target

	0	500	1000	1500	2000	2500	3000	3500	4000	4500
2100	1	1	1	1	1	0	0	0	0	0
1700	1	1	1	1	1	1	0	0	0	0
1300	1	1	1	1	1	1	1	0	0	0
900	1	1	1	1	1	1	1	0	0	0
500	1	1	1	1	1	1	1	1	0	0
100	1	1	1	1	1	0	0	0	0	0

4.1.2.2 **Miss Distance Contours**

In this sub-section, launch envelope is analyzed from a different perspective. Miss distance values in the defined field are calculated using a more refined mesh. Contours will not be shown for BSBPN since lock-on-failure happens for most of the field.

Table 11 Simulation Properties

Parameters	Values
Missile Initial Position	Varies in the defined field
Missile Initial Position Sampling Interval	100 meters for downrange 80 meters for altitude
Target Initial Position	(5000,0)

Target Velocity	Stationary
Missile Velocity	250 m/sec
Missile Initial Orientation	+15 degrees
Gravity	Neglected
Desired Impact Angle	-45 degrees
Acceleration Limits	+7g/-7g

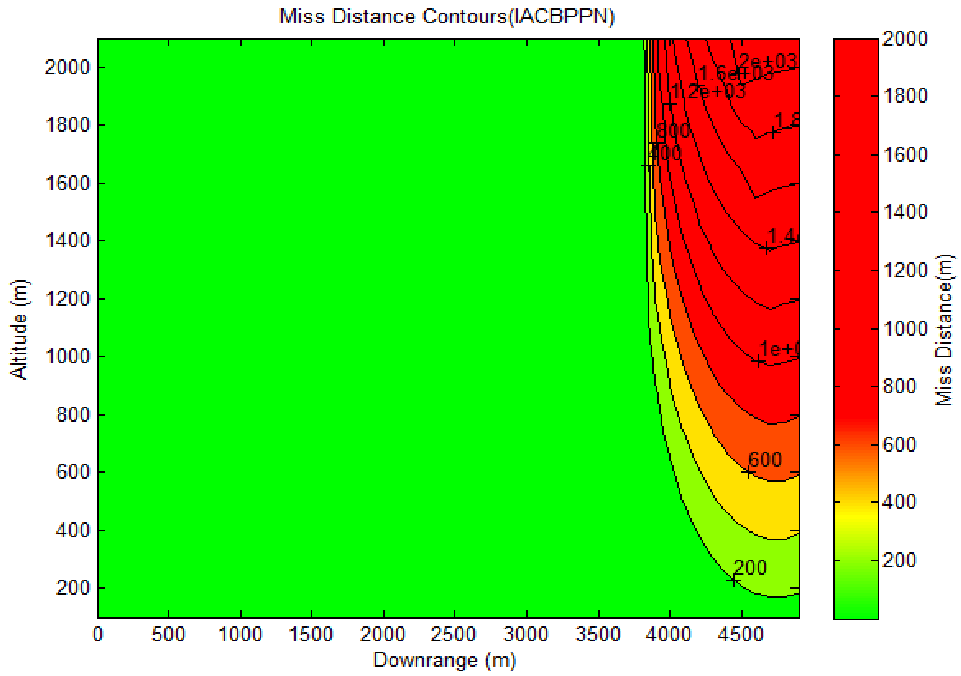

Figure 14 Miss Distance Contours for IACBPPN (Stationary)

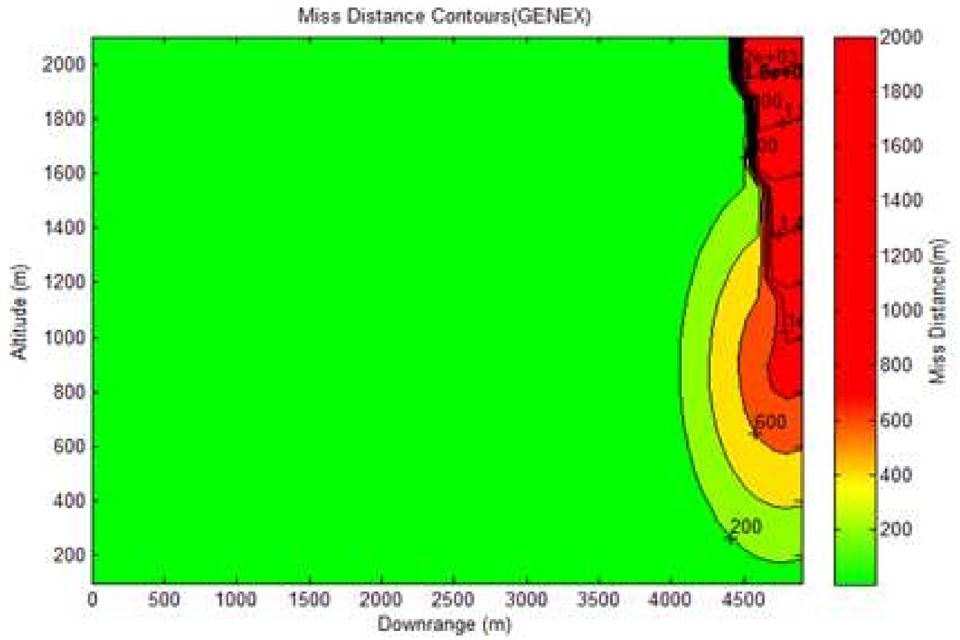

Figure 15 Miss Distance Contours for IACBPPN (Stationary)

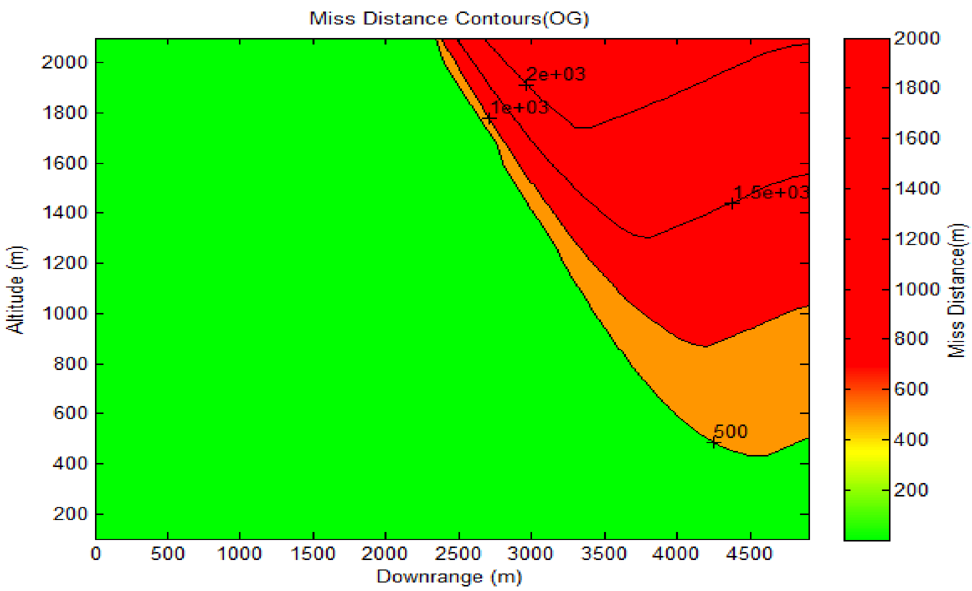

Figure 16 Miss Distance Contours for OG (Stationary)

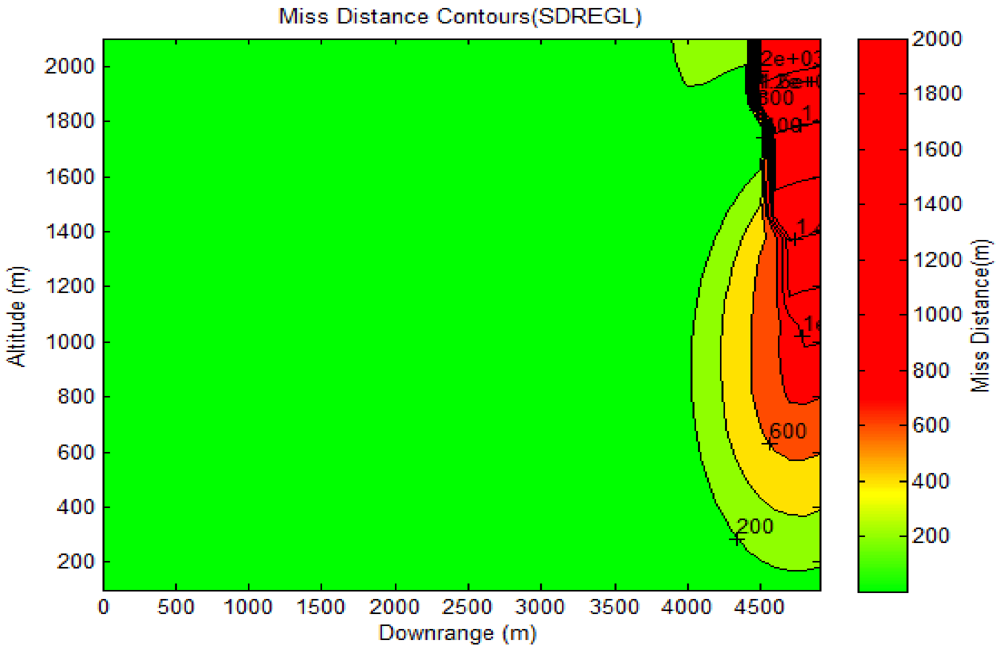

Figure 17 Miss Distance Contours for SDREGL (Stationary)

4.1.2.3 **Cost Function Contours**

Investigating only the miss distance might be misleading. Hence, a cost function is defined which would help to judge the picture in another sense. Cost function is defined as:

$$Cost\ Function = \frac{Miss\ Distance}{Initial\ Distance} \tag{85}$$

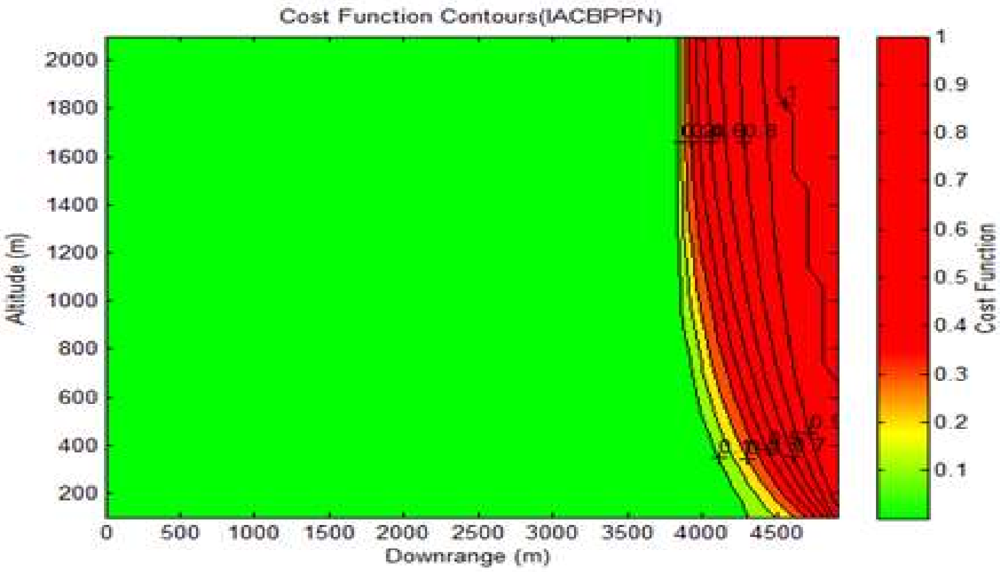

Figure 18 Cost Function Contours for IACBPPN (stationary)

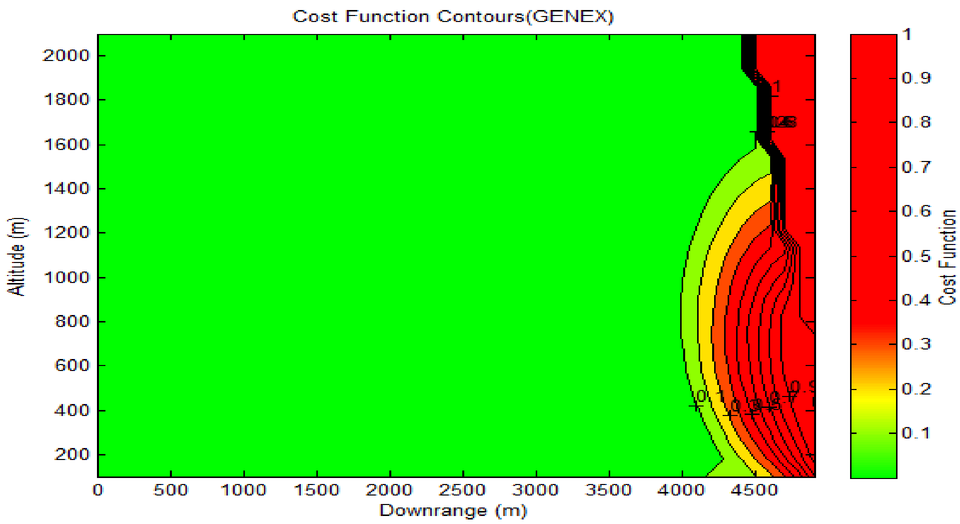

Figure 19 Cost Function Contours for GENEX (stationary)

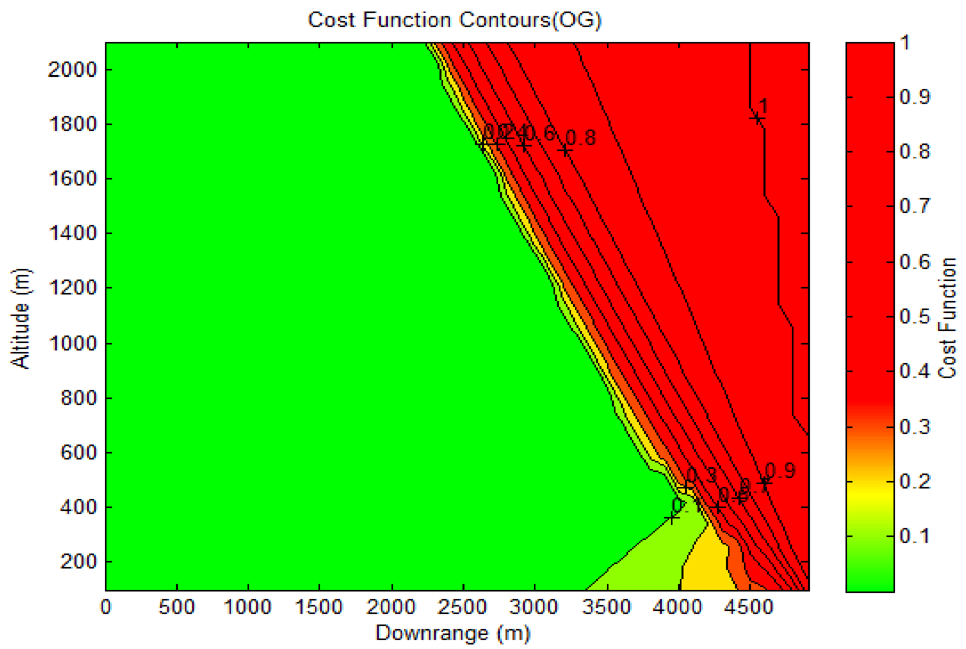

Figure 20 Cost Function Contours for OG (stationary)

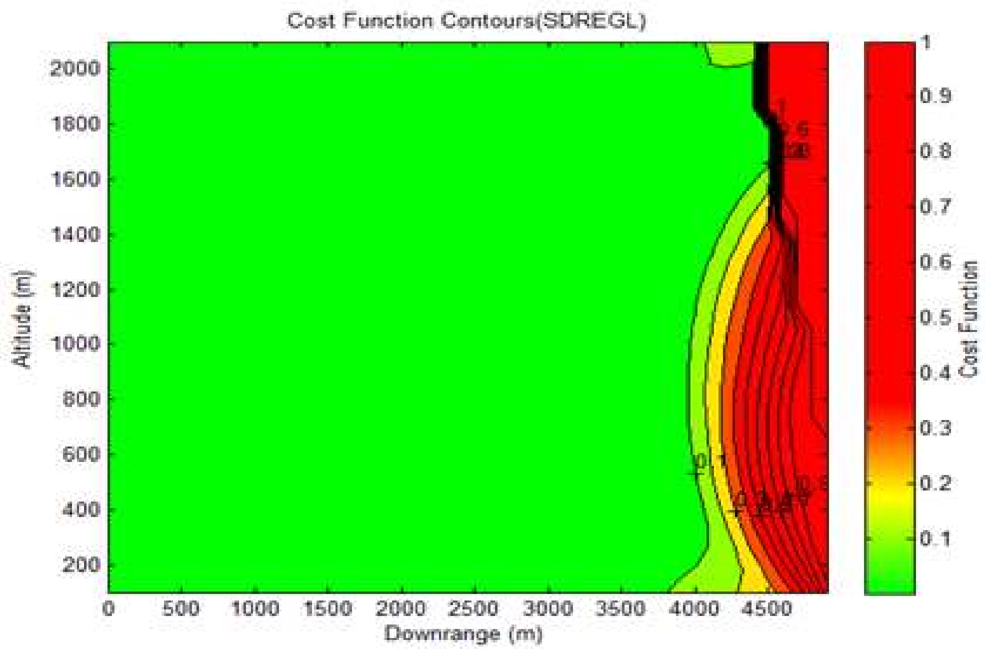

Figure 21 Cost Function Contours for SDREGL (stationary)

It is not surprising that OG has the worst cost function characteristic of above all since its miss distance contours also showed poor performance. GENEX and

SDREGL show similar characteristic. IACBPPN can be concluded to be having a moderate performance.

4.1.3 Run Type III

TGH orientation varies depending on the scenario defined. For this reason, analyses carried out to see the impact of variation of TGH orientation to the impact angle and miss distance. Recalling the missile envelope extraction (see section 4.1.2) for initial orientation of +15 degrees, not all points in launch envelope will be analyzed. Only 4 points which might be considered as critical are analyzed and these points vary depending on the law due to fact that their successful and unsuccessful launch points are different. For each law, the points that are considered to be critical and tested for robustness against initial TGH angle are presented in Table 11.

Table 12 TGH Angle Test Points

Law / Point #	BSBPN	IACBPPN	GENEX	SDREGL	OG
Point I	(0,100)	(3000,900)	(3500,900)	(3500,900)	(3500,500)
Point II	(0,500)	(3000,1300)	(3500,1300)	(3500,1300)	(3500,900)
Point III	(500,100)	(3500,900)	(4000,900)	(4000,900)	(4000,500)
Point IV	(500,500)	(3500,1300)	(4000,1300)	(4000,1300)	(4000,900)

TGH angles are changed as below:

$$\gamma_{m0} = -10, -5, 0, 5, 10, 15 \tag{86}$$

For all laws, point I trajectories will be visualized whereas other points' only results will be given for sake of brevity.

4.1.3.1 BSBPN Success Investigation

Trajectories for the five TGH angles shown in (86) for the TGH point I are plotted in Figure 22. Numerical assessment of these trajectories together with the results of other TGH angle test points is tabulated in Table 13.

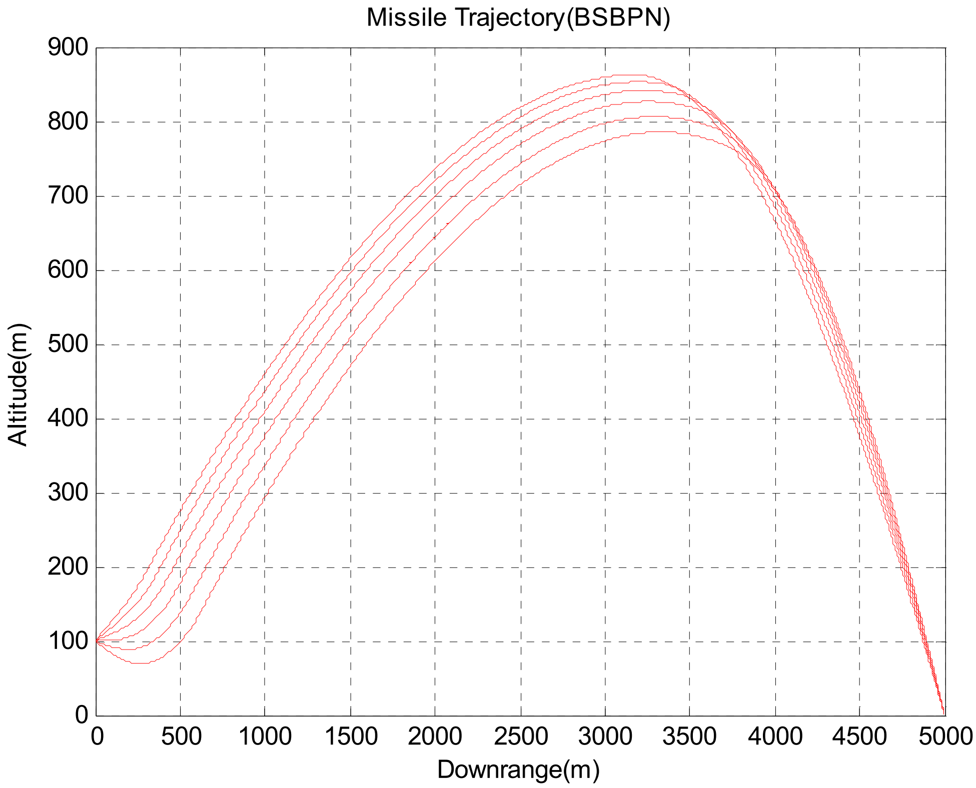

Figure 22 Missile Trajectory for Different TGH Orientation

Table 13 Success Chart of BSBPN for Various TGH Orientation

	-10	-5	0	5	10	15
(0,100)	1	1	1	1	0	0
(0,500)	1	1	1	1	1	1
(500,100)	1	1	1	0	0	0
(500,500)	1	1	1	1	1	1

4.1.3.2 **IACBPPN Success Investigation**

For point I, the figure below illustrates the trajectory of missiles subjected to different initial TGH angles for IACBPPN.

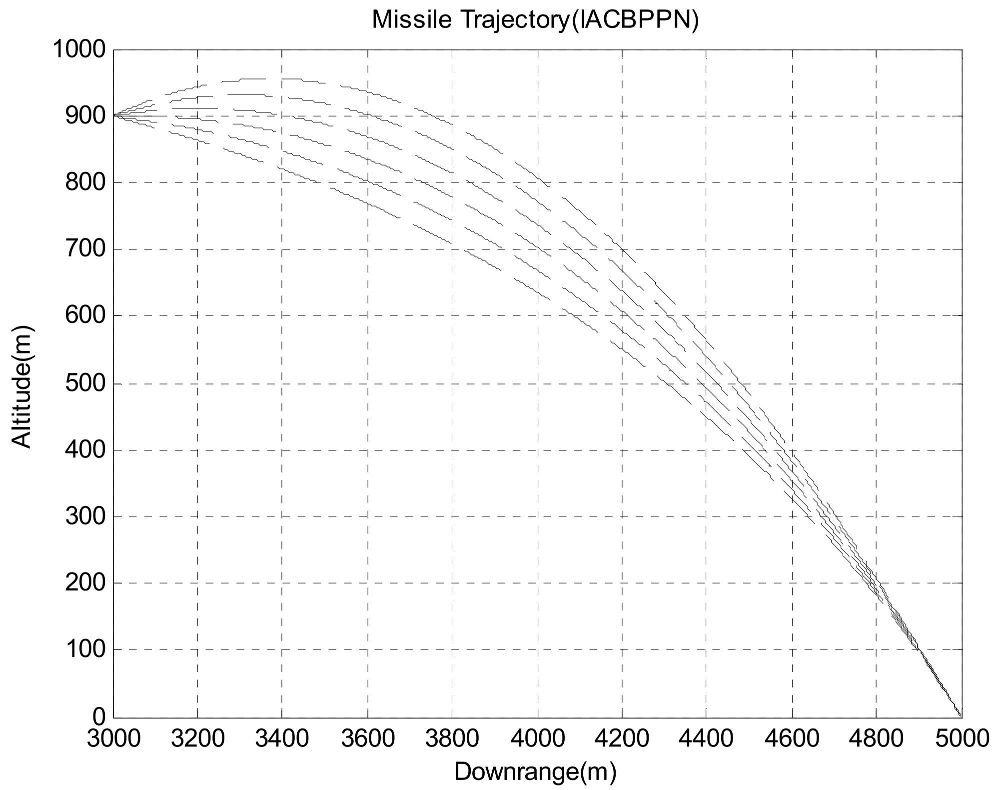

Figure 23 Missile Trajectory History for Various TGH Orientation (IACBPPN)

Table 14 Success Chart of IACBPPN for Various TGH Orientation

	-10	-5	0	5	10	15
(3000,900)	1	1	1	1	1	1
(3000,1300)	1	1	1	1	1	1
(3500,900)	1	1	1	1	1	1
(3500,1300)	1	1	1	1	0	0

4.1.3.3 **GENEX Success Investigation**

For point I, the figure below illustrates the trajectory of missiles subjected to different TGH angles for GENEX. The figure shows that when the missile switches to the terminal guidance at point I, the missile successfully intercepts the target at the commanded angle for all TGH angles tested. Results for all test points are tabulated in Table **15**.

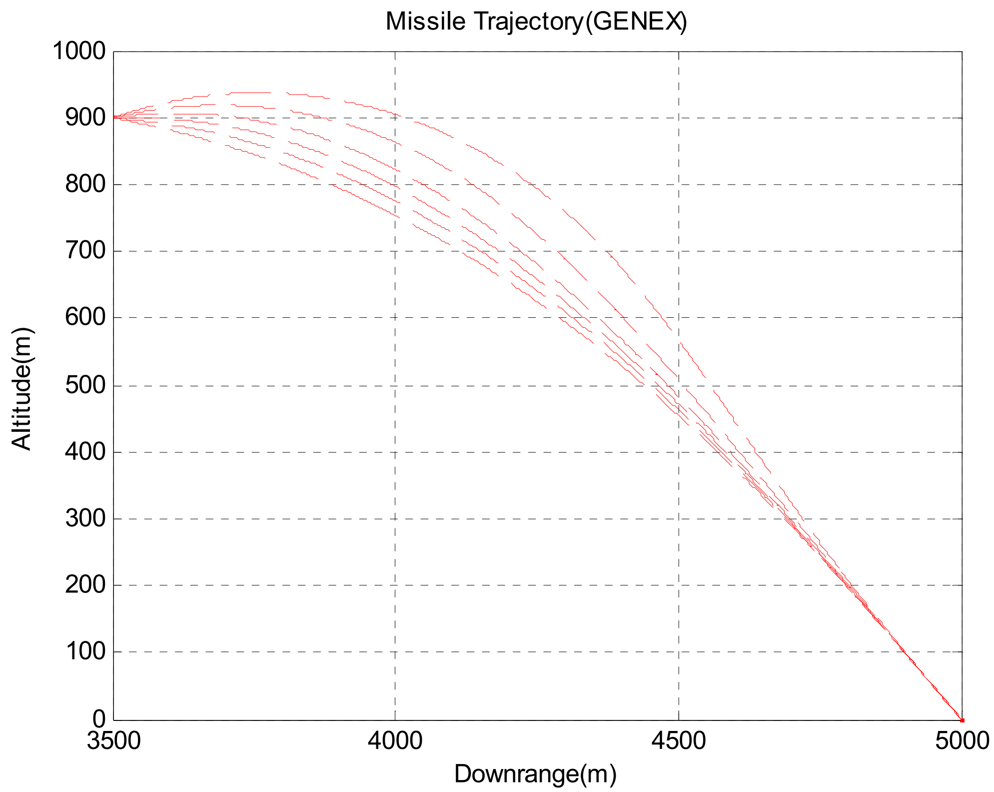

Figure 24 Missile Trajectory History for Various TGH Orientation (GENEX)

Table 15 Success Chart of GENEX for Various TGH Angles

	-10	-5	0	5	10	15
(3500,900)	1	1	1	1	1	1
(3500,1300)	1	1	1	1	1	1
(4000,900)	1	1	0	0	0	0
(4000,1300)	1	0	0	0	0	0

4.1.3.4 **SDREGL Success Investigation**

For point I, the figure below illustrates the trajectory of missiles subjected to different TGH angles for SDREGL. Similar to the previous cases, all five TGH angles lead to successful intercept. Test points III and IV should be considered outside the allowable launch zone since the missile fails for almost all TGH angles tested as seen in Table 16.

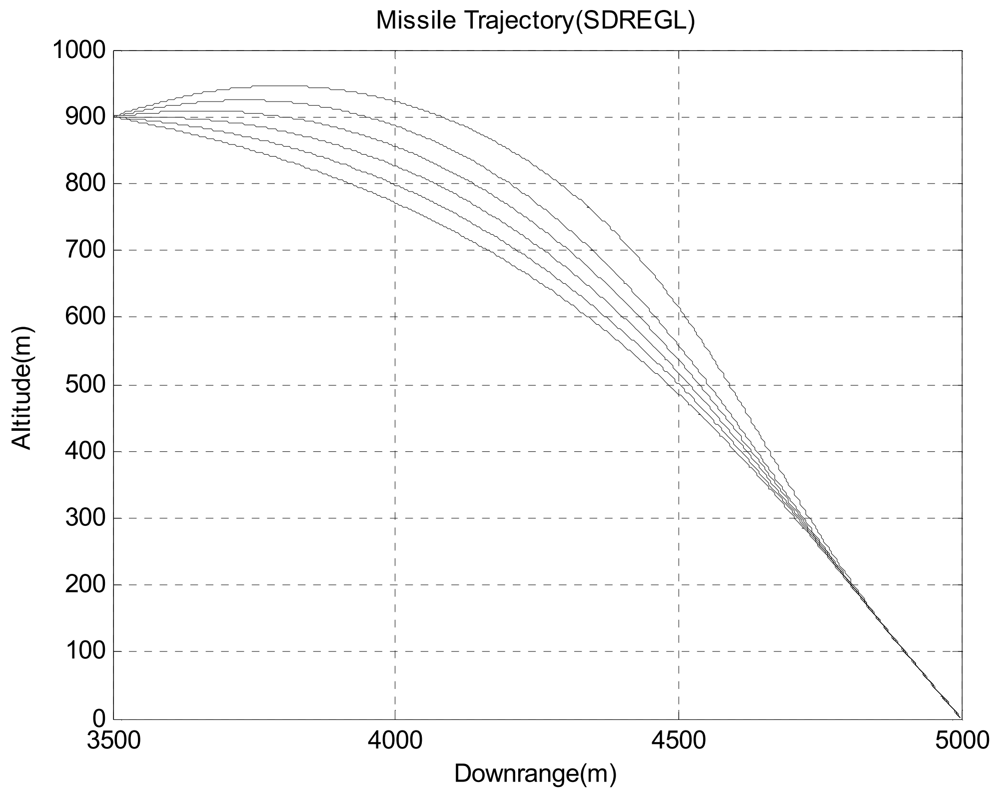

Figure 25 Missile Trajectories for Various TGH Angles (SDREGL)

Table 16 Success Chart of SDREGL for Various TGH Angles

	-10	-5	0	5	10	15
(3500,900)	1	1	1	1	1	1
(3500,1300)	1	1	1	1	1	1
(4000,900)	1	0	0	0	0	0
(4000,1300)	0	0	0	0	0	0

4.1.3.5 **OG Success Investigation**

For point I, the figure below illustrates the trajectory of missiles subjected to different TGH angles for OG. . The figure shows that for point I TGH angle is critical and should be chosen to be positive as for the negative angles tested the missile fails to satisfy performance requirements. Results for all test points are presented in Table 17.

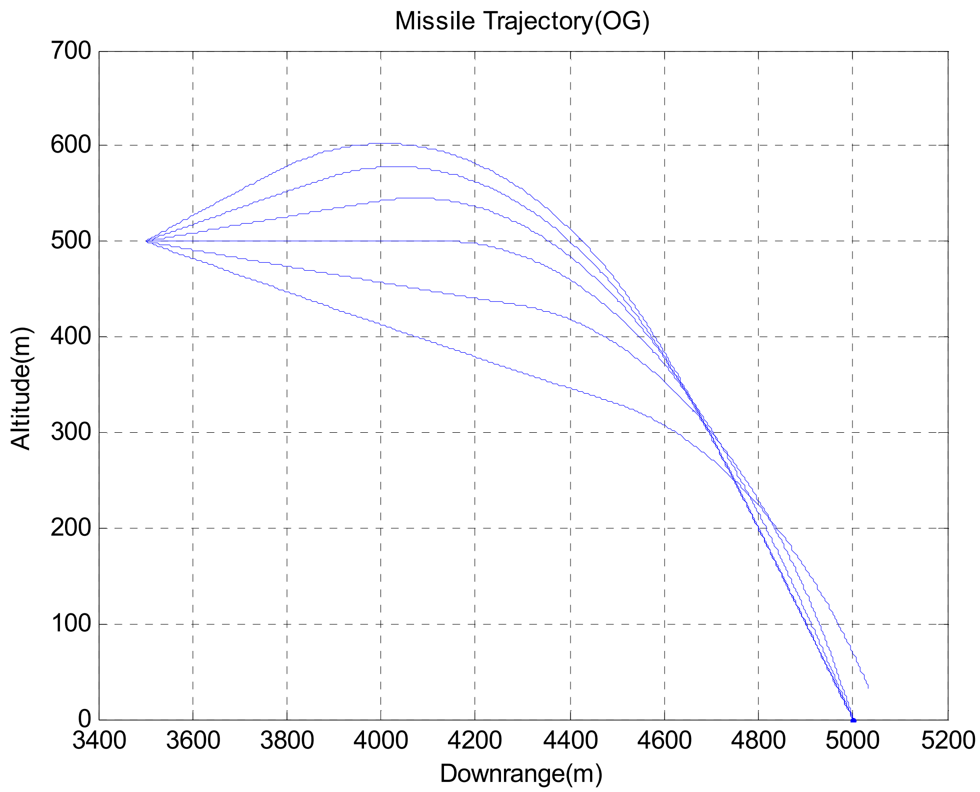

Figure 26 Missile Trajectories for Various TGH Angles (OG)

Table 17 Success Chart of OG for Various TGH Angles

	-10	-5	0	5	10	15
(3500,500)	0	0	1	1	1	1
(3500,900)	1	1	1	1	1	0
(4000,500)	1	1	1	0	0	0
(4000,900)	0	0	0	0	0	0

4.1.3.6 **Comments on Run Type III**

As seen in all tables in this sub-section, success varies upon the TGH angle. This results show that, in practice, it would be important to carefully approach the target so that at the TGH point, the missile orientation is appropriate for a successful strike. Results obtained by run types II and III can be used to increase the success rate of a missile. The missile should be taken by the midcourse guidance algorithm to a safe point in the allowable launch zone before switching to terminal guidance such that even moderate errors in reaching the desired TGH point should not jeopardize the mission. While selecting the TGH point, sensitivity to TGH angle should also be taken into account in order to maximize the chances of success.

4.2 Non-Stationary Target

In this subsection, investigated algorithms will be analyzed in the case of a non-stationary non-maneuvering target.

4.2.1 Run Type I

GENEX and OG are the laws that take the target motion into account. Hence, satisfactory performance is expected from those algorithms. The other algorithms are for stationary targets; however they will also be analyzed in this section to illustrate the reader that these algorithms cannot satisfy either or both of the performance criterions in case of non-stationary targets.

The algorithm parameters are the same as used in section 4.1.1. The engagement parameters are the same expect that in this case there is a target motion which is 15 m/sec symbolizing a main battle tank target. The parameters are given in Table 18. Trajectories with all five guidance laws for this sample scenario are presented in Figure 27.

Table 18 Scenario II Run I Parameters

Parameters	Values
Missile Initial Position	(3000,500)
Target Initial Position	(5000,0)
Target Velocity	15 m/sec
Missile Initial Velocity	250 m/sec
Missile Initial Orientation	+15 degrees
Gravity	Neglected
Desired Impact Angle	-45 degrees
Acceleration Limits	+7g/-7g

The target is intercepted by all guidance laws, however the impact angle error is within acceptable limits for only GENEX and OG as expected. This can clearly be seen in Figure 28. While both of these laws satisfy the performance requirements, they have considerably different acceleration profiles as seen in Figure 29. The OG starts off with a very little acceleration command and at around $t = 3$ seconds it suddenly commands a very large acceleration reaching the acceleration limit due to the fact that guidance phases are switched. After about 1.5 seconds it comes out of saturation and reaches the target with a decaying acceleration command. GENEX algorithm on the other hand never reaches acceleration limit up until the intercept point. Numerical comparison of all five performances is presented in Table 19.

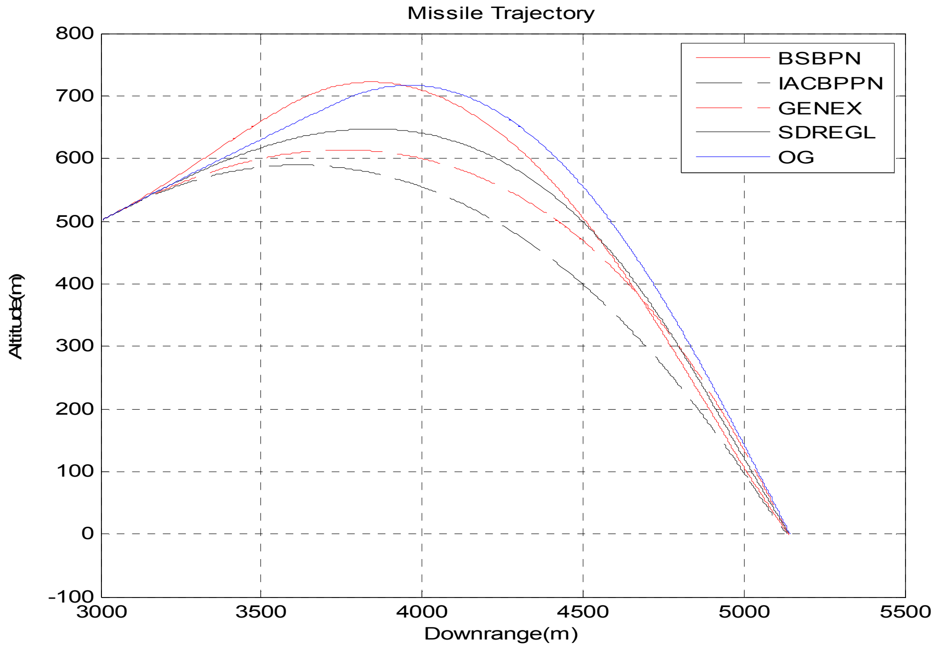

Figure 27 Missile Trajectory Histories

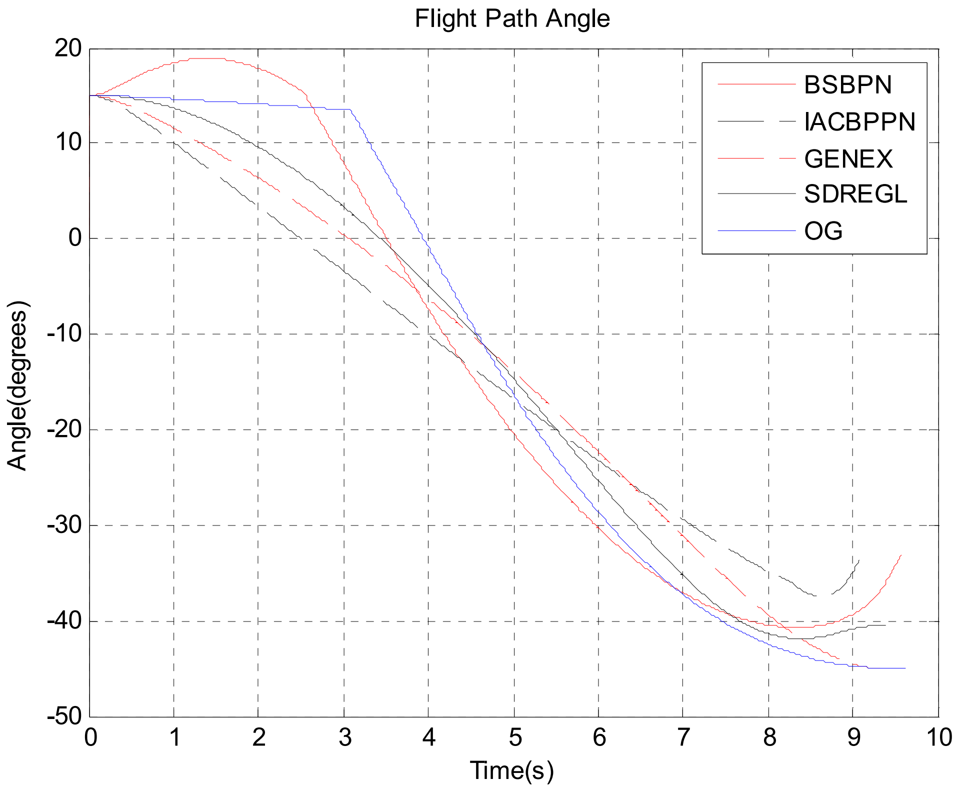

Figure 28 Flight Path Angle Histories

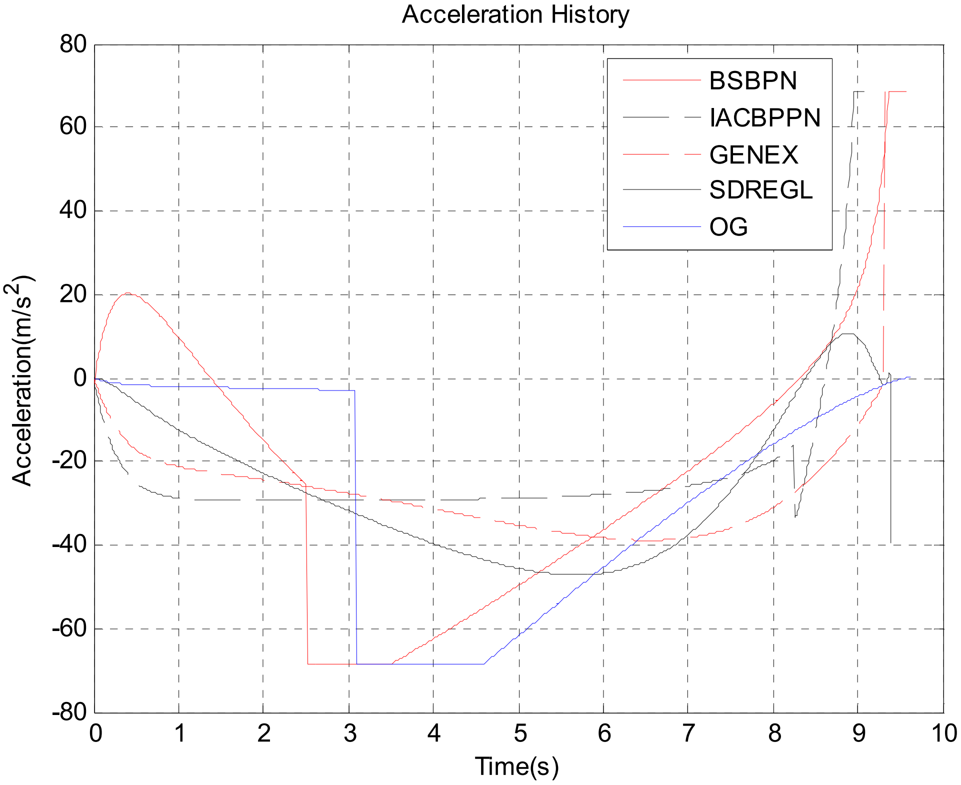

Figure 29 Acceleration Histories

Table 19 Scenario II Run I Results

	BSBPN	IACBPPN	GENEX	SDREGL	OG
Miss Distance(m)	1.97	1.51	3.27	2.29	0.72
Impact Angle(degrees)	-33.1	-32.5	-45.0	-40.56	-45.0
Control Effort(m/s)	311.9	251.56	263.4	254.8	261.9

BSBPN, IACBPPN and SDREGL are not expected to satisfy the desired criterions. The results met this expectation since they are not designed to intercept non-stationary targets. GENEX and OG as expected perfectly satisfy success criterions.

Moreover, it should be noted that BSBPN needs more control effort to intercept the target than that others do.

4.2.1.1 **Simulation with Gravity ON for Non-Stationary Target**

Simulation parameters are seen below in Table 20.

Table 20 Simulation Parameters for Non-Stationary Targets with Gravity

Parameters	Values
Missile Initial Position	(3000,500)
Target Initial Position	(5000,0)
Missile Initial Velocity	250 m/s
Missile Initial Orientation	+15 degrees
Target Velocity	15 m/sec
Target Orientation	+x direction
Gravity	Neglected
Desired Impact Angle	-45 degrees
Acceleration Limits	+7g/-7g
Gravity	ON

Table 21 Results with Gravity for Non-Stationary Target

	BSBPN	IACBPPN	GENEX	SDREGL	OG
Miss Distance(m)	2.4	1.0	4.0	0.1	2.4
Impact Angle(degrees)	-34.0	-33.9	-44.9	-40.8	-45.0
Control Effort(m/s)	306.7	244.2	264.3	276.2	257.6

One should compare Table 19 and Table 21 to see the effects of gravity. The results are the same with the stationary target case. Almost no difference exists for this scenario between gravity on and gravity off cases. This shows that gravity compensation can successfully remove the effect of gravity even though the component of gravity along the body x axis cannot be compensated for.

4.2.2 **Run Type II**

4.2.2.1 **Discrete TGH Region**

In this section, the same procedure that was applied in section 4.1.2 will be processed but for this time the target is non-stationary whose velocity is 15 m/sec in +x direction. The aim is again to extract the allowable missile launch regions in terms of successful intercept with the desired impact angle. Parameters of the run are below.

Table 22 Scenario II Run II Parameters

Parameters	Values
Missile Initial Position	Varies in the defined field
Target Initial Position	(5000,0)
Target Velocity	15 m/sec
Target Orientation	+x direction
Missile Initial Velocity	250 m/sec
Missile Initial Orientation	+15 degrees
Gravity	Neglected
Desired Impact Angle	-45 degrees
Acceleration Limits	+7g/-7g

Since the only law designed for non-stationary targets is GENEX, only launch envelope extracted is GENEX for non-stationary targets case.

Table 23 GENEX Launch Envelope for Non-Accelerating Missile against Non-Stationary Target

	0	500	1000	1500	2000	2500	3000	3500	4000	4500
2100	1	1	1	1	1	1	1	1	0	0
1700	1	1	1	1	1	1	1	1	0	0
1300	1	1	1	1	1	1	1	1	0	0
900	1	1	1	1	1	1	1	1	0	0
500	1	1	1	1	1	1	1	1	0	0
100	1	1	1	1	1	1	1	1	0	0

Table 24 OG Launch Envelope for Non-Accelerating Missile against Non-Stationary Target

	0	500	1000	1500	2000	2500	3000	3500	4000	4500
2100	1	1	1	1	1	0	0	0	0	0
1700	1	1	1	1	1	1	0	0	0	0
1300	1	1	1	1	1	1	1	0	0	0
900	1	1	1	1	1	1	1	1	0	0
500	1	1	1	1	1	1	1	1	0	0
100	1	1	1	1	1	0	0	0	0	0

4.2.2.2 **Miss Distance Contours**

The analysis in section 4.1.2.2 will be repeated for the case of non-stationary target.

Table 25 Simulation Properties

Parameters	Values
Missile Initial Position	Varies in the defined field
Missile Initial Position Sampling Interval	100 meters for downrange 80 meters for altitude
Target Initial Position	(5000,0)
Target Velocity	15 m/sec in +x direction
Missile Velocity	250 m/sec
Missile Initial Orientation	+15 degrees
Gravity	Neglected
Desired Impact Angle	-45 degrees
Acceleration Limits	+7g/-7g

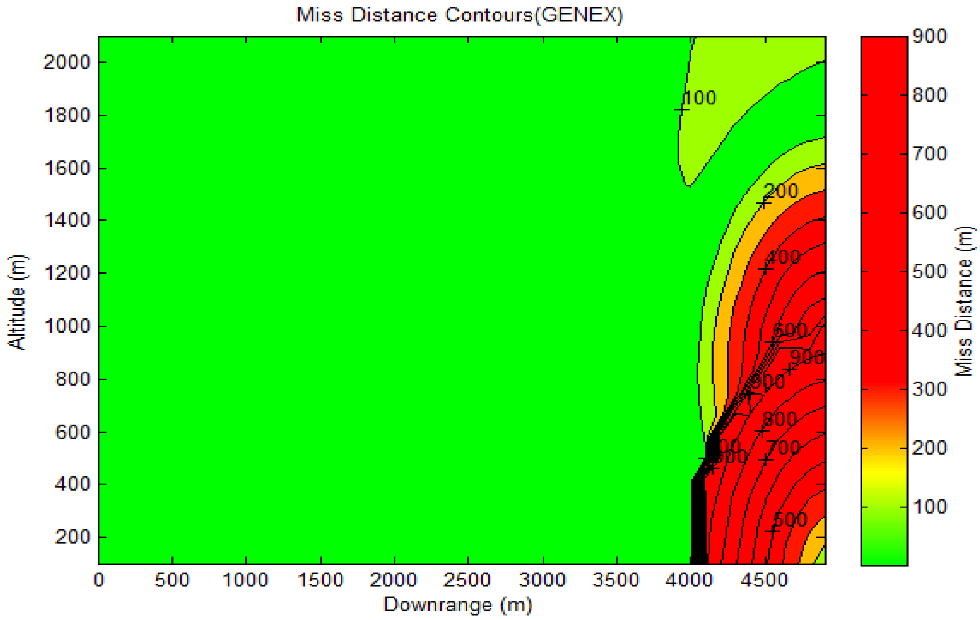

Figure 30 Miss Distance Contours for GENEX (non-stationary)

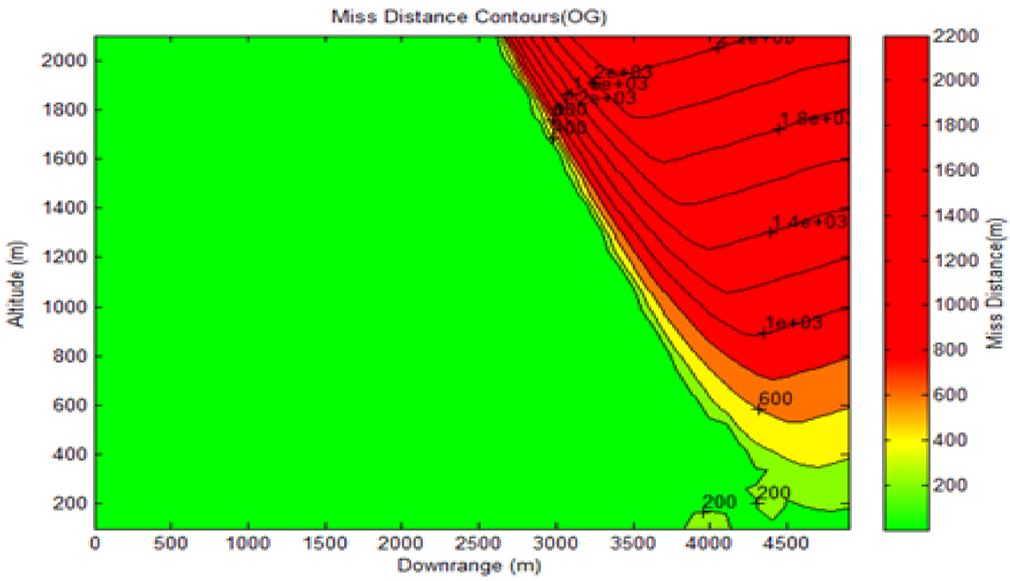

Figure 31 Miss Distance Contours for OG (non-stationary)

4.2.2.3 **Cost Function Contours**

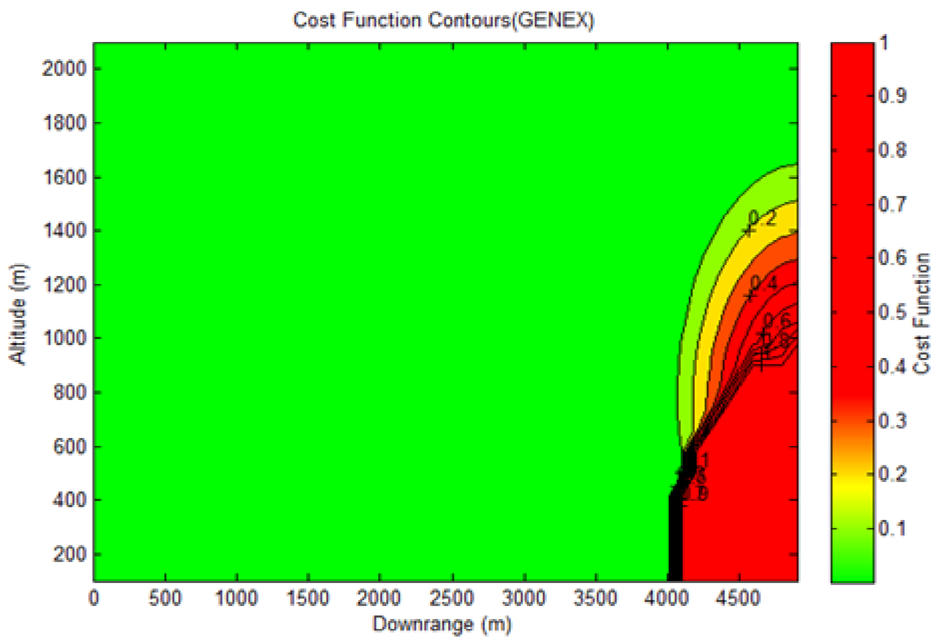

Figure 32 Cost Function Contours for GENEX (non-stationary)

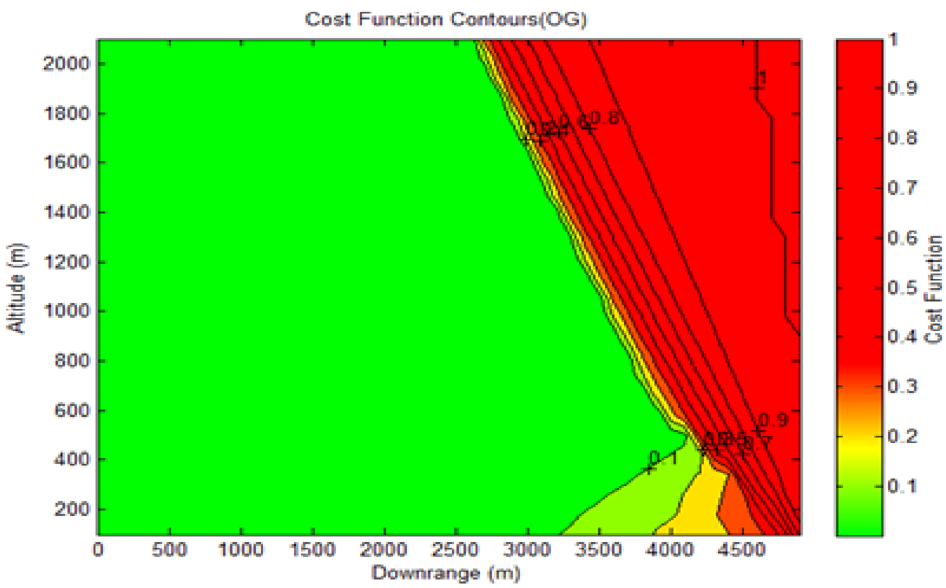

Figure 33 Cost Function Contours for OG (non-stationary)

4.2.3 **Run Type III**

This is the same run type in section 4.1.2.2. However, in this section, target will be non-stationary with the orientation and velocity being +x and +15 m/sec respectively. The TGH coordinates are seen in the table below.

Table 26 TGH Test Points

Law / Point #	GENEX	OG
Point I	(3500,500)	(3500,900)
Point II	(3500,900)	(3500,1300)
Point III	(4000,500)	(4000,900)
Point IV	(4000,900)	(4000,1300)

For all laws, point I trajectories will be visualized only.

4.2.3.1 **GENEX Success Investigation**

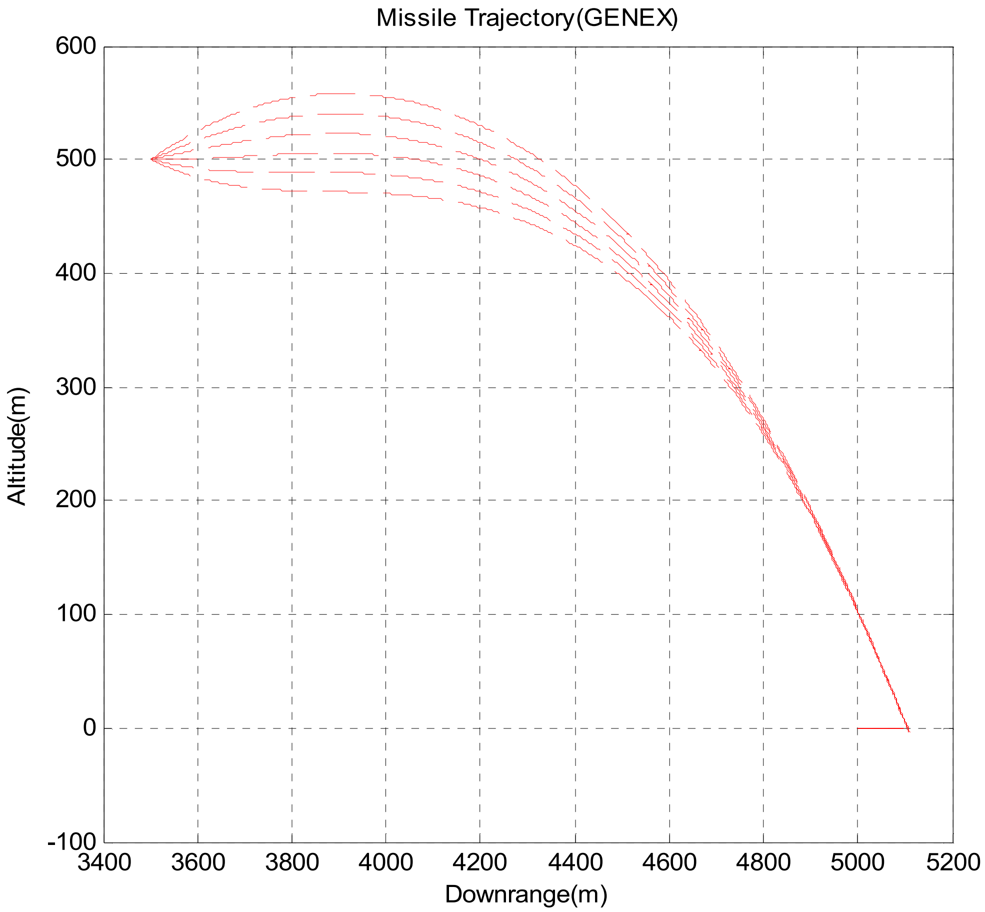

Figure 34 Missile Trajectory for Various TGH Angles

Table 27 Success Chart of GENEX for TGH Angles (non-stationary target)

	-10	-5	0	5	10	15
(3500,500)	1	1	1	1	1	1
(3500,900)	1	1	1	1	1	1
(4000,500)	1	1	1	1	1	0
(4000,900)	1	1	1	0	0	0

4.2.3.2 **OG Success Investigation**

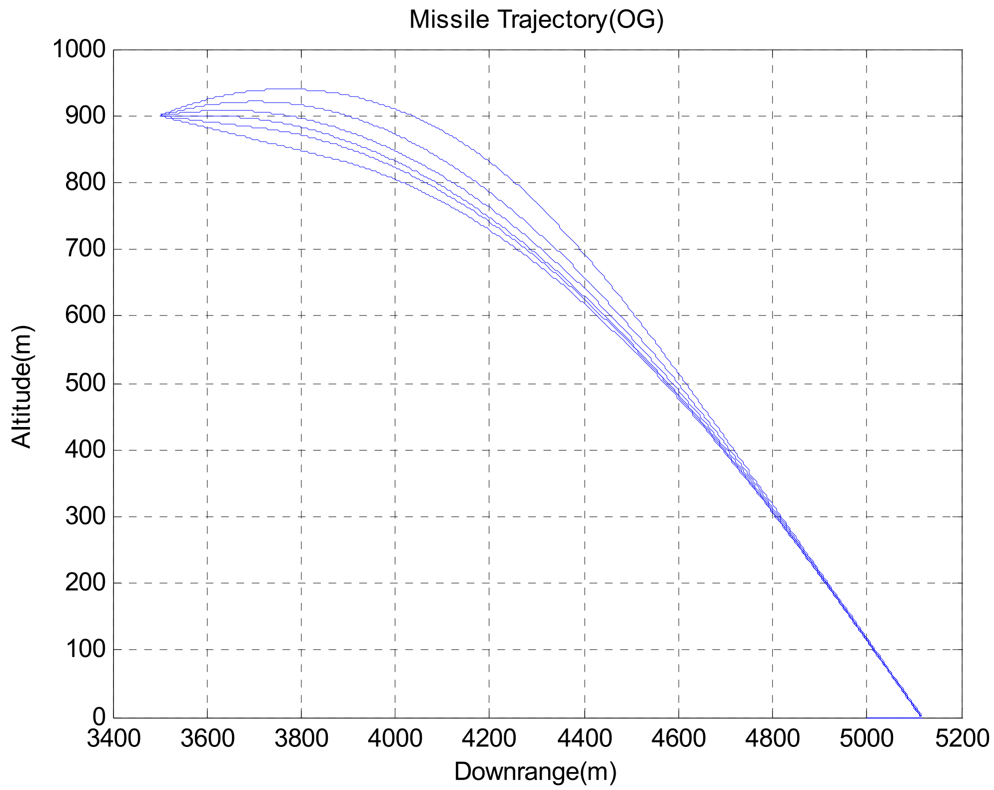

Figure 35 Missile Trajectory for TGH Angles

Table 28 Success Chart of GENEX for Various TGH Angles (non-stationary target)

	-10	-5	0	5	10	15
(3500,900)	1	1	1	1	1	1
(3500,1300)	1	1	0	0	0	0
(4000,900)	0	0	0	0	0	0
(4000,1300)	0	0	0	0	0	0

4.2.3.3 **Comments on Run Type III**

Results are similar with the results explained in section 4.1.3.6. Recalling that, in order to ensure a satisfactory performance, missile firing officer and/or pilot should be careful when directing the missile to the target.

4.2.4 **Run Type IV**

In this section, target velocity will be varied between -30 and +30 m/sec and the success of algorithms will be investigated.

It would be good to discriminate 5 algorithms that are investigated in detail to 2 parts in this test. In the first part, the algorithms that are designed for stationary targets will be tested whereas in the second part the algorithms that are designed for non-stationary targets will be tested against non-stationary targets.

Output will be scatter graphs in which the intercept angles and miss distances exist. Below, there exist the parameters of the run.

Table 29 Scenario II Run IV Parameters

Parameters	Values
Missile Initial Position	(3000,500)
Target Initial Position	(5000,0)
Target Velocity	Varies between -30 to +30 m/sec with 5 m/sec intervals
Missile Initial Velocity	250 m/sec
Missile Initial Orientation	+15 degrees
Gravity	Neglected
Desired Impact Angle	-45 degrees
Acceleration Limits	+7g/-7g

4.2.4.1 **Run Type IV for Stationary Type Algorithms**

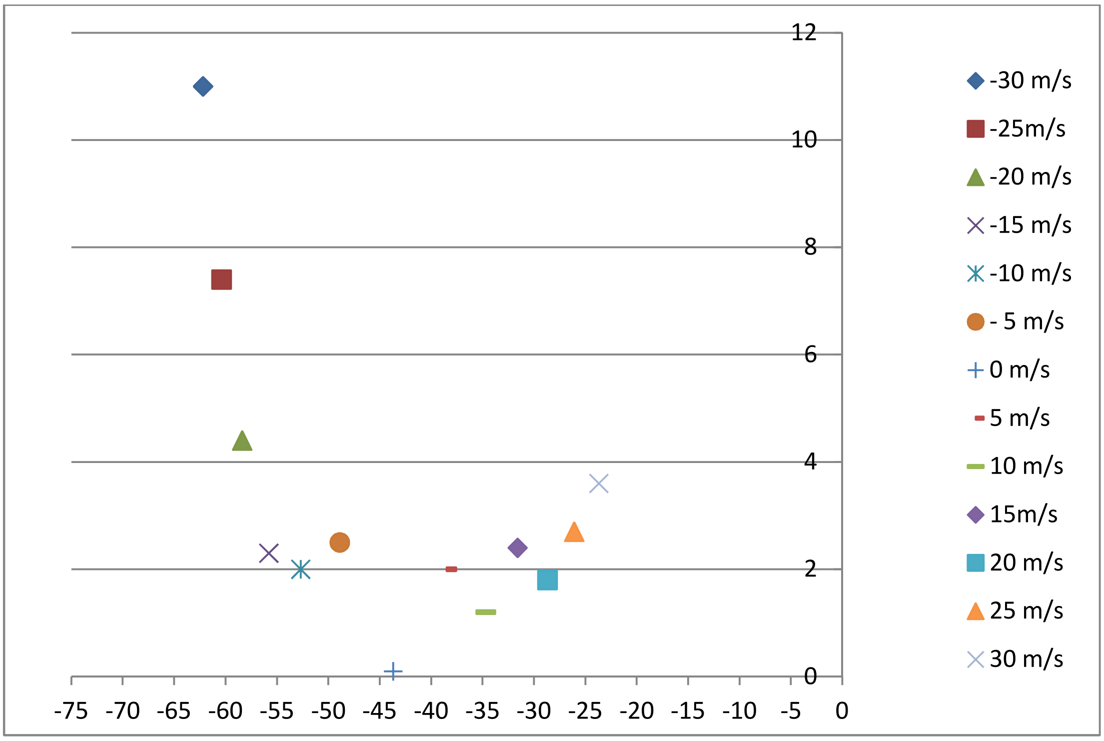

Figure 36 Scatter Graph for BSBPN

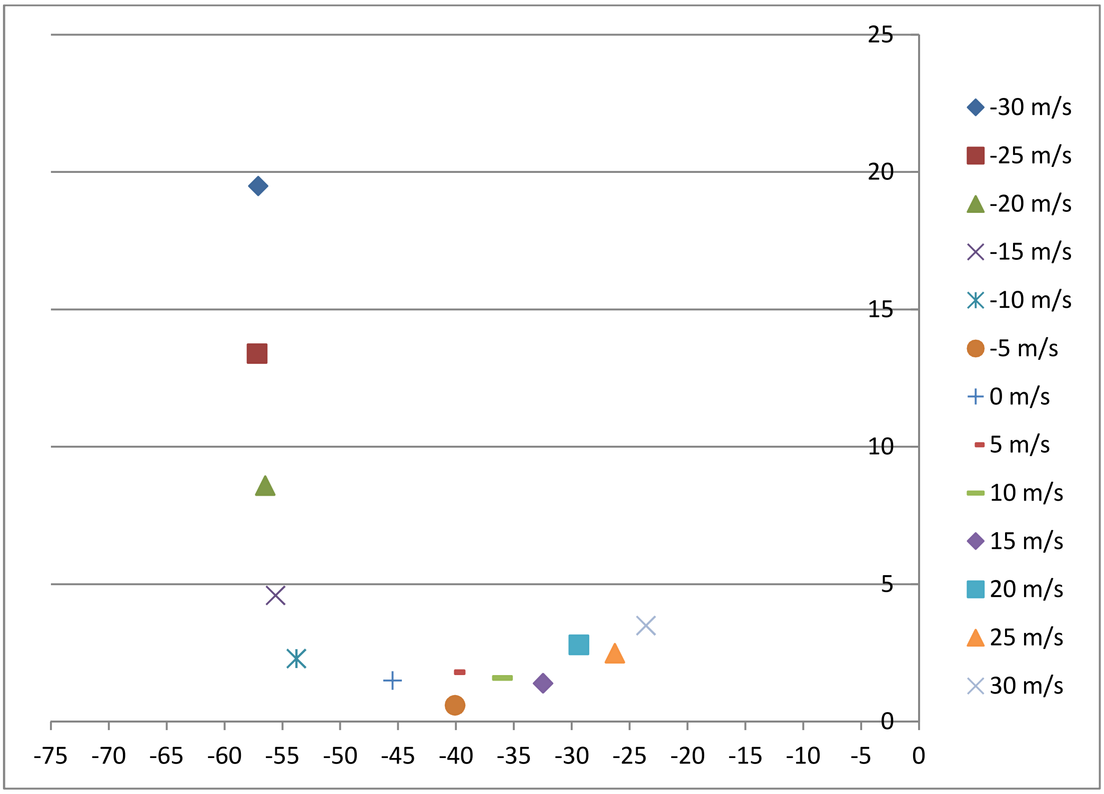

Figure 37 Scatter Graph for IACBPPN

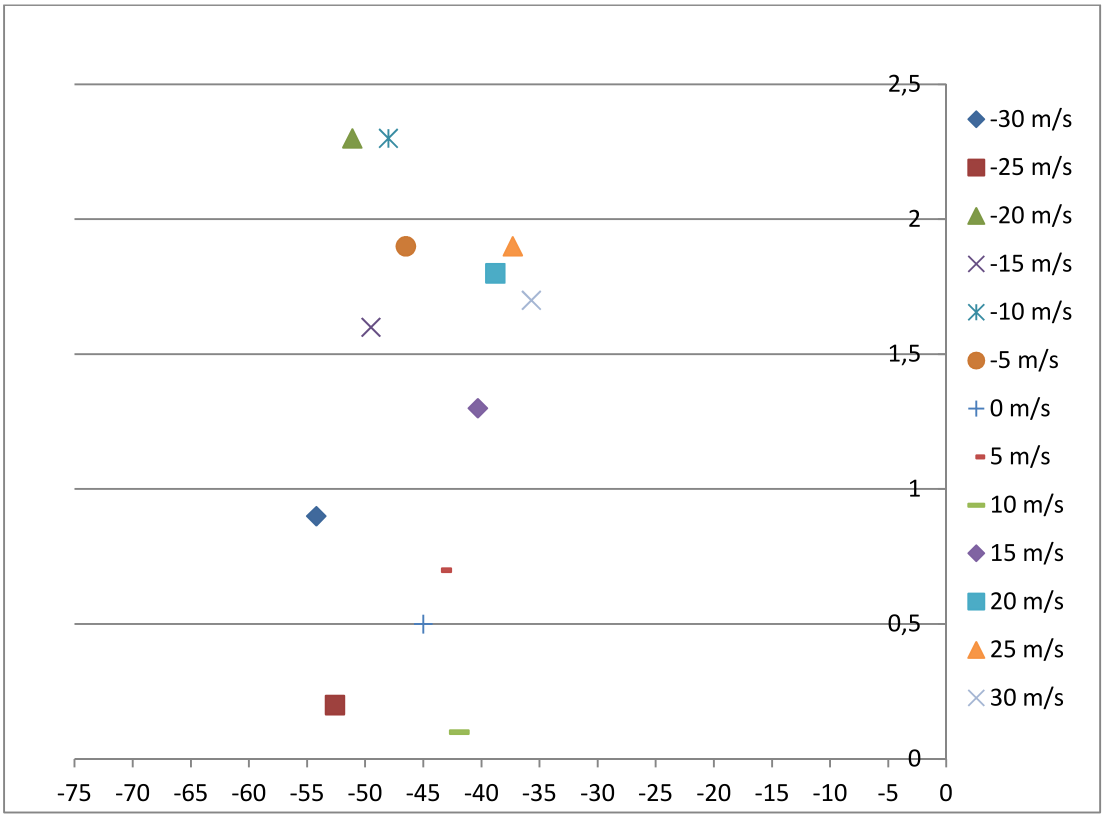

Figure 38 Scatter Graph for SDREGL

In Figure 36, Figure 37 and Figure 38, it is observed that for different target velocities, miss distances and impact angles vary. A "good" algorithm should not have a very big variance of miss distance and impact angle for different target speeds. In this manner, the best algorithm of above algorithms is SDREGL.

4.2.4.2 Run Type IV for Non-Stationary Type Algorithms

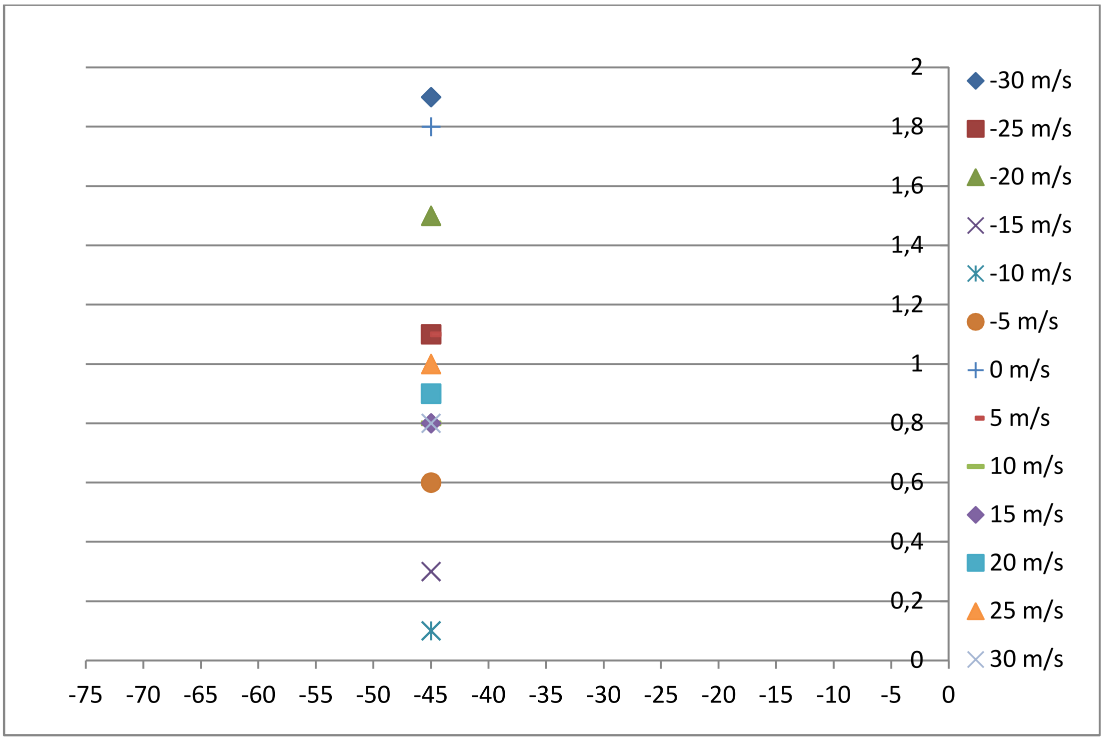

Figure 39 Scatter Graph for GENEX

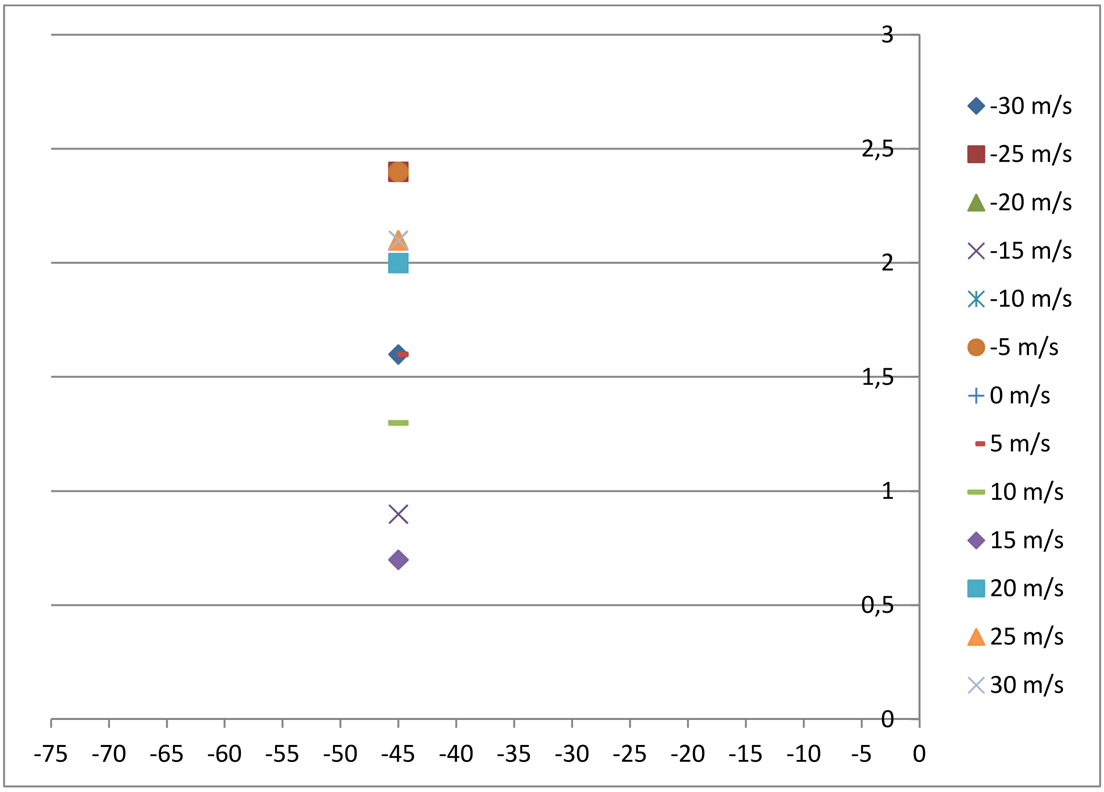

Figure 40 Scatter Graph for OG

For both GENEX and OG, not much variance is observed and they can be considered as successful for the target speeds defined.

4.3 Robustness to Time Constant

In all analyses above, time constant of the missile was taken to be 0.25 seconds. However, it may depend from the missile to missile in real applications. In this section, all of the 5 laws will be tested against various time constant values and success of them in terms of miss distance and impact angle is analyzed.

4.3.1 Robustness to Time Constant Against Stationary Target

All 5 laws will be analyzed against stationary target with the time constants being in the range between 0 and 1. Simulation parameters are the same as those shown in Table 1**.**

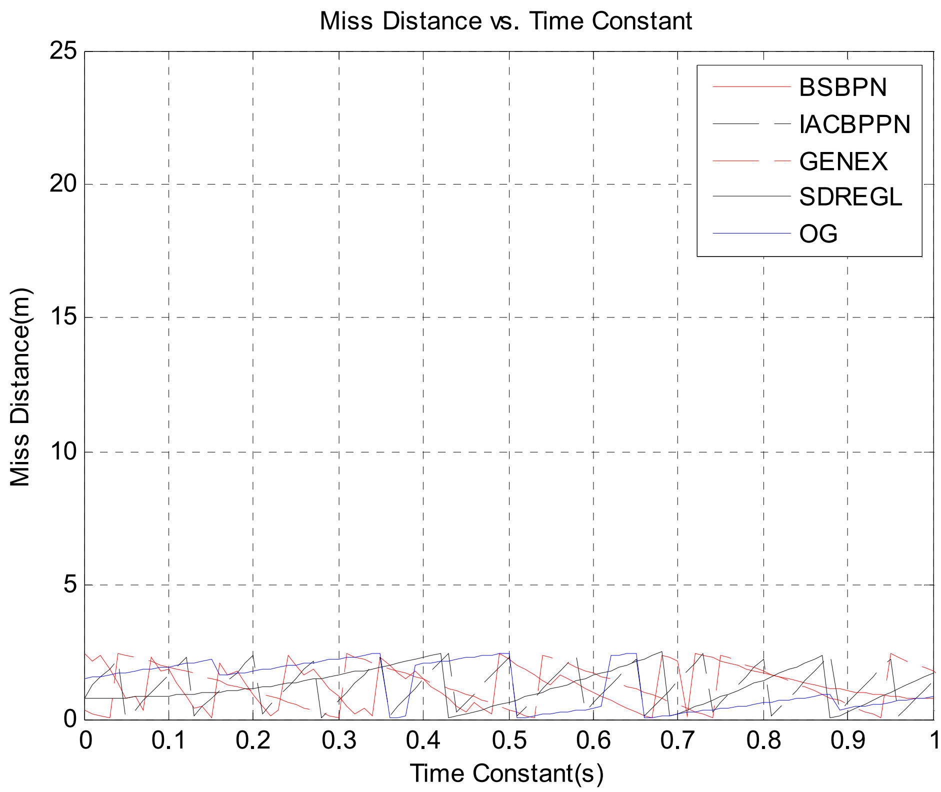

Figure 41 Miss Distance vs. Time Constant (stationary target)

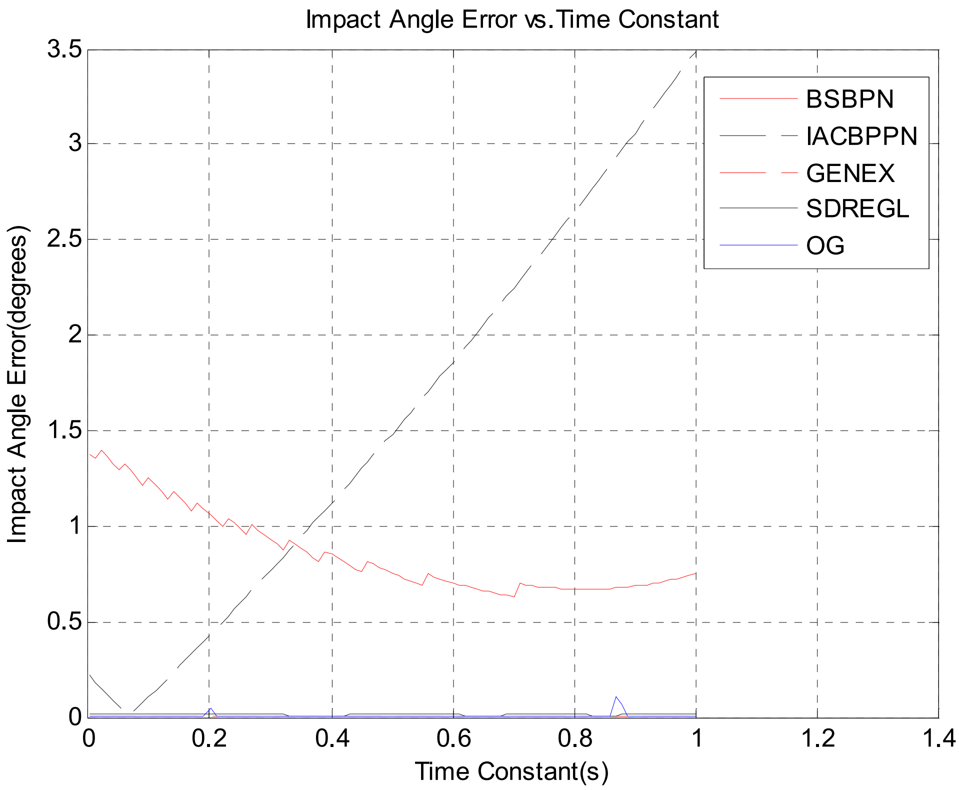

Figure 42 Impact Angle Error vs. Time Constant (stationary target)

In Figure 41, it is observed that miss distances of all laws are in acceptable range in the specified time constant interval. The jumpiness of the curves in Figure 41 is caused by the way miss distance is calculated. To reduce simulation run times, integration time step is chosen as 0.01 seconds as explained in the beginning of section 4. At a speed of 250 m/s, the missile travels about 2.5 meters in one time step. Hence the accuracy of miss distance calculation is less than 2.5 meters. Hence the results in Figure 41 in fact demonstrate perfect hit within the accuracy of miss distance calculations.

In Figure 42, it is seen that GENEX, SDREGL and OG are more robust than the other two laws in terms of impact angle error. They virtually have no impact angle error in the specified time constant interval. On the contrary, IACBPPN has an increasing trend of impact angle error. This would badly affect the performance of the missile when the time constant gets larger. On the other hand, BSBPN has a stable impact angle error characteristic which might be an advantage in the case of an unknown system, i.e. a missile in conceptual design phase.

4.3.2 Robustness to Time Constant Against Non-Stationary Targets

In this subsection, contrary to previous section, simulations are run for non-stationary targets for 2 laws that are designed for non-stationary targets. Simulation parameters are the same as Table 18.

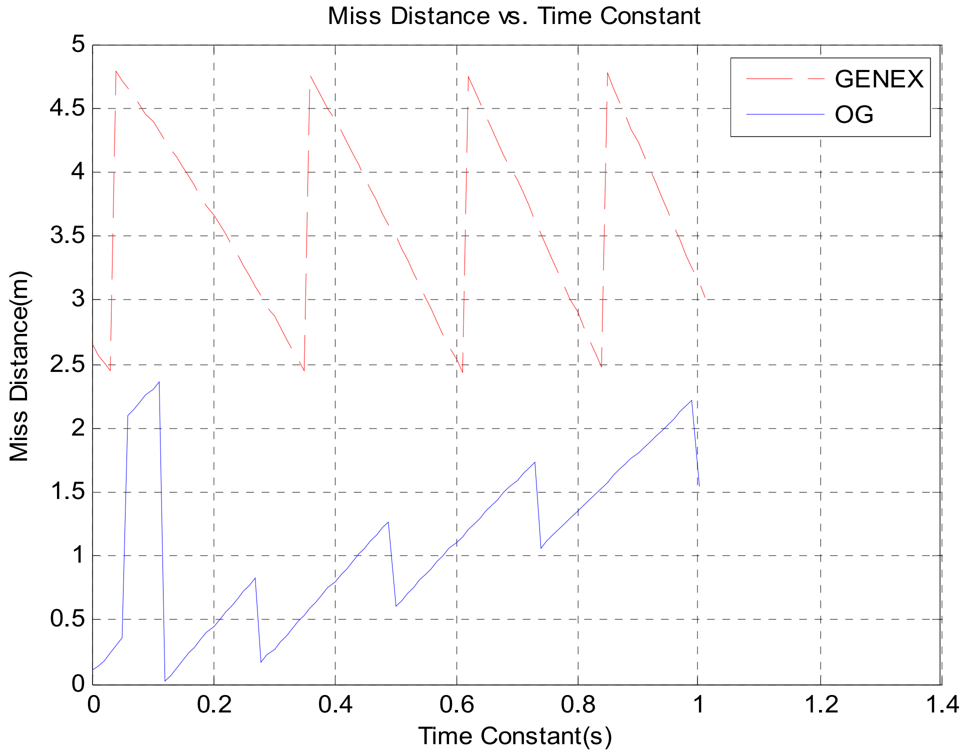

Figure 43 Miss Distance vs. Time Constant (non-stationary target)

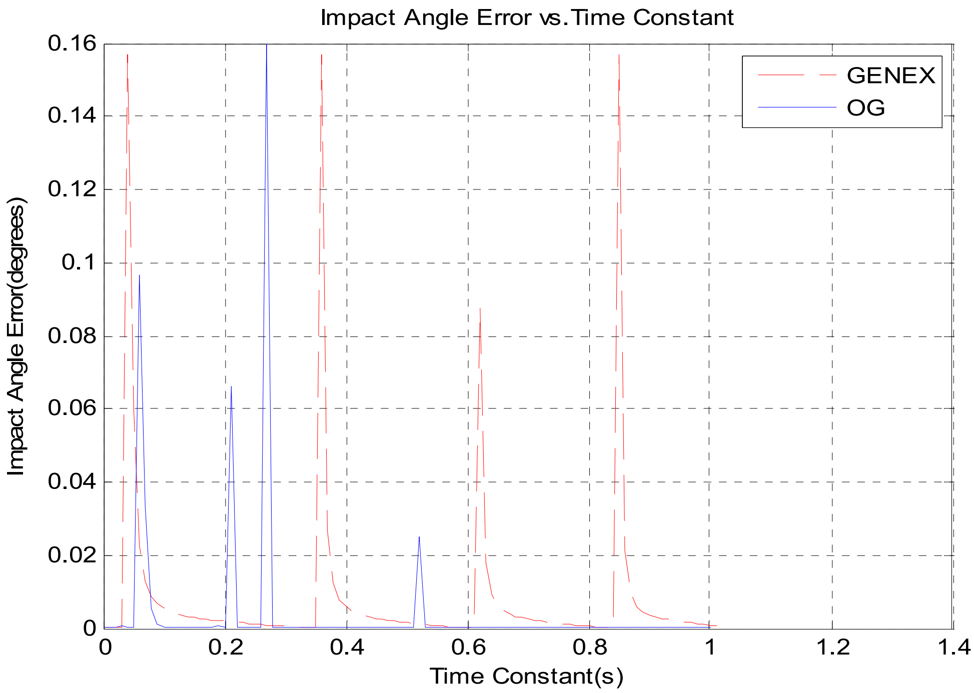

Figure 44 Impact Angle vs. Time Constant (non-stationary target)

In Figure 43 and in Figure 44, it is seen that impact angle and miss distance performance of both GENEX and OG are not distorted by the time constants up to 1 seconds.

4.4 Time-to-Go Error Analysis

Time to go information is needed in **GENEX** and **SDREGL.** Hence, it would be good to analyze the effect of time-to-go error. The error model is taken from [11] and is simply stated as following:

$$t'_{go} = kt_{go} + \Delta t_{go} \qquad (87)$$

Effects of proportional and additive terms will be analyzed separately. One important note is that the impact angle error is only meaningful where the impact really happens. Otherwise, it is nothing but the flight path angle at the location where it is closest to the target. Hence, the portion of the impact angle error graphs where the miss distance is less than 20 m. will be zoomed so that conclusions can be drawn more easily. If there are two laws being compared, depending on the miss distance history, all portion of impact angle error graph may be visualized since the miss distance history may be different for two laws. Nevertheless, reader should still stick to the same logic that is explained above.

4.4.1 **Effect of Additive Term**

To see the effect of additive term, k is held constant as 1. Δt_{go} is changed between -5 and +5. Simulations will be run for stationary targets (both SDREGL and GENEX) and non-stationary targets. (GENEX only)

4.4.1.1 **Effects of Additive Terms in the Case of Stationary Target**

The simulation parameters are shown below.

Table 30 Simulation Parameters

Parameters	Values
Missile Initial Position	(3000,500)
Target Initial Position	(5000,0)
Target Velocity	0 m/sec
Missile Initial Velocity	250 m/sec
Missile Initial Orientation	+15 degrees
Gravity	Neglected
Desired Impact Angle	-45 degrees
Acceleration Limits	$a_{max} = 7g$ $a_{min} = -7g$

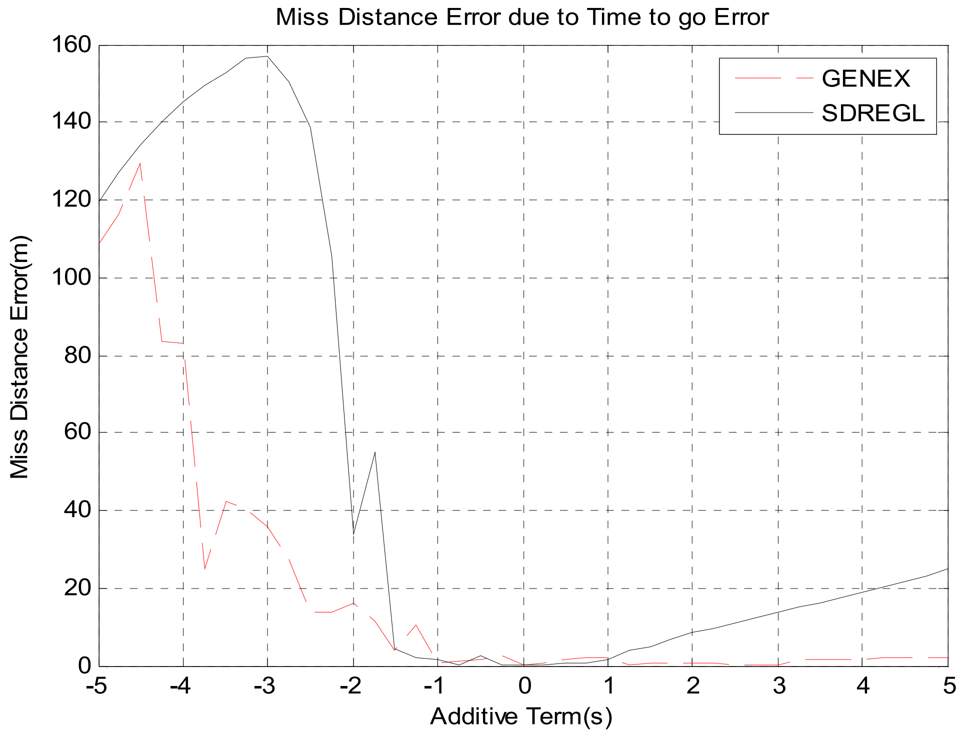

Figure 45 Miss Distance Error due to Time to go Error (additive/ stationary target)

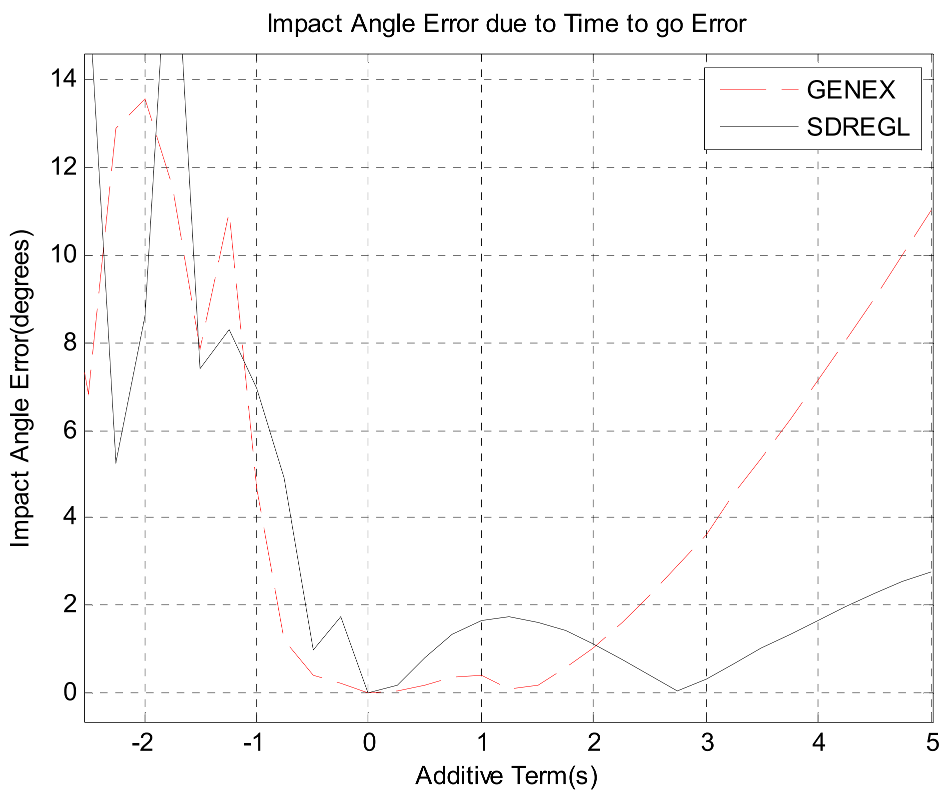

Figure 46 Impact Angle Error due to Time to go Error (additive/ stationary target)

In the case explained above, it is observed that additive term has a distorting effect when it is negative which means time-to-go is **under-estimated**. On the contrary, when it is positive, it doesn't have a much disturbance which means time-to-go is **over-estimated.** The advantage of one law over the other is highly dependent on the specific error interval. The sharp jumps occurring in the additive term type graphs are due to acceleration saturation difference between the corresponding error terms.

4.4.1.2 Effects of Additive Terms in the Case of Non-Stationary Target

SDREGL is not designed for non-stationary targets. Hence it would not make any sense to evaluate its performance in this analysis. Only GENEX will be analyzed in this subsection.

The simulation parameters are shown below.

Table 31 Simulation Parameters

Parameters	Values
Missile Initial Position	(3000,500)
Target Initial Position	(5000,0)
Missile Initial Velocity	250 m/sec
Missile Initial Orientation	+15 degrees
Target Orientation	+x direction
Target Velocity	15 m/sec
Gravity	Neglected
Desired Impact Angle	-45 degrees
Acceleration Limits	$a_{max} = 7g$ $a_{min} = -7g$

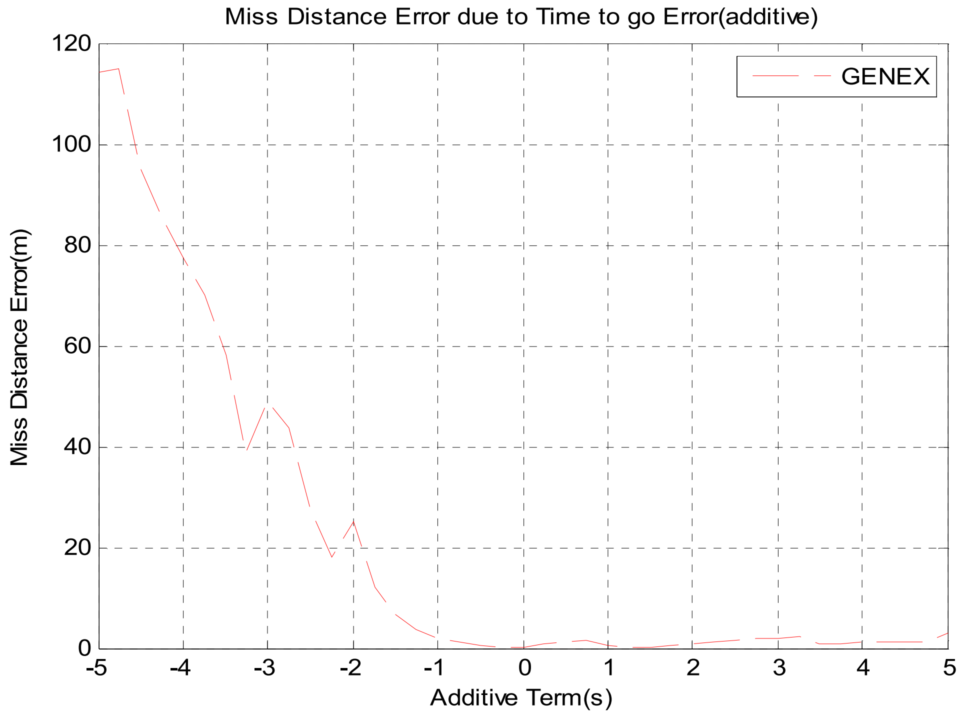

Figure 47 Miss Distance Error due to Time to go Error (additive/non-stationary target)

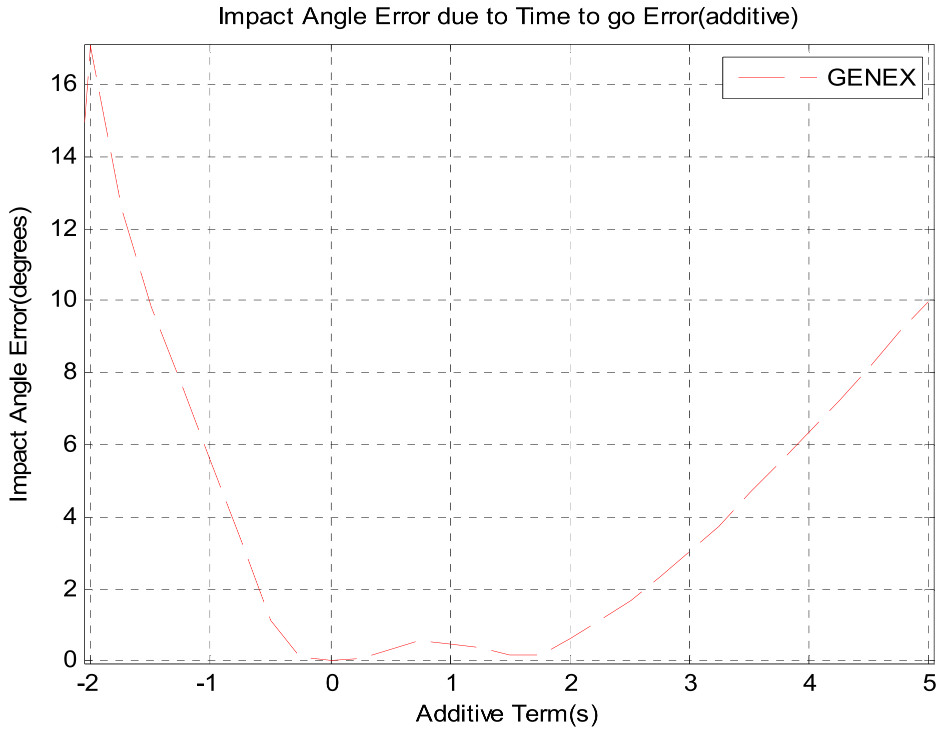

Figure 48 Impact Angle Error due to Time to go Error (additive/ non-stationary target)

GENEX has almost same trend with the stationary type case. One can comment with confidence that over-estimation is advantageous than under-estimation. The sharp jumps occurring in the additive term type graphs are due to acceleration saturation difference between the corresponding error terms.

4.4.2 **Effect of Proportional Term**

To see the effect of proportional term, Δt_{go} is set to 0 whereas k is changed between 0.4 and 2. Simulations will be run for stationary targets (both SDREGL and GENEX) and non-stationary targets. (GENEX only)

4.4.2.1 **Effects of Proportional Term in the Case of Stationary Target**

Simulation parameters are the same as Table 30.

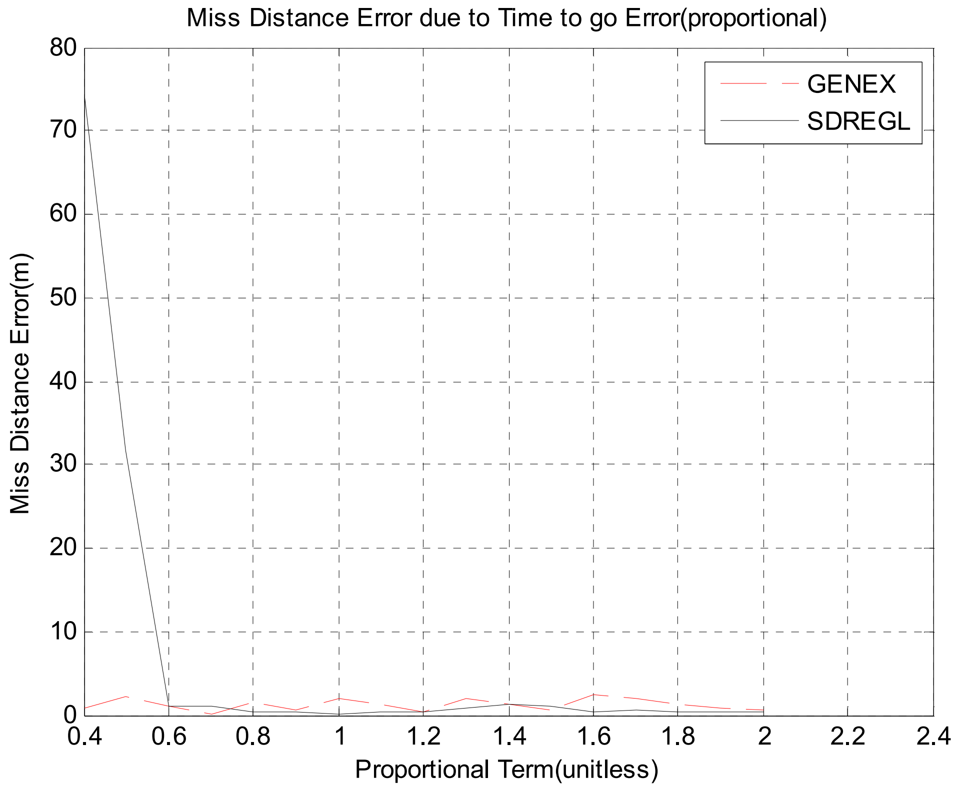

Figure 49 Miss Distance Error due to Time to go Error (proportional/stationary)

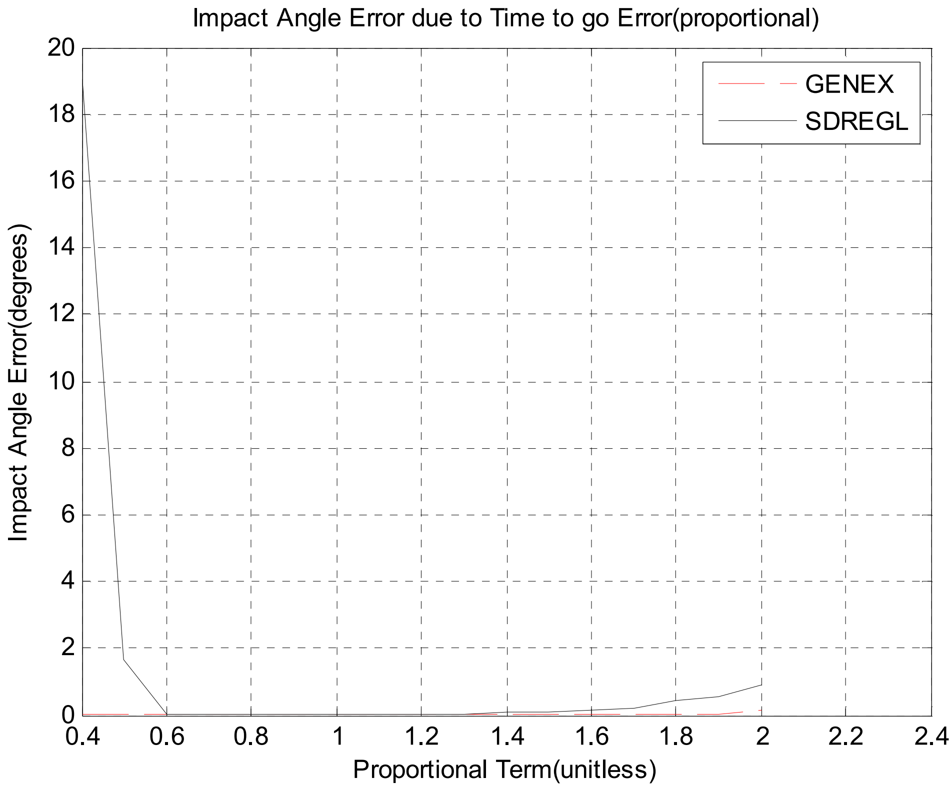

Figure 50 Impact Angle Error due to Time to go Error (proportional/stationary)

It is worth to note that for proportional term between 0.6 and 2 (for GENEX, whole range between 0.4 and 2) both laws show superior performance. It means under-estimation of 40% and over-estimation of 100% does not affect the performance.

4.4.2.2 **Effects of Proportional Terms in the Case of Non-Stationary Target**

Simulation parameters are the same as Table 31.

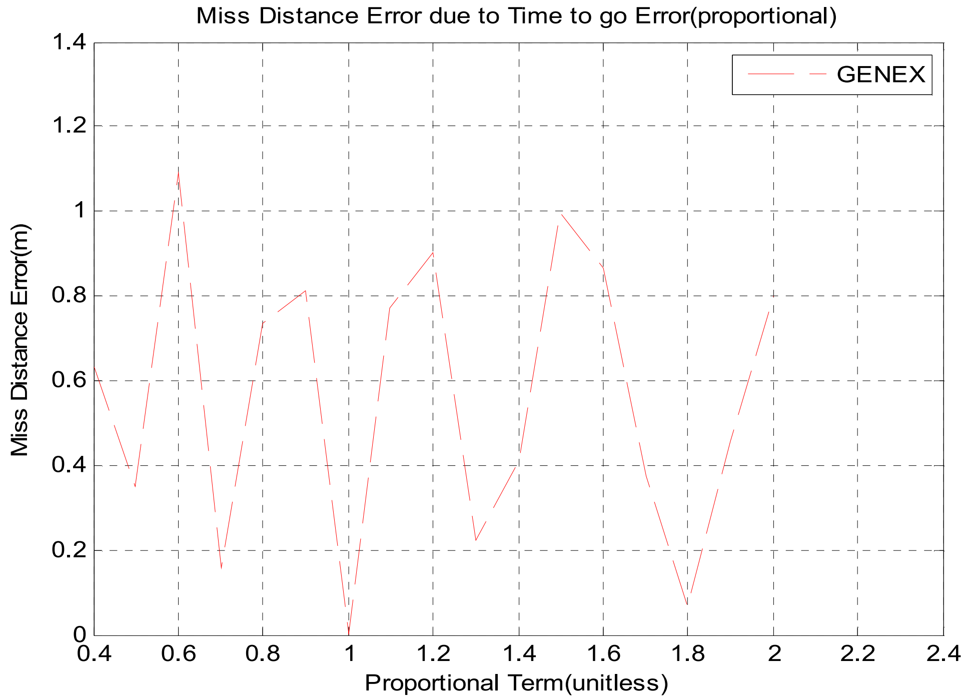

Figure 51 Miss Distance Error due to Time to go Error (proportional/non-stationary)

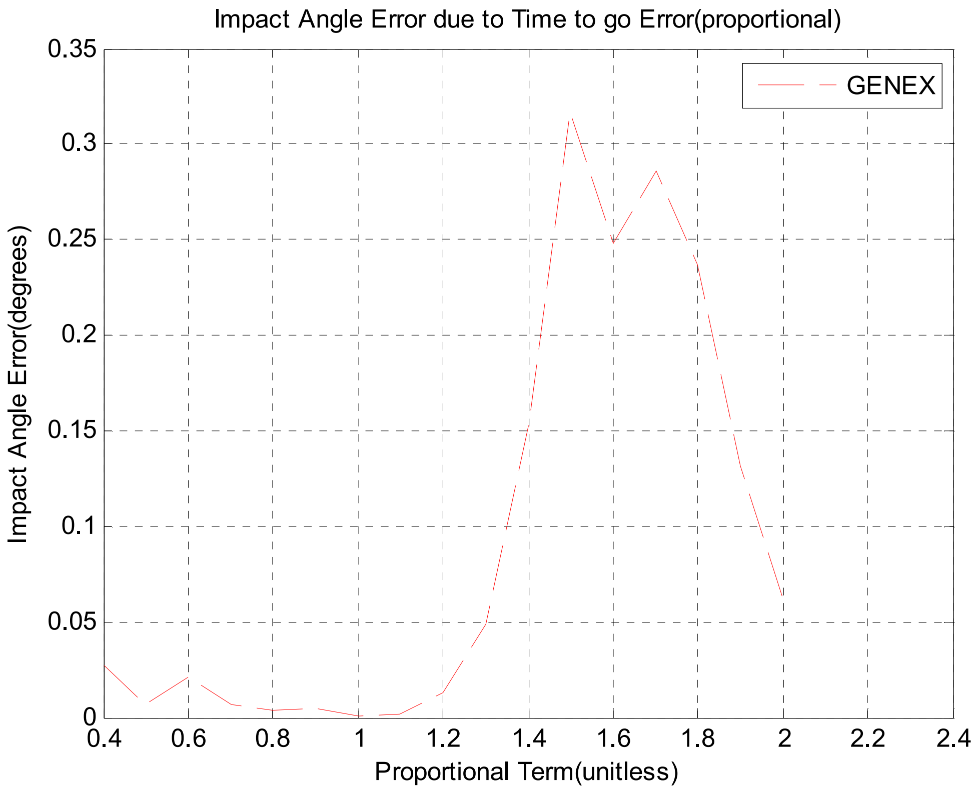

Figure 52 Impact Angle Error due to Time to go Error (proportional /non-stationary)

GENEX shows good performance in the case of non-stationary target also.

4.5 **Time-to-go Error Analysis with Non-Traditional Time-to-Go Method**[1]

In both of the two algorithms that require time-to-go information, time-to-go is calculated by the traditional formulation which is nothing but range divided by missile velocity. However, as seen in [1], there are other methods that can be used to calculate time-to-go which might improve the guidance performance. This section is devoted to the time-to-go error analysis' with traditional and new time-to-go method described in [1].

There are two time-to-go calculation methods in [1] both of which will be explained in the appendix section. In simulations, method 2 shall be used for the reasons that are explained in the appendix.

4.5.1 **Additive Term Varying Case**

4.5.1.1 **GENEX Time-to-go Error Analysis Comparison with New Time-to-go Method Against Non-Stationary Target**

The simulation parameters are shown below.

Table 32 Simulation Parameters

Parameters	Values
Missile Initial Position	(3000,500)
Target Initial Position	(5000,0)
Missile Initial Velocity	250 m/sec
Missile Initial Orientation	+15 degrees
Target Orientation	+x direction

Target Velocity	15 m/sec
Gravity	Neglected
Desired Impact Angle	-45 degrees
Acceleration Limits	$a_{max} = 7g$ $a_{min} = -7g$

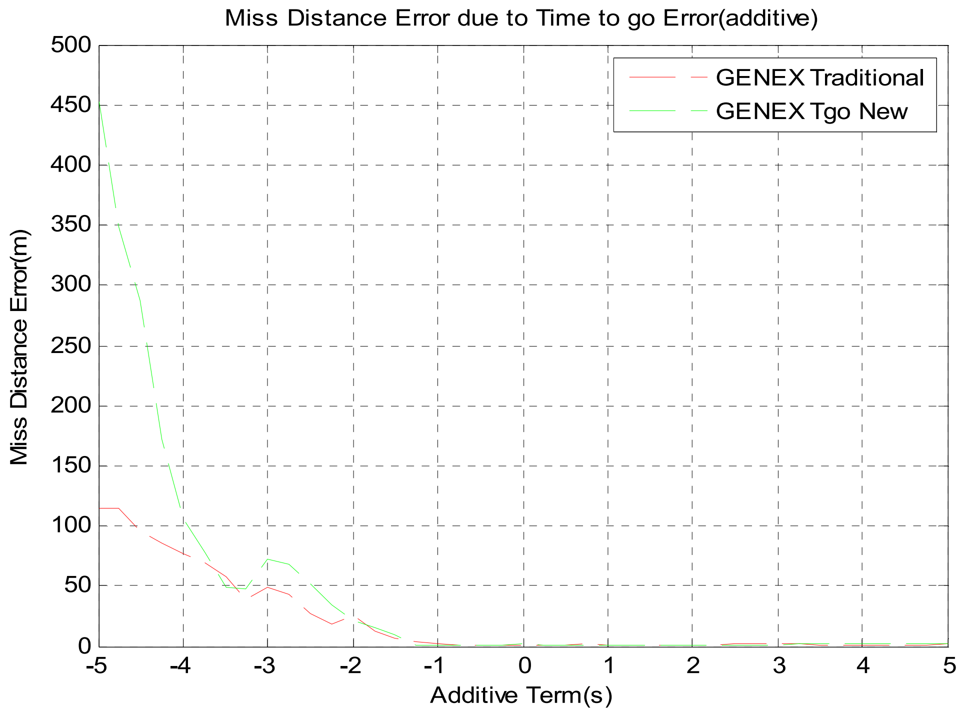

Figure 53 Miss Distance Error due to Time to go Error (additive/non-stationary)

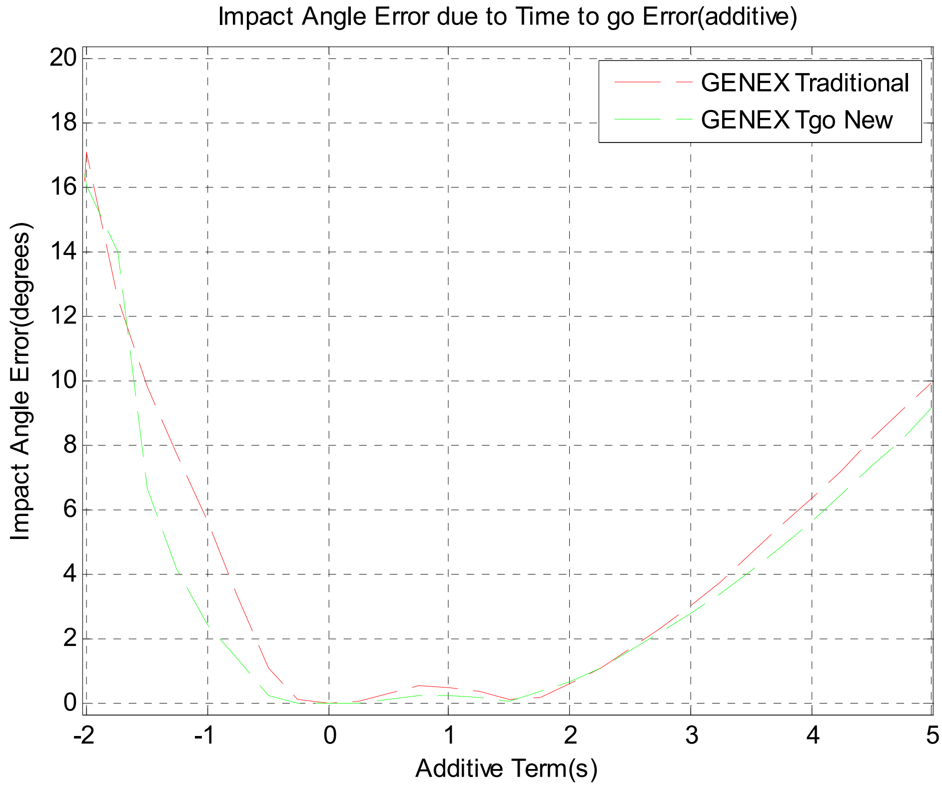

Figure 54 Impact Angle Error due to Time to go Error (additive/non-stationary)

As seen in the figures above, for terms from -2 to 5 seconds both method show similar performance. From -5 to -2, traditional method shows better performance though both cannot satisfy success criterions in that interval.

4.5.1.2 SDREGL Time-to-go Error Analysis Comparison with New Time-to-go Method against Stationary Target

Simulation parameters are shown below.

Parameters	Values
Missile Initial Position	(3000,500)
Target Initial Position	(5000,0)
Target Velocity	0 m/sec
Missile Initial Velocity	250 m/sec
Missile Initial Orientation	+15 degrees
Gravity	Neglected
Desired Impact Angle	-45 degrees
Acceleration Limits	$a_{max} = 7g$ $a_{min} = -7g$

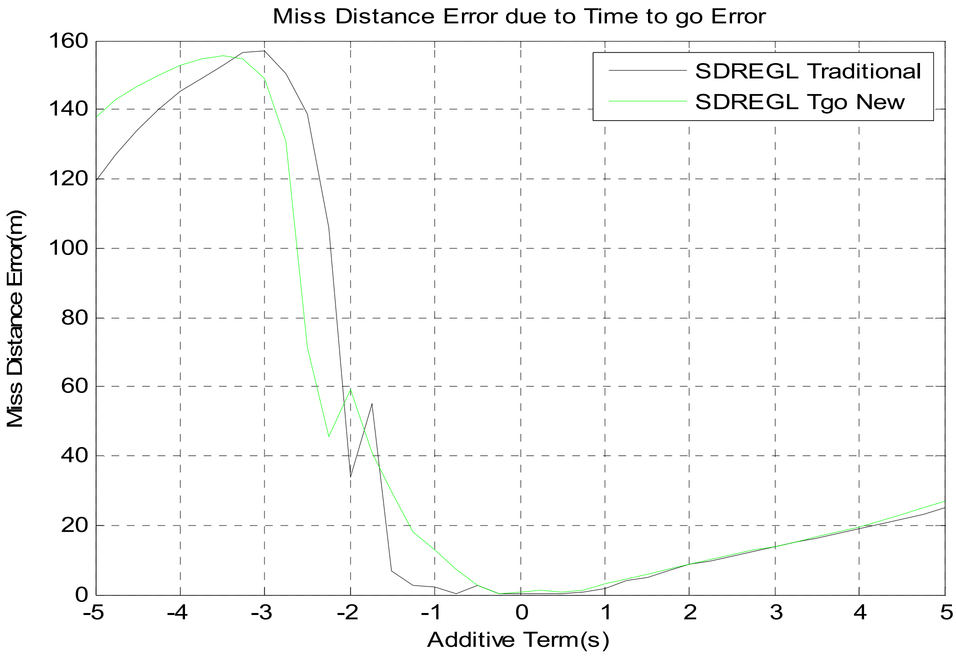

Figure 55 Miss Distance Error due to Time to go Error (additive/stationary)

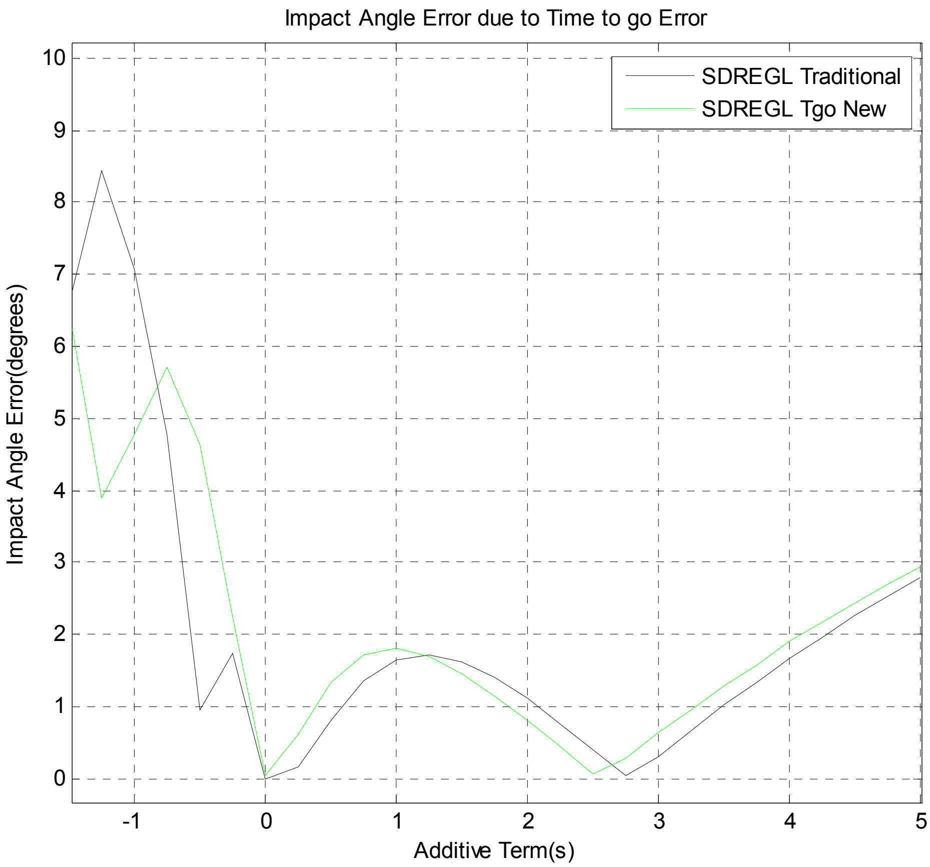

Figure 56 Impact Angle Error due to Time to go Error (additive/stationary)

For SDREGL, new time-to-go method does not produce much difference.

4.5.2 **Proportional Term Varying Case**

4.5.2.1 **GENEX Time-to-go Error Analysis Comparison with New Time-to-go Method Against Non-Stationary Target**

Simulation parameters are same as in Table 31.

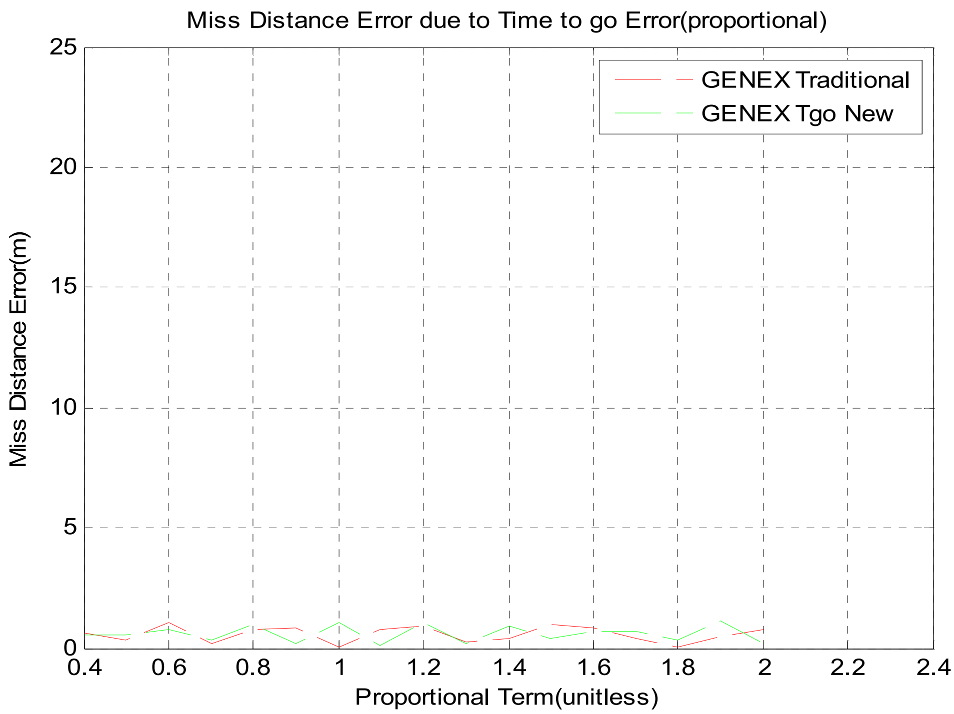

Figure 57 Miss Distance Error due to Time to go Error (proportional/non-stationary)

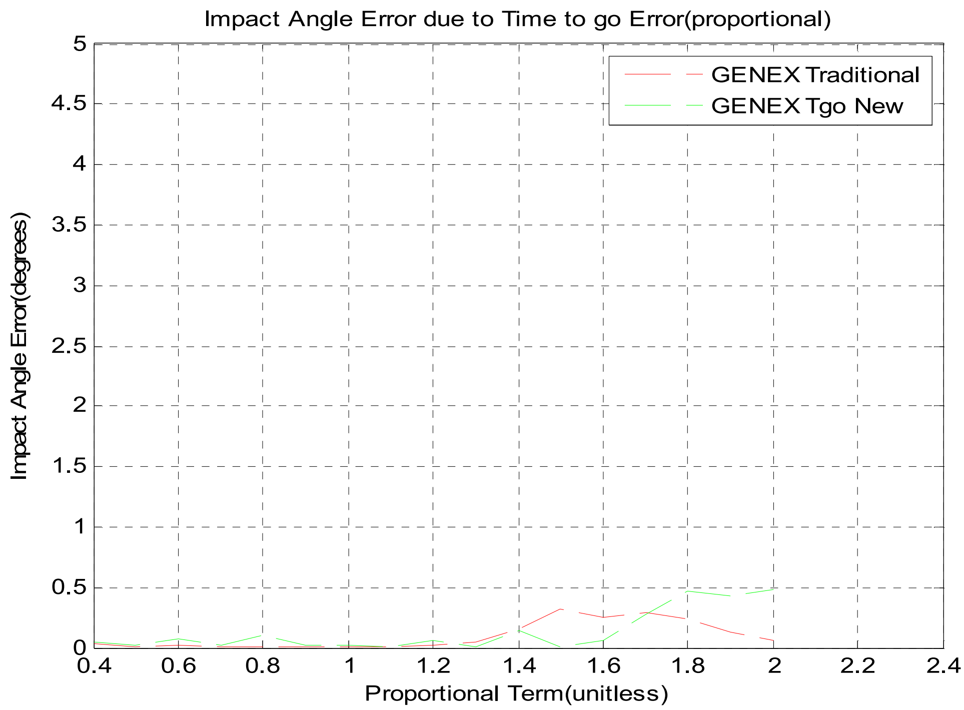

Figure 58 Impact Angle Error due to Time to go Error (proportional/non-stationary)

GENEX law with new time-to-go method also shows superior performance in the existence of proportional error term.

4.5.2.2 **SDREGL Time-to-go Error Analysis Comparison with New Time-to-go Method Against Stationary Target**

Simulation parameters are same as in Table 32.

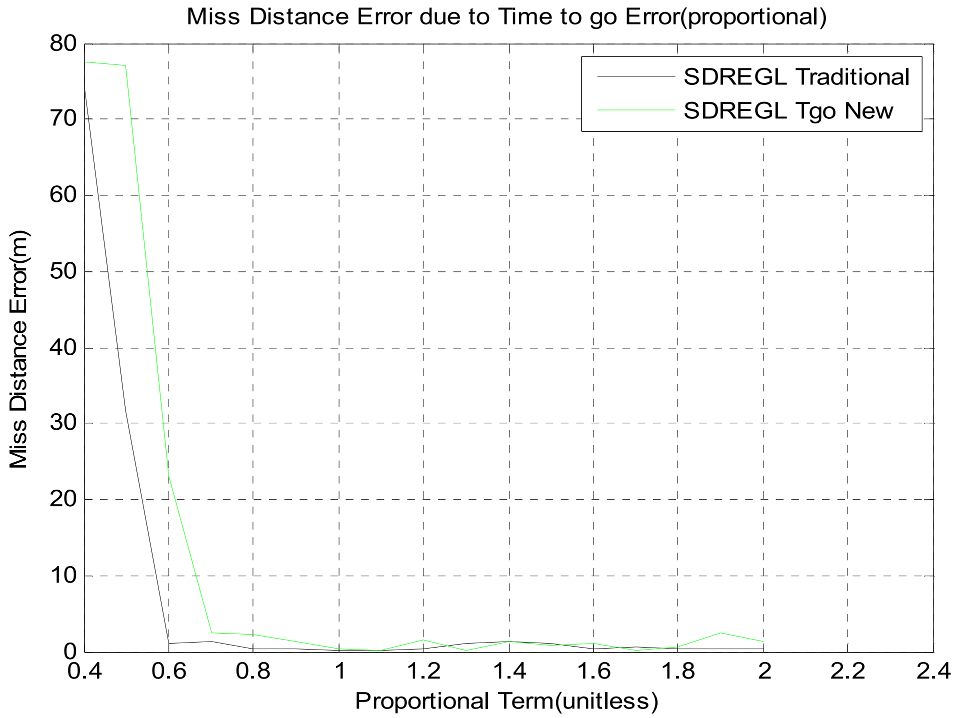

Figure 59 Miss Distance Error due to Time to go Error (proportional/ stationary)

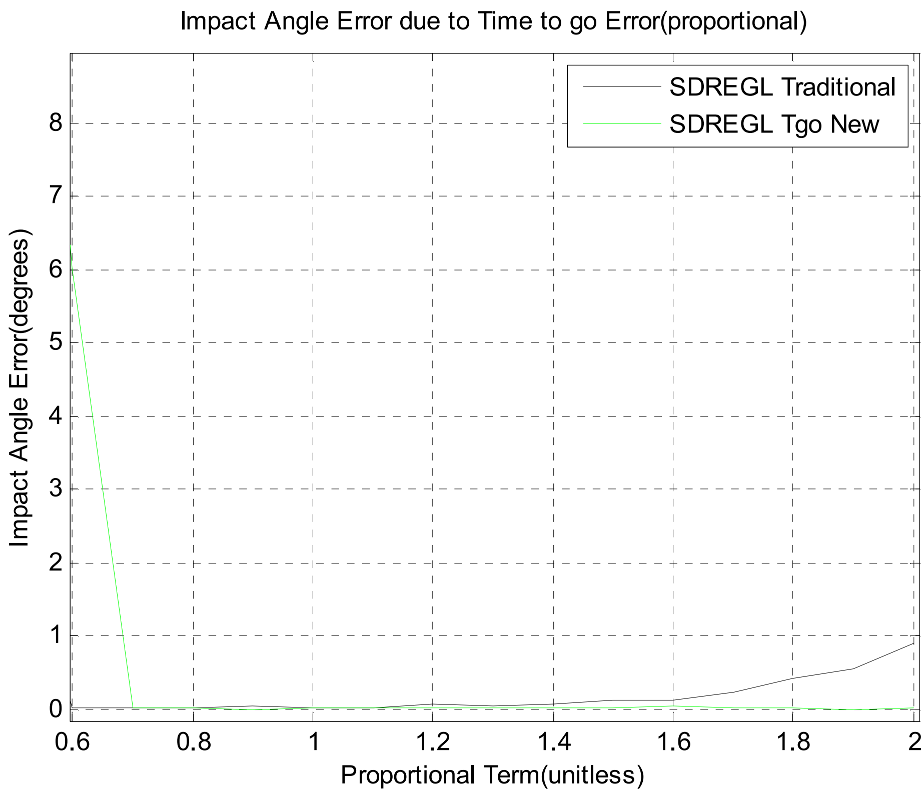

Figure 60 Impact Angle Error due to Time to go Error (proportional/ stationary)

SDREGL with new time-to-go method shows good performance like with the traditional case. However, its performance degrades as the error term gets smaller than 0.7.

In overall picture, it can confidently be concluded that non-traditional time-to-go method does not provide an improved t-go error performance.

CHAPTER 5

CONCLUSIONS AND FUTURE WORK

In this thesis, 5 impact angle constrained guidance laws have been investigated by means of different analysis techniques. In order to sum up, it would be useful to tabulate the merits of performance in a single table which is given below.

Table 33 Summary of Merits of Performance

	BSBPN	IACBPPN	SDREGL	GENEX	OG
Range Information Necessity	●	◐	○	○	●
Implementation Issues	●	●	○	○	●
Robustness to Time Constant	◐	○	●	●	●
Feasible Engagement Zone(stationary)	N/A	◐	●	●	○
Feasible Engagement Zone(non-stationary)	N/A	N/A	N/A	●	○
Success Variance of Handover Orientation	◐	●	●	◐	○
Variance of Impact Angle and Miss Distance with respect to Different Target Speeds	○	○	◐	●	●
Sensitivity to T-go Error(traditional T-go method)	●*	●*	◐	●	●*
Sensitivity to T-go Error(non-traditional T-go method)	●*	●*	◐	●	●*

● Superior ◐ Moderate ○ Poor

Range information necessity is an important parameter for implementation. However, it is stressed here as another merit due to its high importance. SDREGL and GENEX require range information and they are considered as poor. IACBPPN requires this information only at the beginning of the engagement, thus it is considered as moderate. OG and BSBPN does not require range information at all, hence they are superior in this sense.

Implementation issues are also important. GENEX requires many angles and range as stated above, hence it is poor. SDREGL requires time-to-go, flight path and LOS angles hence it is also poor. IACBPPN, BSBPN and OG demand only LOS rate information hence they are evaluated as superior.

Robustness to time constant is another important measure of performance. In miss distance comparison, they are all under the bound 2.5 meters which is the error of simulations. Nevertheless, IACBPPN's impact angle error increases considerably as the time constant gets larger. BSBPN has a stable and considerably low impact angle error in the specified time constant interval, thus it is evaluated as moderate. OG, GENEX and SDREGL almost have no impact angle error in the specified interval.

Feasible engagement zones' grades are determined whether the algorithms' engagement zone is bigger or smaller. Reader can refer to sections 4.1.2 and 4.2.2 for detailed information.

Success variance of handover orientation is also important. OG has high variance depending on the TGH angle. Hence it can be considered as poor. GENEX and BSBPN have fairly good variance characteristic. SDREGL and GENEX are more insensitive to the variations of TGH orientation.

Variance of impact angle and miss distance with respect to different target speeds is another performance merit. BSBPN and IACBPPN have impact angles of broader range than others with respect to different target speeds. Hence they are evaluated as poor. SDREGL is better than BSBPN and IACBPPN. OG and GENEX are best since they are designed to intercept non-stationary targets.

Last merit is sensitivity to t-go error. The error model is calculated for both traditional and non-traditional[1] methods and they have almost same performance. (*) symbol means the t-go error analysis is not applied to those algorithms, however they can be considered as superior because they do not require t-go information at all. GENEX is more insensitive to t-go errors than SDREGL. Thus, they are graded accordingly.

This study can be base of a more comprehensive software in which these guidance laws and maybe more other laws are incorporated. Software would have a user-friendly graphical user interface (GUI) that would allow the pilots and/or fire control officer to choose the appropriate guidance law depending on the feasible engagement zones which would be embedded to software. Moreover, more information would be displayed on a screen about the possible miss distance and impact angle limitation of the current situation with the embedded laws. On the other hand, these laws would be embedded to a higher fidelity simulation models which would include auto-pilot and aerodynamic models to be used in software-in-the-loop (SWIL) simulations.

REFERENCES

[1] C.-K. Ryoo, H. Cho, and M.-J. Tahk, “Optimal Guidance Laws with Terminal Impact Angle Constraint,” *J. Guid. Control. Dyn.*, vol. 28, no. 4, pp. 724–732, Jul. 2005.

[2] “Missile.” [Online]. Available: http://en.wikipedia.org/wiki/Missile. [Accessed: 30-Jan-2014].

[3] “List Of Missiles.” [Online]. Available: http://en.wikipedia.org/wiki/List_of_missiles. [Accessed: 15-Jul-2014].

[4] “No Title.” [Online]. Available: http://en.wikipedia.org/wiki/Main_battle_tank. [Accessed: 10-Jan-2014].

[5] Wikipedia, “Missile Guidance.” [Online]. Available: 3,http://en.wikipedia.org/wiki/Missile_guidance#Command_to_Line-Of-Sight_.28CLOS.29. [Accessed: 22-Feb-2014].

[6] ROKETSAN, “No Title.” [Online]. Available: http://www.roketsan.com.tr/urunler-hizmetler/hassas-gudumlu-fuzeler/umtas-uzun-menzilli-anti-tank-fuzesi/. [Accessed: 30-Jun-2014].

[7] Wikipedia, “No Title.” [Online]. Available: http://en.wikipedia.org/wiki/Warship#Modern_warships. [Accessed: 17-Mar-2014].

[8] George M.SIORUS, *Missile Guidance and Control Systems*. Springer.

[9] Wikipedia, “Harpoon(missile).” [Online]. Available: http://en.wikipedia.org/wiki/Harpoon_(missile). [Accessed: 15-Jul-2014].

[10] P. B. Jackson, “Overview of Missile Flight Control Systems,” pp. 9–24.

[11] J. Yao, Q. Xia, and Z. Qi, “Study of the trajectory shaping guidance law with terminal constraints,” *2010 3rd Int. Symp. Syst. Control Aeronaut. Astronaut.*, pp. 172–177, Jun. 2010.

[12] I. Jeon, J. Lee, and M. Tahk, "Impact-Time-Control Guidance Law for Anti-Ship Missiles," vol. 14, no. 2, pp. 260–266, 2006.

[13] K. S. Erer and O. Merttopçuoglu, "Indirect Impact-Angle-Control Against Stationary Targets Using Biased Pure Proportional Navigation," *J. Guid. Control. Dyn.*, vol. 35, no. 2, pp. 700–704, Mar. 2012.

[14] S. K. Jeong and S. J. Cho, "Angle Constraint Biased PNG," 2004.

[15] T.-H. Kim, B.-G. Park, and M.-J. Tahk, "Bias-Shaping Method for Biased Proportional Navigation with Terminal-Angle Constraint," *J. Guid. Control. Dyn.*, vol. 36, no. 6, pp. 1810–1816, Nov. 2013.

[16] A. Ratnoo and D. Ghose, "Impact Angle Constrained Interception of Stationary Targets," *J. Guid. Control. Dyn.*, vol. 31, no. 6, pp. 1817–1822, Nov. 2008.

[17] B. S. O. Kim, "Biased PNG Law for Impact with Angular Constraint," vol. 34, no. 1, 1998.

[18] F. Q. Elizabeth, G. Akhil, and D. Ghose, "2012 American Control Conference Biased PN based Impact Angle Constrained Guidance Using a Nonlinear Engagement Model," 2012.

[19] A. Ratnoo and D. Ghose, "Impact Angle Constrained Guidance Against Nonstationary Nonmaneuvering Targets," *J. Guid. Control. Dyn.*, vol. 33, no. 1, pp. 269–275, Jan. 2010.

[20] Y.-I. Lee, S.-H. Kim, J.-I. Lee, and M.-J. Tahk, "Analytic Solutions of Generalized Impact-Angle-Control Guidance Law for First-Order Lag System," *J. Guid. Control. Dyn.*, vol. 36, no. 1, pp. 96–112, Jan. 2013.

[21] P. Zarchan, "Tactical and Strategic Missile Guidance 6th Ed.PDF." p. 178, 2012.

[22] Kim M.;Grider V.Kelly, "Terminal Guidance for Impact Attitude Angle Constrained Flight Trajectories," no. 6, pp. 852–859, 1973.

[23] S. Subchan, "TRAJECTORY SHAPING OF SURFACE-TO-SURFACE MISSILE WITH TERMINAL IMPACT ANGLE CONSTRAINT," vol. 11, no. 2, pp. 65–70, 2007.

[24] G. Gede, "The Direct Collocation Method for Optimal Control," 2011.

[25] C. Ryoo, H. Cho, and M. Tahk, "Time-to-Go Weighted Optimal Guidance With Impact Angle Constraints," vol. 14, no. 3, pp. 483–492, 2006.

[26] C.-H. Lee, M.-J. Tahk, and J.-I. Lee, “Generalized Formulation of Weighted Optimal Guidance Laws with Impact Angle Constraint,” *IEEE Trans. Aerosp. Electron. Syst.*, vol. 49, no. 2, pp. 1317–1322, Apr. 2013.

[27] A. Ratnoo and D. Ghose, “State-Dependent Riccati-Equation-Based Guidance Law for Impact-Angle-Constrained Trajectories,” vol. 32, no. 1, 2009.

[28] B.-G. Park, T.-H. Kim, and M.-J. Tahk, “Optimal impact angle control guidance law considering the seeker’s field-of-view limits,” *Proc. Inst. Mech. Eng. Part G J. Aerosp. Eng.*, vol. 227, no. 8, pp. 1347–1364, Jun. 2012.

[29] Y.-I. Lee, S.-H. Kim, and M.-J. Tahk, “Analytic solutions of optimal angularly constrained guidance for first-order lag system,” *Proc. Inst. Mech. Eng. Part G J. Aerosp. Eng.*, vol. 227, no. 5, pp. 827–837, May 2012.

[30] a. V. Savkin, P. N. Pathirana, and F. a. Faruqi, “Problem of precision missile guidance: LQR and H//sup∞/ control frameworks,” *IEEE Trans. Aerosp. Electron. Syst.*, vol. 39, no. 3, pp. 901–910, Jul. 2003.

[31] E. J. Ohlmeyer and C. a. Phillips, “Generalized Vector Explicit Guidance,” *J. Guid. Control. Dyn.*, vol. 29, no. 2, pp. 261–268, Mar. 2006.

[32] I. R. Manchester and A. V. Savkin, “Circular-Navigation-Guidance Law for Precision Missile/Target Engagements,” *J. Guid. Control. Dyn.*, vol. 29, no. 2, pp. 314–320, Mar. 2006.

[33] M.-G. Yoon, “Relative circular navigation guidance for the impact angle control problem,” *IEEE Trans. Aerosp. Electron. Syst.*, vol. 44, no. 4, pp. 1449–1463, Oct. 2008.

[34] M. Yoon, “Relative Circular Navigation Guidance for Three-Dimensional Impact Angle Control Problem,” no. October, pp. 300–309, 2010.

[35] B. Özkan, “DYNAMIC MODELING, GUIDANCE, AND CONTROL OF HOMING MISSILES,” Middle East Technical University, 2005.

[36] R. Yanushevsky, *Modern Missile Guidance*. 2007.

APPENDIX

For the time-to-go method proposed in [1], a new frame of reference is proposed which represents the flight path of the missile. The reference frame and its angles are seen below. Note that the notations are the same as in paper since it is a new reference frame that is not used in the thesis.

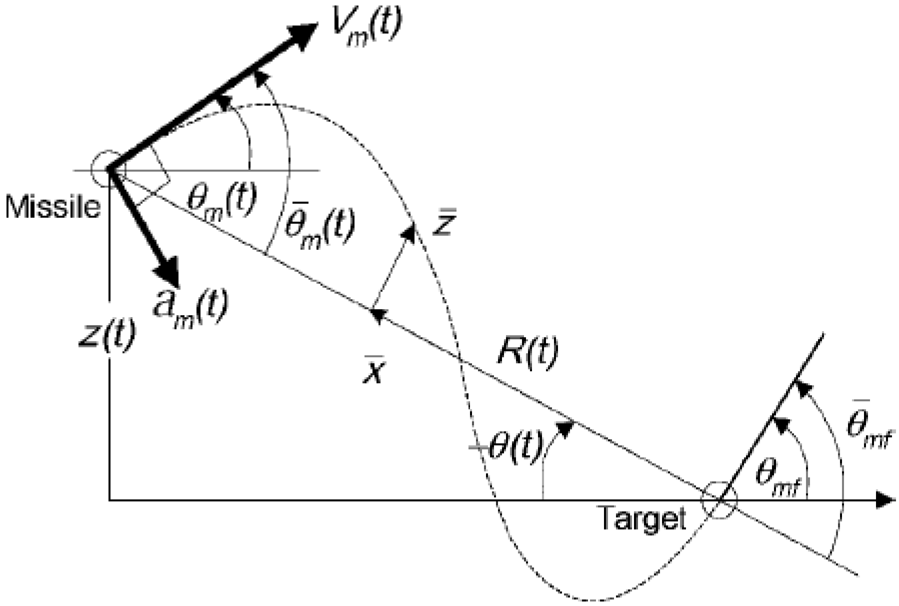

Assuming that $\bar{z}$ can be expressed as third order polynomials of $\bar{x}$;

$$\bar{z}(x) = a_3\bar{x}^3 + a_2\bar{x}^2 + a_1\bar{x} + a_0 \tag{88}$$

Knowing that;

$$\dot{z}(t) = V_m\theta_m(t) \tag{89}$$

Combining (87) and (88);

$$\bar{\theta}_m(\bar{x}) = \frac{\dot{\bar{z}}}{V_m} = \frac{\dot{\bar{x}}}{V_m}\left(3a_3\bar{x}^2 + 2a_2\bar{x} + a_1\right) = -\left(3a_3\bar{x}^2 + 2a_2\bar{x} + a_1\right) \tag{90}$$

Boundary conditions for this problem are given as:

$$\overline{z} = 0\,, \overline{\theta}_m = \overline{\theta}_m(t) \;\; and\; \overline{x} = R\; at\; t$$
$$\overline{z} = 0, \overline{\theta}_m = \overline{\theta}_{mf} \;\; and\; \overline{x} = 0\; at\; t_f \tag{91}$$

Coefficients of (87) and (89) can then be obtained as following:

$$a_3 = \frac{\left[-\overline{\theta}_m(t) - \theta_{mf}\right]}{R^2}\,, a_2 = \frac{\left[2\overline{\theta}_m(t) + \overline{\theta}_{mf}\right]}{R}\,, a_1 = -\overline{\theta}_{mf}\,, a_0 = 0 \tag{92}$$

For time-to-go calculation, two methods are proposed. First method uses length of the curved path over velocity while second method incorporates range over the average velocity which is defined as projection of the velocity vector on the LOS.

Simple definitions of the formulas whose details can be accessed in [21] are seen below.

Table 34 Time-to-go Formulas

Method #	Formula
1	$t_{go} = \frac{1}{V_m}\int_0^R \sqrt{1 + (z')^2}dx\,, z' = \frac{dz}{dx}$
2	$t_{go} = {}^{R}\!/_{\overline{V}_m}\,, \overline{V}_m = \frac{1}{R}\int_0^R V_m \cos\overline{\theta}_m\, dx$

To evaluate the integrals above, two approximations are used.

$$\sqrt{1 + (z')^2} \approx 1 + \frac{1}{2}(z')^2 - \frac{1}{8}(z')^4 \tag{93}$$

$$\cos\overline{\theta}_m \approx 1 - \frac{\overline{\theta}_m^{\,2}}{2!} + \frac{\overline{\theta}_m^{\,4}}{4!} \tag{94}$$

The important point here is that the approximation (92) is valid only for $-1 < (z')^2 < 1$ while for (93) is valid for $-\infty < \overline{\theta}_m < +\infty$. When $\theta_{m0}$and θ_{mf} are closer to ${}^{\pi}\!/_{2}$, $(z')^2 \geq 1$ happens. Hence, approximation for the formula does not hold producing large errors. However, there is no such a situation for method 2. For this reason, method 2 is employed.